Defense Nuclear Agency
Alexandria, VA 22310-3398

DNA-TR-91-224

Advanced Development of Diagnostics for Non-Ideal Blast Flows

Dariush Modarress
Thomas Hoeft
Physical Research, Inc.
25500 Hawthorne Boulevard
Suite 2300
Torrance, CA 90505-6828

July 1992

Technical Report

CONTRACT No. DNA 001-89-C-0018

DESTRUCTION NOTICE:

FOR CLASSIFIED documents, follow the procedures in DoD 5200.22-M, Industrial Security Manual, Section II-19.

FOR UNCLASSIFIED, limited documents, destroy by any method that will prevent disclosure of contents or reconstruction of the document.

Retention of this document by DoD contractors is authorized in accordance with DoD 5220.22-M, Industrial Security Manual.

PLEASE NOTIFY THE DEFENSE NUCLEAR AGENCY, ATTN: CSTI, 6801 TELEGRAPH ROAD, ALEXANDRIA, VA 22310-3398, IF YOUR ADDRESS IS INCORRECT, IF YOU WISH IT DELETED FROM THE DISTRIBUTION LIST, OR IF THE ADDRESSEE IS NO LONGER EMPLOYED BY YOUR ORGANIZATION.

DISTRIBUTION LIST UPDATE

This mailer is provided to enable DNA to maintain current distribution lists for reports. (We would appreciate your providing the requested information.)

NOTE:
Please return the mailing label from the document so that any additions, changes, corrections or deletions can be made easily.

☐ Add the individual listed to your distribution list.

☐ Delete the cited organization/individual.

☐ Change of address.

NAME: _____

ORGANIZATION: _____

OLD ADDRESS	CURRENT ADDRESS
_____	_____
_____	_____
_____	_____

TELEPHONE NUMBER: (___) _____

DNA PUBLICATION NUMBER/TITLE	CHANGES/DELETIONS/ADDITIONS, etc.) (Attach Sheet if more Space is Required)
_____	_____
_____	_____
_____	_____

DNA OR OTHER GOVERNMENT CONTRACT NUMBER: _____

CERTIFICATION OF NEED-TO-KNOW BY GOVERNMENT SPONSOR (if other than DNA):

SPONSORING ORGANIZATION: _____

CONTRACTING OFFICER OR REPRESENTATIVE: _____

SIGNATURE: _____

CUT HERE AND RETURN

DEFENSE NUCLEAR AGENCY
ATTN: TITL
6801 TELEGRAPH ROAD
ALEXANDRIA, VA 22310-3398

DEFENSE NUCLEAR AGENCY
ATTN: TITL
6801 TELEGRAPH ROAD
ALEXANDRIA, VA 22310-3398

REPORT DOCUMENTATION PAGE

Form Approved OMB No. 0704-0188

1. AGENCY USE ONLY *(Leave blank)*	2. REPORT DATE	3. REPORT TYPE AND DATES COVERED
	920701	Technical 890401-910601

4. TITLE AND SUBTITLE
Advanced Development of Diagnostics for Non-Ideal Blast Flows

5. FUNDING NUMBERS
C -DNA 001-89-C-0018
PE-62715H
PR-RW
TA-RS
WU-DH056140

6. AUTHOR(S)
Dariush Modarress and Thomas Hoeft

7. PERFORMING ORGANIZATION NAME(S) AND ADDRESS(ES)
Physical Research, Inc.
25500 Hawthorne Boulevard
Suite 2300
Torrance, CA 90505-6828

8. PERFORMING ORGANIZATION REPORT NUMBER

9. SPONSORING/MONITORING AGENCY NAME(S) AND ADDRESS(ES)
Defense Nuclear Agency
6801 Telegraph Road
Alexandria, VA 22310-3398
SPSP/Castleberry

10. SPONSORING/MONITORING AGENCY REPORT NUMBER
DNA-TR-91-224

11. SUPPLEMENTARY NOTES
This work was sponsored by the Defense Nuclear Agency under RDT&E RMC Code B4662D RW RS 00029 PRAS 1940A 25904D.

12a. DISTRIBUTION/AVAILABILITY STATEMENT
Approved for public release; distribution is unlimited.

12b. DISTRIBUTION CODE

13. ABSTRACT *(Maximum 200 words)*

Investigations of non-ideal airblast are performed at the Ernst Mach Institute in a shock tube that simulates a radiation-induced thermal layer. Visualization techniques were adequate for overall study of the flow, but did not provide the detailed data for validation of computer codes. Under this contract three tasks were performed to provide needed data. The first task was to develop a software package for analysis of interferogram fringes. This package translates fringes shift due to the presence of helium into densities over the image area. This package was installed at EMI. The second task was to evaluate and test techniques for direct time-varying measurement of gas species concentration. Absorption spectroscopy of NO_2 was selected to be used, but had corrosion problems and was abandoned. As a replacement, filtered Rayleigh scattering from Freon gas was identified. The third task was to fabricate and install a multi-location laser Doppler velocimeter system for the shock tube. This unit was installed in the shock tube and preliminary velocity measurements of flow over a rough surface were made. The developed boundary layer over the rough surface was found to be similar to those developed in dusty flows.

14. SUBJECT TERMS
Shock Tube
Shock Boundary Layer Interaction
Laser Doppler Velocimeter
Interferogram Fringe Analysis

15. NUMBER OF PAGES
102

16. PRICE CODE

17. SECURITY CLASSIFICATION OF REPORT	18. SECURITY CLASSIFICATION OF THIS PAGE	19. SECURITY CLASSIFICATION OF ABSTRACT	20. LIMITATION OF ABSTRACT
UNCLASSIFIED	UNCLASSIFIED	UNCLASSIFIED	SAR

CLASSIFIED BY:

N/A since Unclassified.

DECLASSIFY ON:

N/A since Unclassified.

SUMMARY

DNA-sponsored experimental investigations of non-ideal airblast are being carried out at the Ernst Mach Institute (EMI) in a shock tube fitted for introduction of a helium layer to simulate a radiation-induced thermal layer. Direct visualization techniques available were adequate for study of the overall features of the flow, but did not provide the detailed data for validation of computer code prediction methods. Under contract DNA-001-89-C-0018, Physical Research, Inc. (PRi) performed three tasks: 1) a software package for analysis of interferogram fringes in flowfield images was developed and implemented; 2) techniques for direct time-varying measurement of gas species concentration versus height in the shock tube were evaluated and tested, and basic system design parameters were established; 3) a multi-location laser Doppler velocimeter (LDV) system for the shock tube was developed and tested.

The fringe analysis computer program compares interference fringe patterns recorded before and after introduction of helium to the shock tube. Fringe shifts due to the presence of helium are translated into partial densities over the field of view of the imaging system. The operation manual for this program is included as an appendix to this report.

For time-varying concentration measurements, a number of techniques were reviewed. Absorption spectroscopy using NO_2 as the seed gas was chosen as most promising, and successful tests with a prototype system were carried out. Further development of this technique was stopped because of corrosion problems due to formation of nitric acid in the shock tube. After review of additional techniques, filtered Rayleigh scattering from Freon gas was identified as a promising technique, and an experiment for testing the technique, with several options, is proposed in this report.

A LDV system for simultaneous velocity measurements at four locations was fabricated and installed in the shock tube. Preliminary velocity measurements made with the four-location instrument were of flow over a rough surface (carpet). The developed boundary layer for this rough surface was found to be similar to those for dusty flows.

CONVERSION TABLE

Conversion factors for U.S. Customary to metric (SI) units of measurement

MULTIPLY →	BY →	TO GET
TO GET	BY	DIVIDE
angstrom	1.000 000 X E -10	Meters (m)
atmosphere (normal)	1.013 25 X E +2	Kilo pascal (kPa)
bar	1.000 000 X E +2	Kilo pascal (kPa)
barn	1.000 000 X E -28	meter^2 (m^2)
British thermal unit (thermochemical)	1.054 350 X E +3	joule (J)
cal (thermochemical)/cm^2	4.184 000 X E -2	mega joule/m^2 (MJ/m^2)
calorie (thermochemical)	4.184 000	joule (J)
calorie (thermochemical/g)	4.184 000 X E +3	joule per kilogram (J/kg)
curies	3.700 000 X E +1	giga becquerel (Gbq)*
degree Celsius	$t_K = t°_K + 273.15$	degree kelvin (K)
degree (angle)	1.745 329 X E -2	radian (rad)
degree Fahrenheit	$t_K = t°_K + 459.67/1.8$	degree kelvin (K)
electron volt	1.602 19 X E -19	joule (J)
erg	1.000 000 X E -7	joule (J)
erg/second	1.000 000 X E -7	watt (W)
foot	3.048 000 X E -1	meter (m)
foot-pound-force	1.355 818	joule (J)
gallon (U.S. liquid)	3.785 412 X E -3	meter^3 (m^3)
inch	2.540 000 X E -2	meter (m)
jerk	1.000 000 X E +9	joule (J)
joule/kilogram (J/kg) (radiation dose absorbed)	1.000 000	gray (Gy)
kilotons	4.183	terajoules
kip (1000 lbf)	4.448 222 X E +3	newton (N)
kip/inch^2 (ksi)	6.894 757 X E +3	kilo pascal (kPa)
ktap	1.000 000 X E +2	newton-second/m^2 ($N-s/m^2$)
micron	1.000 000 X E -6	meter (m)
mil	2.540 000 X E -5	meter (m)
mile (international)	1.609 344 X E +3	meter (m)
ounce	2.834 952 X E -2	kilogram (kg)
pound-force (lbf avoirdupois)	4.448 222	newton (N)
pound-force inch	1.129 848 X E -1	newton-meter (N-m)
pound-force/inch	1.751 268 X E +2	newton/meter (N/m)
pound-force/foot^2	4.788 026 X E -2	kilo pascal (kPa)
pound-force/inch^2 (psi)	6.894 757	kilo pascal (kPa)
pound-mass (lbm avoirdupois)	4.535 924 X E -1	kilogram (kg)
pound-mass-foot^2 (moment of inertia)	4.214 011 X E -2	kilogram-meter^2 ($kg-m^2$)
pound/mass/foot^3	1.061 846 X E +1	kilogram-meter^3 (kg/m^3)
rad (radiation dose absorbed)	1.000 000 X E -2	gray (Gy)**
roentgen	2.579 760 X E -4	coulomb/kilogram (C/kg)
shake	1.000 000 X E -8	second (s)
slug	1.459 390 X E -1	kilogram (kg)
torr (mm Hg, O°C)	1.333 22 X E -1	kilo pascal (kPa)

* The becquerel (Bq) is the SI unit of radioactivity. 1 Bq = 1 event/s

** The Gray (Gy) is the SI unit of absorbed radiation

TABLE OF CONTENTS

Section			Page
	SUMMARY		iii
	CONVERSION TABLE		iv
	LIST OF ILLUSTRATIONS		vi
1	INTRODUCTION		1
	1.1	BACKGROUND	1
2	INSTALLATION OF FRINGE REDUCTION SOFTWARE AT EMI		3
3	HELIUM CONCENTRATION MEASUREMENT		8
	3.1	MEASUREMENT REQUIREMENTS	8
	3.2	SELECTED TECHNIQUE	9
	3.3	TESTING	10
	3.4	ALTERNATE TECHNIQUE	14
4	VELOCITY MEASUREMENT		37
	4.1	LASER DOPPLER CELOCIMETER	37
	4.2	LDV PROBE DESIGN	37
	4.3	PRELIMINARY TESTS AT ERNST MACH INSTITUTE	38
5	CONCLUSION AND RECOMMENDATIONS		61
6	LIST OF REFERENCES		63
Appendicies			
	A	Operation Manual	A-1
	B	Required Equipment for Rayleigh Scattering	B-1

LIST OF ILLUSTRATIONS

Figure		Page
1	Pre-helium reference interferogram	5
2	Post-helium, pre-shock interferogram	6
3	Mach-Zehnder interferometers of shock/Helium layer interaction obtained at EMI	7
4	Weak-line parameter for NO_2 at 300 K	20
5	Weak-line parameter for NO_2 at 500 K	21
6	Weak-line parameter for NO_2 at 750 K	22
7	Absorption coefficient of NO_2 vd wavelength and wavenumber.	23
8	Transmission of light through 10 cm test cell containing 3% nitric dioxide in air.	24
9	Transmission of light through shock tube behind normal shock at M=2.0.	25
10	Schematic of NO_2 absorption test setup.	26
11	Schematic of double pass NO_2 absorption measurement apparatus.	27
12	Photograph of double pass NO_2 absorption apparatus.	28
13	Laser transmission vs water bath temperature.	29
14	Laser transmission versus time.	30
15	Pressure trace for run 13479.	31
16	Laser attenuation time history for run 13479.	32
17	Pressure trace for run 13480.	33
18	Laser attenuation time history for run 13480.	34
19	Laser attenuation versus NO_2 concentration.	35
20	Transmission versus frequency for Freon 12.	36
21	Reference beam LDV principle of operation.	42
22	Dual beam LDV principle of operation.	43
23	Sample burst and FFT from a tracer particle for single point LDV.	44
24	Schematic of four location LDV system at EMI.	45

LIST OF ILLUSTRATIONS (Continued)

Figure		Page
25	Optical schematic of 4 position LDV for EMI.	46
26	Photograph of LDV system installed at EMI.	47
27	Photograph of probe's transmitting optics.	48
28	Photograph of probe's receiving optics.	49
29	Typical pressure traces for 1) smooth floor and b) rough floor.	50
30	Freestream velocity data/pressure trace.	51
31	Individual velocity data 0.4 mm off smooth floor.	52
32	Velocity time histories for two different runs, smooth floor.	53
33	Velocity time histories for boundary layer developed behind a shock wave over a smooth floor.	54
34	Photograph of test bed with carpet.	55
35	Three simultaneous freestream velocity time history.	56
36	Normalized velocity time history for boundary layer developed behind a shock wave over rough surfaces.	57
37	RMS velocity time history at different elevations.	58
38	Normalized velocity profile.	59
39	Comparison of normalized velocity profiles.	60

SECTION 1
INTRODUCTION

1.1 BACKGROUND.

Analysis of experimental data such as those of the DNA-sponsored large-scale field tests indicates that the evolution of thermo-nuclear generated air blasts is strongly affected by the initial shock interactions with the flow in the vicinity of the ground. Propagation of a blast wave into a thermal radiation-generated ground layer of high sound speed produces a flow pattern with an outrunning precursor shock followed by a recirculation region with a strong forward flow along the ground. The flow field generated by the accelerated shock can have significant influence on the loadings on the objects located along the path of the precursor shock. Understanding of these phenomena requires detailed understanding of the shock behavior in such an environment.

Presently, experimental investigations of the non-ideal airblast are being carried out at Ernst Mach Institute (EMI). Characterization of the flow is being carried out by direct visualization techniques. These include schlieren photography, shadowgraphs, and Mach-Zehnder interferometry. These data are adequate for study of the overall features of the flow. However, they do not provide detailed measurement data necessary for code validation.

Flow diagnostics are the key to characterization of the non-ideal blast wave environment. Methods employed to date are not able to provide the required information and precision, and improved techniques are needed. Laser measurement technology available today offers candidate non-intrusive methods for the required data acquisition. Interpretation of experimental data and correlation with analytical predictions also are

required for further understanding of this complex flow field.

Shock tube experiments at Ernst Mach Institute (EMI) are being carried out to study development of the flow behind a shock wave in the presence of a high sound-speed region. For example, helium is injected through a series of porous plates located at the roof of the shock tube to generate a high sound speed layer near the wall. Visualization of the flow behind the incident shock using techniques such as shadowgraph, schlieren photography, and interferometry techniques has been used by EMI. The data obtained from these techniques are reduced to provide an index of refraction profiles. To further reduce the data into primary variables, an independent measurement of velocity, density, temperature, and species concentration is required.

The objective of the research reported here was a) to install fringe reduction software at EMI, and b) to evaluate the feasibility of optical techniques for direct measurement of species concentration and gas velocity time history at the EMI shock tube. Task a was completed and a copy of the manual is included in Appendix A. For Task b, two techniques were developed and implemented at EMI: 1) direct measurement of species concentration using NO_2 as the seed constituent, and 2) simultaneous measurement of velocity time history at four locations. The design and results of the investigation performed at EMI. Section 2 describes the fringe reduction software installed at EMI. Section 3 includes the description of the laser absorption technique that was used for direct measurement of helium concentration. Section 4 includes the design and development of a multi-location LDA system developed for the EMI facility.

SECTION 2

INSTALLATION OF FRINGE REDUCTION SOFTWARE AT EMI

Mach-Zehnder interferometry is customarily used as a flow visualization and data recording means at the EMI shock tube for non-ideal air blast studies. The multi-line Mach-Zehnder (M-2) interferometry photographs obtained represent the map of refractive index in the test section. Typical interferograms for the cases of pre-shock no helium (reference), pre-shock with helium, and shock passage are shown in Figures 1 through 3 respectively. Due to the complexity of and lack of knowledge of the helium concentration, processing interferograms taken during shock passage was not possible. The software developed for fringe reduction concentrated on the first two cases of pre-shock interferograms.

An interference fringe analysis software package using an image processing system at EMI was developed for automated evaluation of interference fringe patterns. The pre-helium interferogram is used as a reference to compensate for spherical aberration in both the photograph and the digitized image and for conditions that exist previous to the injection of helium that will distort the fringes. It is assumed that the temperature is uniform in both cases and the fringe distortions are related to the concentration of helium.

The following formula is used for calculation of the partial air pressure from the measured fringe shift at any location.

$$\frac{\rho_{qu}}{\rho_{total}} = 1 - \frac{\rho_{helium}}{\rho_{total}} = -3.270218 + 18.234761 - \frac{D_n}{KM\rho_o k_1} \qquad (2.1)$$

where

$$D_n = D_f \frac{W}{D}$$

D_f = Fringe Shift

W = Wave Length = .00045 mm

D = Optical path = 40 mm

$$K = 1 - \frac{k_2}{k_1} = 0.1355$$

$$M = 1 - \frac{M_2}{M_1} = 0.8618$$

k_1 = 0.2265 cm^3/gr

ρ_o = Density = 1.204 gr/liter

Required for this calculation is automatic detection of each fringe line and calculation of the fringe shift due to presence of helium (from the case for pure air).

A code was developed and delivered to EMI for this purpose. A complete Operation Manual describing the steps in the program and sample results are included in Appendix A.

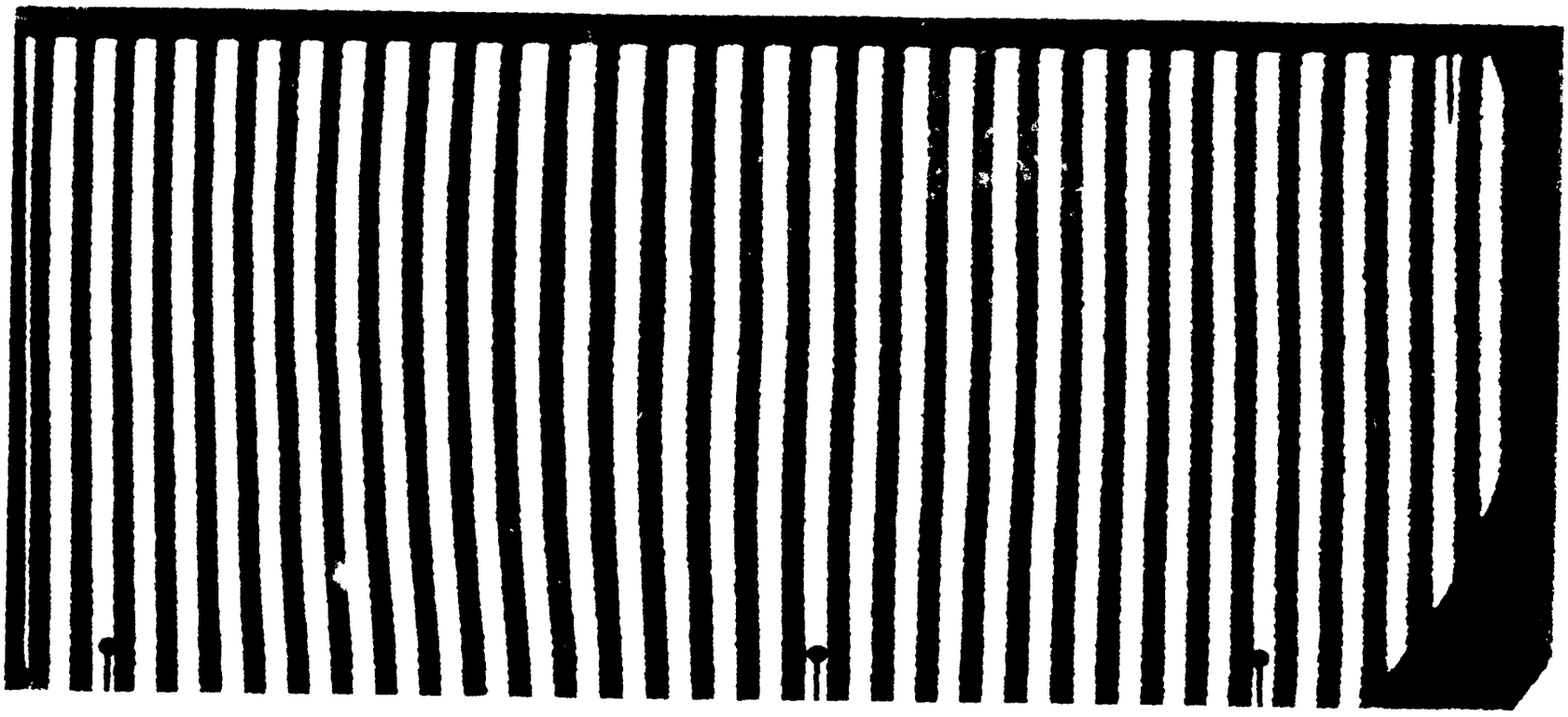

Figure 1. Pre-helium reference interferogram.

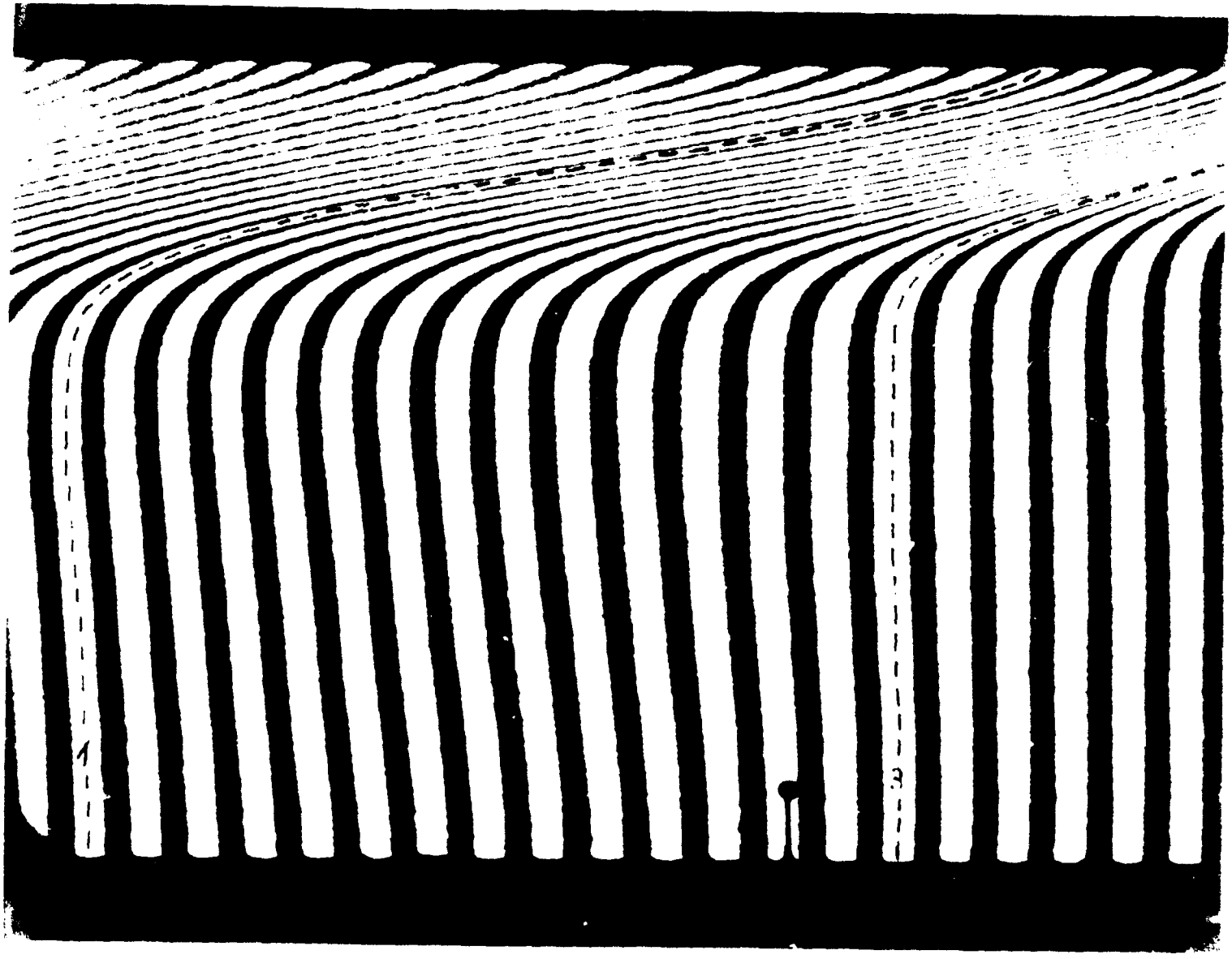

Figure 2. Post-helium, pre-shock interferogram.

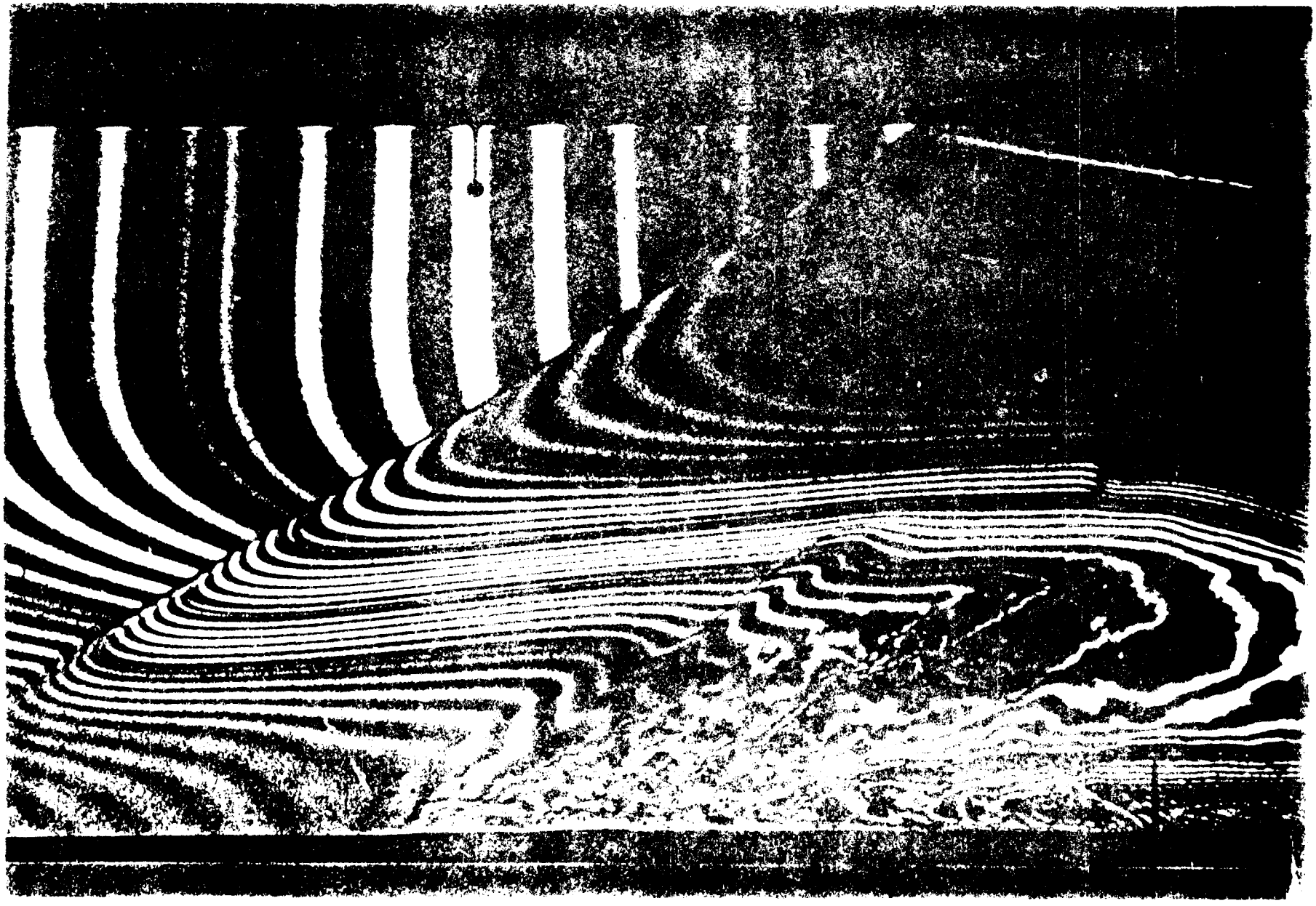

SECTION 3

HELIUM CONCENTRATION MEASUREMENT

3.1 MEASUREMENT REQUIREMENTS.

This task required measurement of the density or mass fraction of helium (or air) in the shock tube versus height and time. The spatial requirements are modest; 5 to 10 detector stations versus height would be adequate. The temporal requirements are more difficult. For a shock speed of 700 m/s, the flow duration is 1 to 2 ms. The measurement frequency requirements was estimated at 100 kHz. The desired measurement resolution is 1 to 2 per cent.

A number of measurement techniques were reviewed. Since helium gas has a closed electronic shell in its outer orbit, ionization spectroscopy is almost the only adequate method to measure helium concentration. N_2 and O_2 do not absorb below the UV. The absorption curve for the ambient air shows some absorption by O_2 at .76 μm. It should be noted however, that the absorption by the O_2 "atmospheric bond" is very weak but is observed in the solar spectrum due to long path lengths. In the shock tube one cannot augment the partial pressure of O_2 much further and therefore might not have the adequate sensitivity required in our studies.

CARS (Coherent Anti-Raman Spectroscopy) can be used to measure these species. This technique is, however, difficult and too expensive to implement.

Atmospheric trace gases offer some hope for absorption in the IR or visible. IR absorption is due to vibration-rotation, while absorption in the visible range is mostly due

to electronic transitions. Possible trace gases for the absorption technique are CO_2, CO, NO, CH_4, SO_2, NO_2, N_2O and H_2O. The best candidates for absorption in the visible were found to be NO_2 (3200 -10000 Å) and SO_2 (3400 - 3900 Å). In the IR region, CO_2 (2 - 15 μm) is most appropriate. SO_2 due to its toxic and corrosive properties was not considered appropriate for use in the shock tube. Another promising technique that was previously reviewed and discounted involved seeding helium with iodine gas. Toxicity and pressure broadening excluded the use of this technique.

3.2 SELECTED TECHNIQUE.

Absorption spectroscopy using NO_2 gas at 0.5 μm was selected as the candidate technique for the measurement of helium concentration. To minimize diffusion of tracer gases in the carrier gas, it is more convenient to add the absorbing gas to air than to helium. The concentration (partial pressure) of the gas is determined from the Lambert-Beer law according to the transmission relation

$$\overline{I_\nu} = \left(\frac{I_\nu}{I_\nu^o}\right) = e^{(-S(T)\rho(\nu)P_{NO_2}L)}$$

where I_ν = transmitted intensity at photon energy ν

I_ν^o = intensity of the source at photon energy ν

S(T) = line strength ($0.0156 cm^{-2}\ atm^{-1}$)

$\varphi(\upsilon)$ = Voight line shape ($\int \varphi(\nu) d\nu = 1$; $\varphi(0) = 1.56\ cr$)

P_{NO_2} = concentration of NO_2

L = absorption path length

The major absorption bands for NO_2 are 25000 cm^{-1} (0.4 μm) and 1500 cm^{-1} (6.2 μm). The absorption coefficients at these wavelengths are 10 and 30 atm^{-1} cm^{-1} (see Figures 4 - 6). For a concentration of 3% NO_2, transmission absorptions of 30% and 2.7% are obtained at visible and infrared bands respectively. No background radiation is present for the NO_2 tracer.

Nitric dioxide gas exists in a dipolar state with NO_2 and N_2O_4 being in an equilibrium. The relative concentration of NO_2 to N_2O_4 increases with temperature. As shown in Figure 7, NO_2 absorbs light above 390 nm whereas N_2O_4 does not. To measure the concentration of NO_2 only, it was decided to use the blue line (λ = 488 nm) of an Argon Ion laser. The predicted absorption of blue light over a 100 mm length by the NO_2 in a 3% nitric dioxide/air mixture versus temperature is shown in Figure 8, and the predicated absorption by the NO_2 behind a shock wave is shown in Figure 9.

3.3 TESTING.

3.3.1 In-House Results.

To examine the absorption by NO_2 versus temperature, absorption measurements of NO_2 were made using a beam from an Argon-Ion laser sent through a gas test cell. This setup is shown in Figure 10. The test cell was submerged in water for two reasons: safety, and to control the gas temperature. To increase the amount of absorption, a double path apparatus was fabricated. A schematic of this apparatus is shown in Figure 11 and a photograph of the apparatus is shown in Figure 12. An extensive series of tests was carried out to verify the optical properties of NO_2 as a tracer gas. Figure 13 shows data taken for two cases varying the water temperature and Figure 14 shows laser absorption over time in

a static test. These tests indicate that within the time scale of our measurement (30 minutes) the NO_2 was reacting with contaminants in the test cell (e.g., water vapor) and breaking down due to its inherent instability. Consequently, the absorption measurements did not agree with the theoretical prediction. This series of tests was abandoned in order to obtain more information regarding the design of the test and handling of the NO_2 gas.

3.3.2 EMI Shock Tube Results.

Testing was conducted at the EMI shock tube to examine whether the absorption by NO_2 behind a shock wave obtains the predicted value and whether the $NO_2 \rightleftharpoons N_2O_4$ interchange reacts instantaneously to the temperature change or if there is a time factor. If there is a time factor then both NO_2 and N_2O_4 concentrations need to be measured. As was seen in Figure 7, concentration measurements of N_2O_4 only can be made with a light source that emits a wavelength less than 250 nm, which would mean obtaining a new light source if the concentration of N_2O_4 needs to be measured.

These tests were performed by EMI staff to evaluate the accuracy of the shock tube concentration measurements using NO_2 as a seed gas. The shock tube was filled with a mixture of NO_2 and air. A normal shock wave was passed through the test section with a reflection shock returning from the closed end shock tube, resulting in three data points for the absorption measurement.

The NO_2/air mixture had an NO_2 content of 3.27% at 0° C. Considering that after pumping out the shock tube there was a residual pressure before the NO_2 mixture was injected, we have the following NO_2 concentration:

Test 13479

$T_1 = 292.5$ K $\quad p_o = 0.022$ bar $\quad p_1 = 1.004$ bar $\quad C_{NO2} = 9.0352 \cdot 10^{-4}$ mol/liter

Test 13480

T_1 = 294.0 K p_o = 0.040 bar p_1 = 0.498 bar $C_{NO2} = 9.0352 \cdot 10^{-4}$ mol/liter

Assuming ideal gas behavior, the following constants were obtained for the gas mixture:

Test 13479

$$\gamma = \frac{C_{pj}}{C_r} = 1.398 \qquad \frac{a_{Mix}}{a_{Air}} = 0.9876 \text{ (sound of velocity)}$$

Test 13480

$$\gamma = 1.398 \qquad \frac{a_{Mix}}{a_{Air}} = 0.9881$$

The pressure time history and the absorption time history for the two tests are shown in Figure 15 through 18. For ideal gas, data were obtained for the conditions before and after shock arrival. The calculated and experimental values are given in Table 1.

Table 1. NO_2 Test Results at EMI.

	TEST 13479		TEST 13480	
	Calculated	Measured	Calculated	Measured
Temperature, T_1	292.5 K		294.0 K	
Shock Mach Number, M_s	1.385		1.366	
Ambient Pressure, P_1 (bar)	1.004		0.998 bar	
Shock Strength	1			
P_{21} (incident) (bar)	2.0709		2.009	
ΔP_2 (reflected)	3.995		3.781	
ΔP_{31}	3.007	3.01	2.775	2.68
Temperature				
T_{21} (Incident)	1.244		1.232	
T_2	363.8 K		362.1 K	
T_{31}	1.512		1.486	
T_3	442.3 K		436.7 K	
NO_2 concentration				
Prior to incident shock, C_1	9.035×10^{-4} mol/l		9.0315×10^{-4} mol/l	
Behind incident shock, C_2	2.194×10^{-3} mol/l		2.104×10^{-3} mol/l	
Behind reflected shock, C_3	3.544×10^{-3} mol/l		3.359×10^{-3} mol/l	
Absorption ratio				
$ln\ (I_1/I_0)$		0.328		0.306
$ln\ (I_2/I_0)$		0.791		0.745
$ln\ (I_3/I_0)$		1.394		1.253

The comparison of the differential pressures Δp_2 and Δp_3 shows a very good agreement between calculated and measured values. The comparison of the laser absorption measurements with the calculated concentrations is also very satisfactory, as can be seen in Figure 19 showing $In(I_1/I_0)$ as a function of NO_2 concentration. Also, in this diagram static values for the absorption as a function of concentration are given which have been obtained by slowly filling up the shock tube with the NO_2 air mixture.

After the above mentioned experiments, the EMI personnel noted extensive corrosion on steel and brass components within the shock tube. This effect was observed even with

an extensive purging of the shock tube. It was postulated that NO_2 gas was absorbed at the shock tube wall and slowly reacted with the air moisture resulting in nitric acid. It was therefore decided that NO_2 could not be used in the shock tube and other species should be used.

3.4 ALTERNATE TECHNIQUES.

3.4.1 Alternate Seed Gas.

During additional searches, Freon 12 was found to be very attractive. Freon 12 is a very strong absorber with a band in the 11 micron region. It should be possible to measure absorption in this region using a grating tunable CO_2 laser. A spectrum for Freon 12 is shown in Figure 20. We could measure on the wing of the band near 10.5 microns (950 cm^{-1}), since the band center absorption will be much too intense. There are a number of CO_2 laser lines in this region. The most appropriate would best be determined by experiment. The laser appropriate for the absorption measurement was found to be the CO_2 laser. No more additional work was performed on this task.

3.4.2 Rayleigh Scattering.

Utilization of Rayleigh scattering imaging for observing instantaneous cross sections of gases and gas mixtures is a promising new development for gas diagnostics. The application of Rayleigh scattering to the observation of mixing phenomena in Freon 12/air or Freon 12/helium at EMI shock tube is briefly discussed. A stratified layer of vapor phase Freon at a pressure of 1 atm is formed at the bottom of the shock tube test section with helium or air above. The aim of this section is to develop a tool which is capable of

measuring a two-dimensional cross section of the gas density coincident with the arrival of a shockwave. Density measurements are desired with an accuracy of approximately 1%.

Possible approaches to obtaining these measurements include visible Rayleigh scattering, ultraviolet Rayleigh scattering (1), and filtered Rayleigh scattering (2). The latter is a new approach to Rayleigh scattering imaging in which the scattered light is passed through a sharp cut-off atomic or molecular filter before being imaged by the camera. By carefully tuning the illuminating laser source frequency, the cut-off filter can eliminate scattering from windows and walls leaving only Rayleigh scattering from the gas to be imaged. This is important since, otherwise, scattering from windows and walls generates background noise which may partially obscure the Rayleigh scattered light. Filtered Rayleigh scattering also has the capability of determining gas velocity since the transmission of the filter is proportional to the Doppler shift and, therefore, the gas velocity. In this section these various approaches with a particular focus on the geometry of the facility and the measurement requirements are discussed. The conclusions may be summarized as follows:

1. Direct Rayleigh scattering in the visible is the most sensible initial approach.
2. Illumination of the flow field with a collimated sheet of light entering through a window in the end wall of the shock tube would be most desirable.
3. Density measurements of approximately 1% with 100 micron spatial resolution can be made with this configuration.
4. By double pulsing the laser, the motion of flow structures can also be observed.
5. With filtered Rayleigh scattering, the potential exists for instantaneous velocity field measurements.

3.4.2.1 Background. Freon 12 has been previously used for Rayleigh scattering measurements in a free jet (3). It is a particularly attractive molecule for Rayleigh scattering since its Rayleigh scattering cross section is 17 times as large as that of nitrogen in the visible portion of the spectrum. From Shardanand and Rao (4), the total scattering cross section at 532 nm is 1.02×10^{-27} cm^2/steradian. This can be compared to nitrogen with a value of 5.86×10^{-28} cm^2/steradian, and helium with a value of 9.0×10^{-30} cm^2/steradian. Note that Freon 12 has a cross section which is 1.134 times as strong as helium. This strong Rayleigh scattering means that when freon/helium mixtures are observed, virtually all the scattering will come from the Freon and the helium will appear dark. In Freon 12/air mixtures, there will be some contribution from the air and that may be important when determining densities to an accuracy of 1%.

Due to the complexity of the spectral analysis, the best approach is to measure the density of Freon 12 by standard Rayleigh scattering rather than filtered Rayleigh scattering. If this is done, great care must be taken to eliminate scattering from windows and walls as well as secondary scattering, since these will significantly complicate the density measurement. With the existing windows on the shock facility (which are not ultraviolet transmitting), the most practical approach is to use a high-power visible laser source. In order to get good mode quality and a short pulse length, a frequency doubled YAG laser operating at 532 nm is an excellent choice. This same laser can be upgraded by the addition of injection-locking to generate narrow line width radiation for filtered Rayleigh scattering work in the future. The good beam quality also allows one to frequency quadruple to 266 nm in order to further enhance the Rayleigh scattering signal and suppress background scattering from windows and walls. The suggested Nd:YAG laser is the Continuum Model NY61 with a rated output energy of 300 mJ at 532 nm. If we assume that of those 300 mJ,

200 mJ enter the test chamber and are focused to a thin sheet, 2 cm high by 260 microns wide (full width between e^{-2} intensity points), then 6.8 x 10^6 photons are scattered into one steradian from each 100 micron x 100 micron resolvable element of the flow. Assuming the collection F number of the optical system is 2, then 0.17 steradians are collected. If the photons fall on an S-20 photocathode with a quantum efficiency of 12%, and the system has another 50% loss due to reflection from optics, etc., the total number of photons collected per 100 x 100 micron resolvable element will be 7 x 10^4. Assuming the detection system is shot noise limited, this leads to a noise of 2.6 x 10^2 photons per resolvable element, or a maximum measurement accuracy of 0.4%. If the frequency of the laser is doubled to 266 nm, then the cross section increases by a factor of 16 to 1.63 x 10^{-25} cm^2/steradian, but the laser output decreases to 50 mJ per pulse. Using the same configuration as before, this gives 9 x 10^4 photons per 100 x 100 micron resolved element. Again, assuming a shot noise limit, this leads to a density measurement accuracy of 0.33%. Background scattering, however, will be decreased so the actual signal-to-noise improvement will be well beyond the factor of 1.2 suggested by the shot noise limit. The problem is that this measurement will require ultraviolet windows on the test section. Any high quality, low fluorescing glass capable of passing light at 266 nm will suffice. Examples include fused silica quartz or Corning 7940 glass.

3.4.2.2 Suppression of scattered light. Great care must be taken to suppress scattered light for all forms of Rayleigh scattering experiments. Background scattering levels should be measured with the tunnel evacuated or filled with pure helium to determine whether they will become a serious problem. It is possible to subtract the background scattering from the signal, but the adds noise and may seriously limit the accuracy of the density measurement.

Also of concern is secondary scattering in the Freon. If the laser sheet can be made to intersect the Freon only in the observation region, this will minimize secondary scattering problems. It will also minimize beam steering effects due to index-of-refraction gradients in the freon. If secondary scattering still remains a problem, it may become necessary to generate a patterned mask so that alternately bright and dark stripes illuminate the sample volume. Secondary scattering can then be removed by subtraction.

3.4.2.3 Proposed experiment. The proposed experiment is to image Rayleigh light scattered from the Freon/Helium or Freon/air interface using a frequency-doubled Nd:YAG laser source and an intensified imaging camera. The laser beam will be expanded to form a light sheet 2 cm high by 300 microns wide. It is expected that a 2 cm high by 2.6 cm wide field-of-view will be observed with an approximately 100 x 100 micron pixel element area. Larger fields-of-view may be observed with correspondingly lower resolution. (Assuming the laser sheet height is expanded to fill the camera field-of-view, and the collection optics stay constant, the number of photons per pixel increases as the square root of the observed area.)

The image collection system may be either a double intensified CCD or CID camera, or possibly a CCD array. The intensified system permits adjustment of the luminous gain as well as a fast shutter capability (1 μsec) to permit operation with room lights on. The intensifier adds noise, reduces resolution, and has a linear range slightly in excess of 2 orders of magnitude. The CCD array, on the other hand, has a much greater linear range, high resolution, and low background noise levels, but cannot be electronically shuttered and does not have a variable gain. It is also not UV sensitive. In either case, non-blooming devices must be used to eliminate streaking when randomly occurring particles are imaged

in the flow field. The images are downloaded to videotape and digitized by an 8 bit or greater frame grabbing digitizer.

The capabilities of this system can be significantly enhanced by purchasing a double Q-switch option from Continuum Corporation. This device allows two Q-switch pulses to emerge from the laser with a separation variable between 20 and 200 μsec. This will produce a double image or, if two cameras are used, two sequential images, which can be used to measure the motion of observable structure in the field-of-view.

A system upgrade may be considered if background scattering cannot be sufficiently suppressed. This upgrade would include the addition of a frequency quadrupling crystal to operate at 266 nm. As previously mentioned, this would require ultraviolet windows and would substantially reduce background scattering. A fourth harmonic system such as this is currently being used to image nitrogen and air in a blow down, Mach 3, tunnel at Princeton (8). A second upgrade would be to incorporate an injection locker with the Nd:YAG laser system in order to permit filtered Rayleigh scattering for flow field and density measurements. This upgrade would eliminate background scattering from windows and walls and generate high contrast images. The interpretation of the intensity of these images would require at lease two camera systems observing through slightly different cut-off filters. The research work for this capability is in its early stages at Princeton. In its present form, filtered Rayleigh scattering would be most appropriate for observing flow features including shock locations and shock generated structures. Quantitative filtered Rayleigh scattering measurements have not yet been done for single pulsed images such as this.

The required equipment and price for the above proposed experiment are listed in Appendix B.

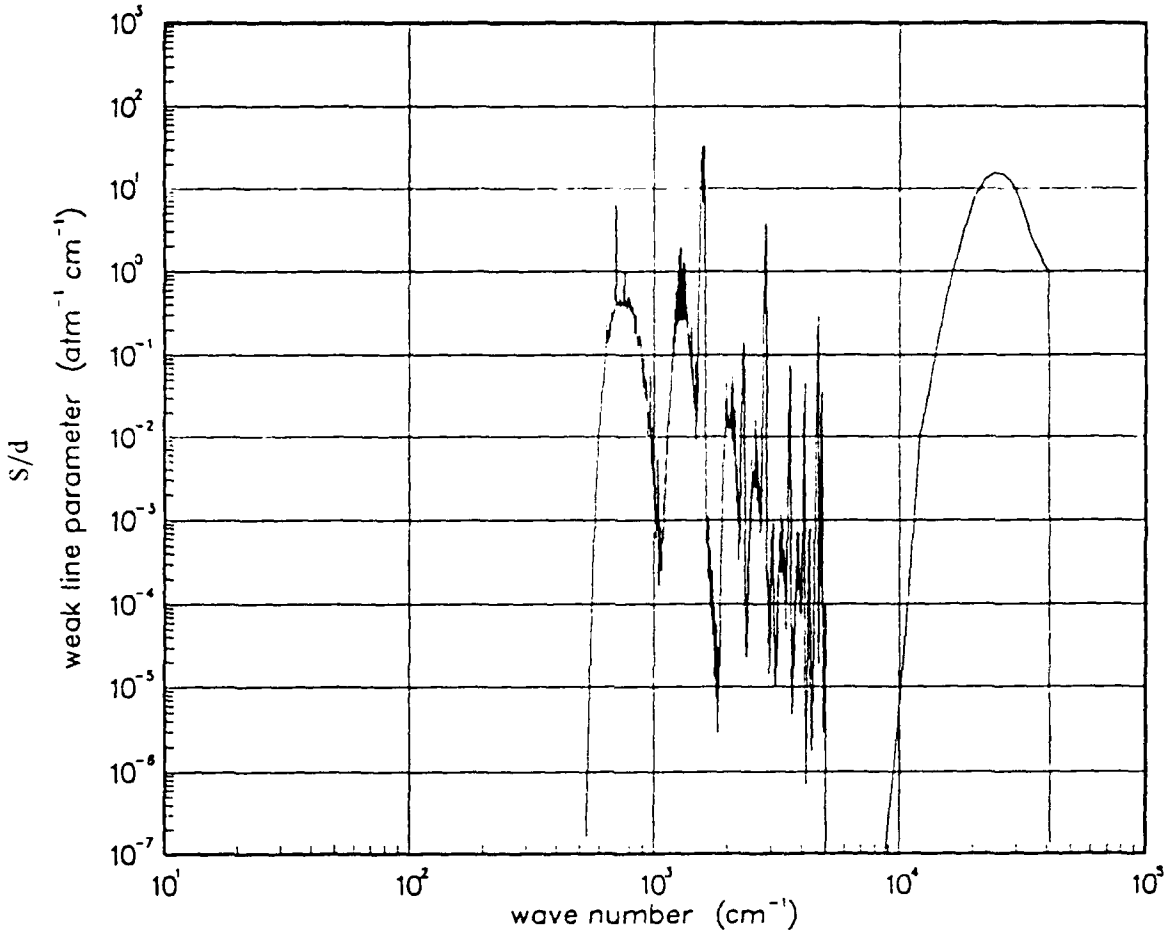

Figure 4. Weak-line parameter for NO_2 at 300°K

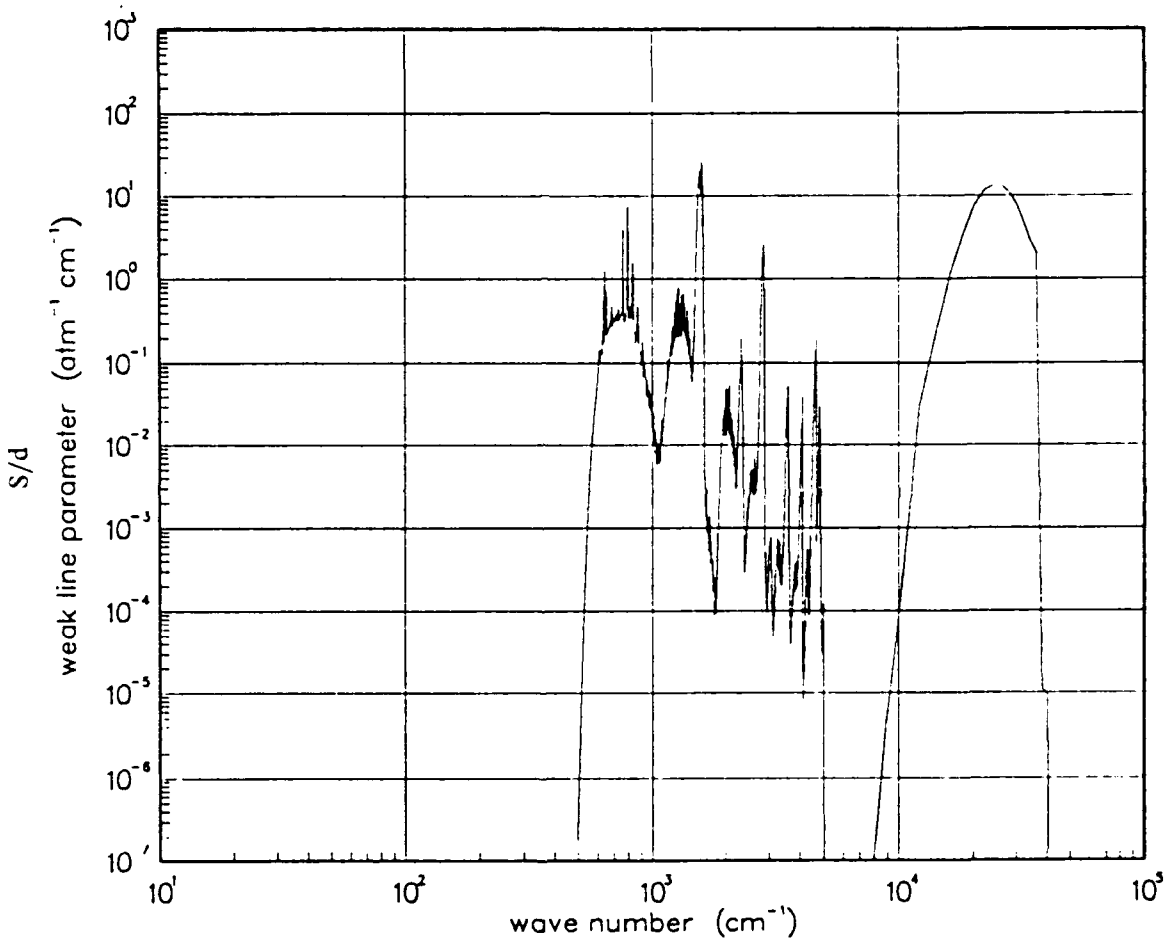

Figure 5. Weak-line parameter for NO_2 at 500°K.

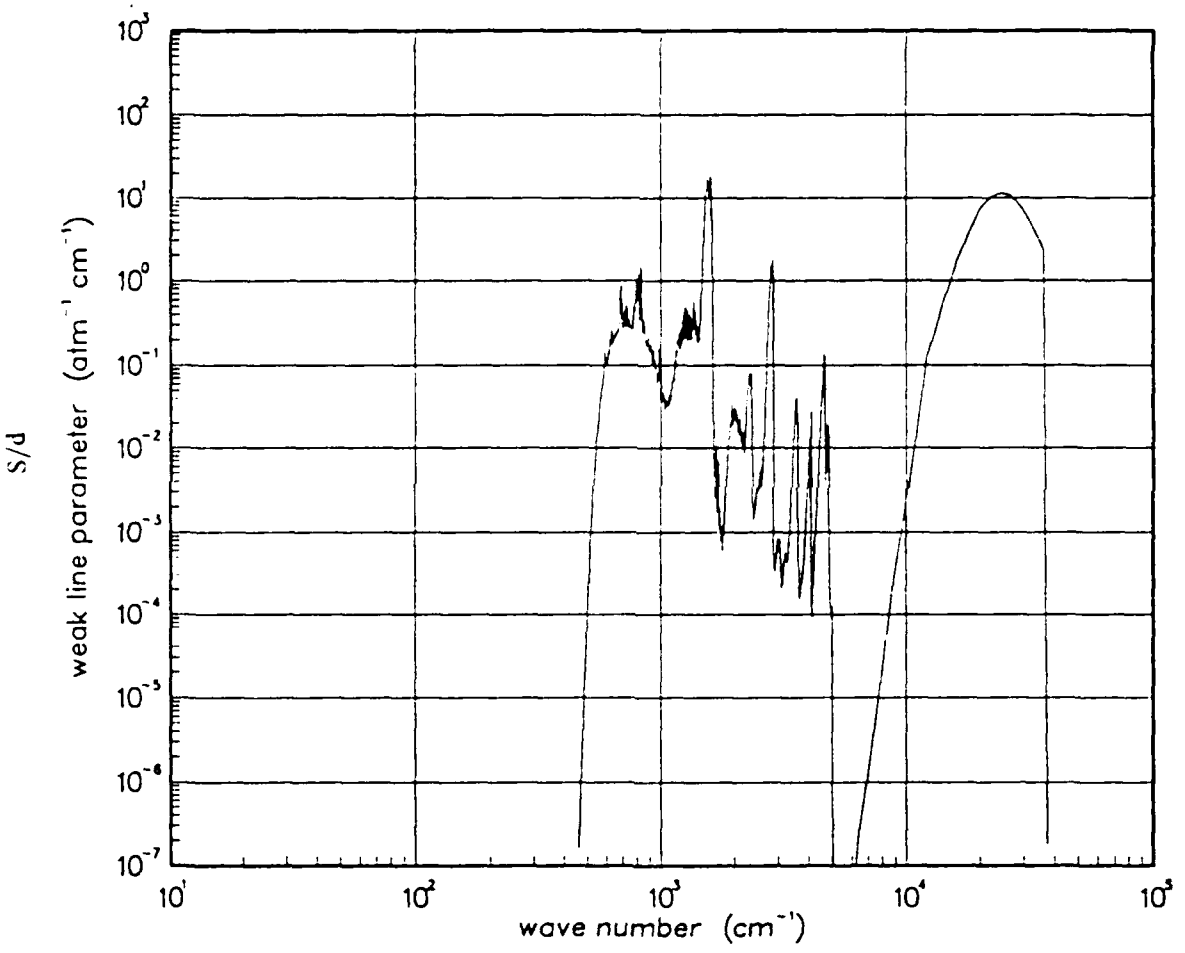

Figure 6. Weak-line parameter for NO_2 at 750°K.

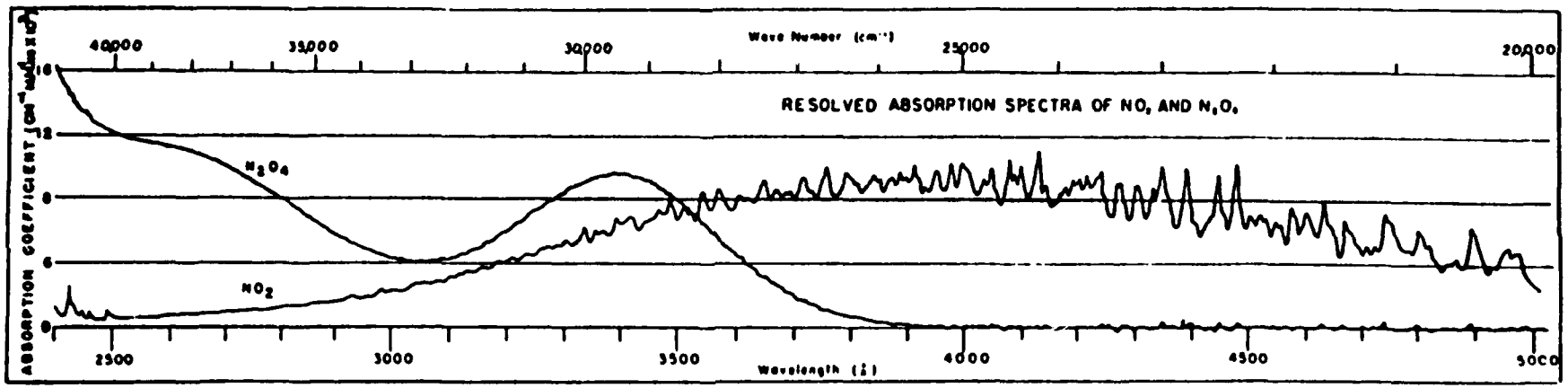

Figure 7. Absorption coefficient of NO_2 and N_2O_4 vs wavelength and wavenumber.

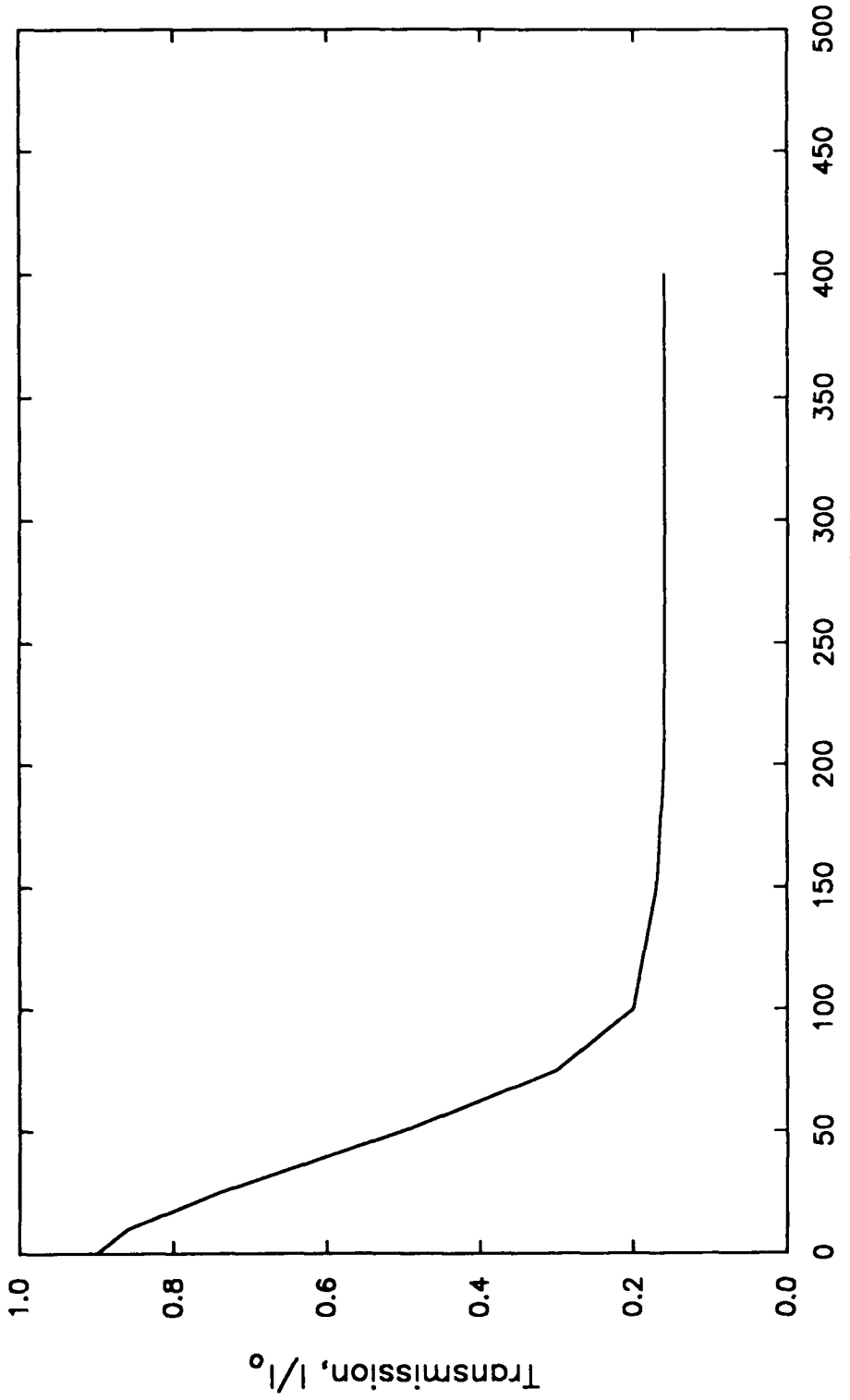

Figure 8. Transmission of light through 10 cm test cell containing 3% nitric dioxide in air.

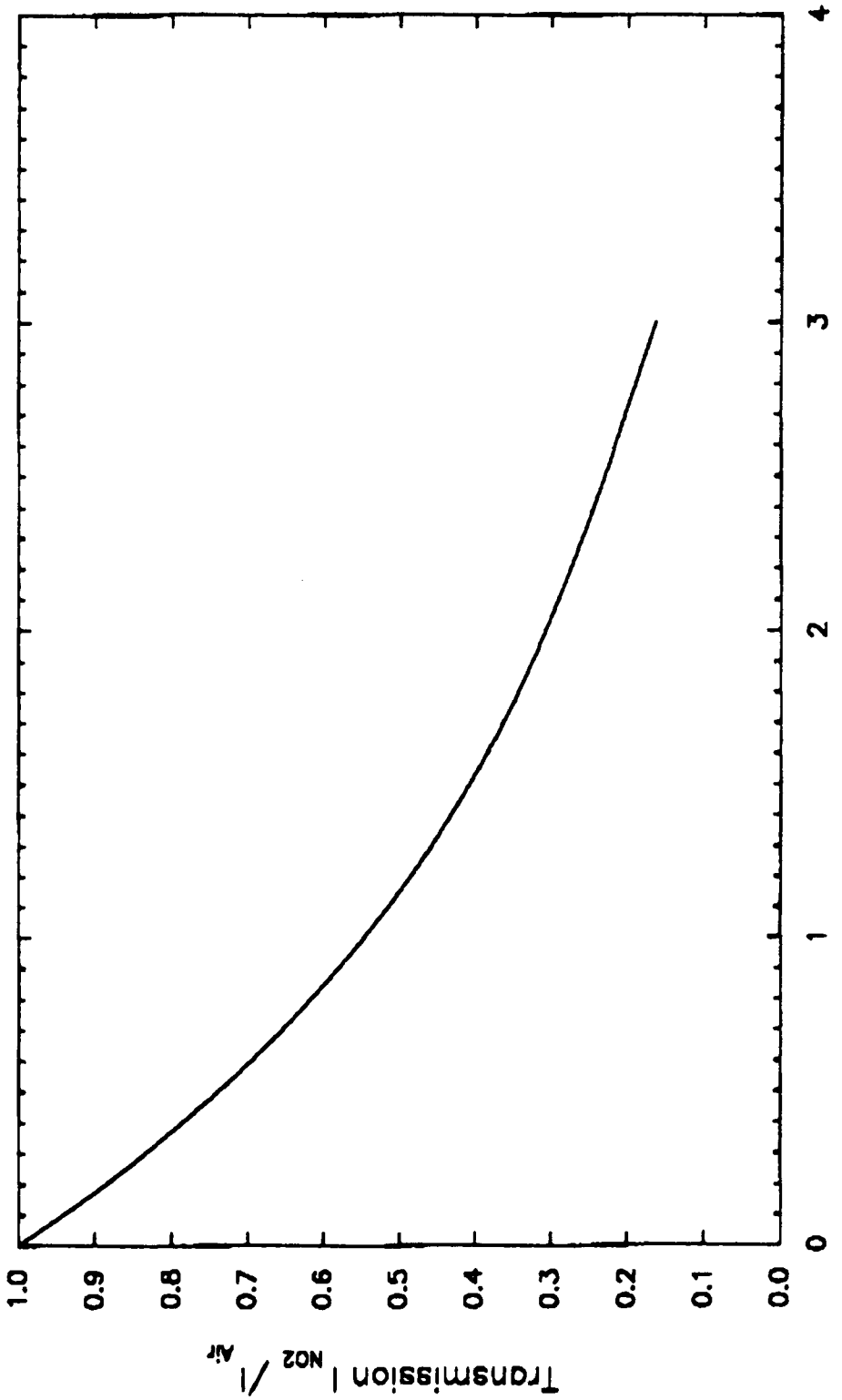

Figure 9. Transmission of light through shock tube behind normal shock at M=2.0.

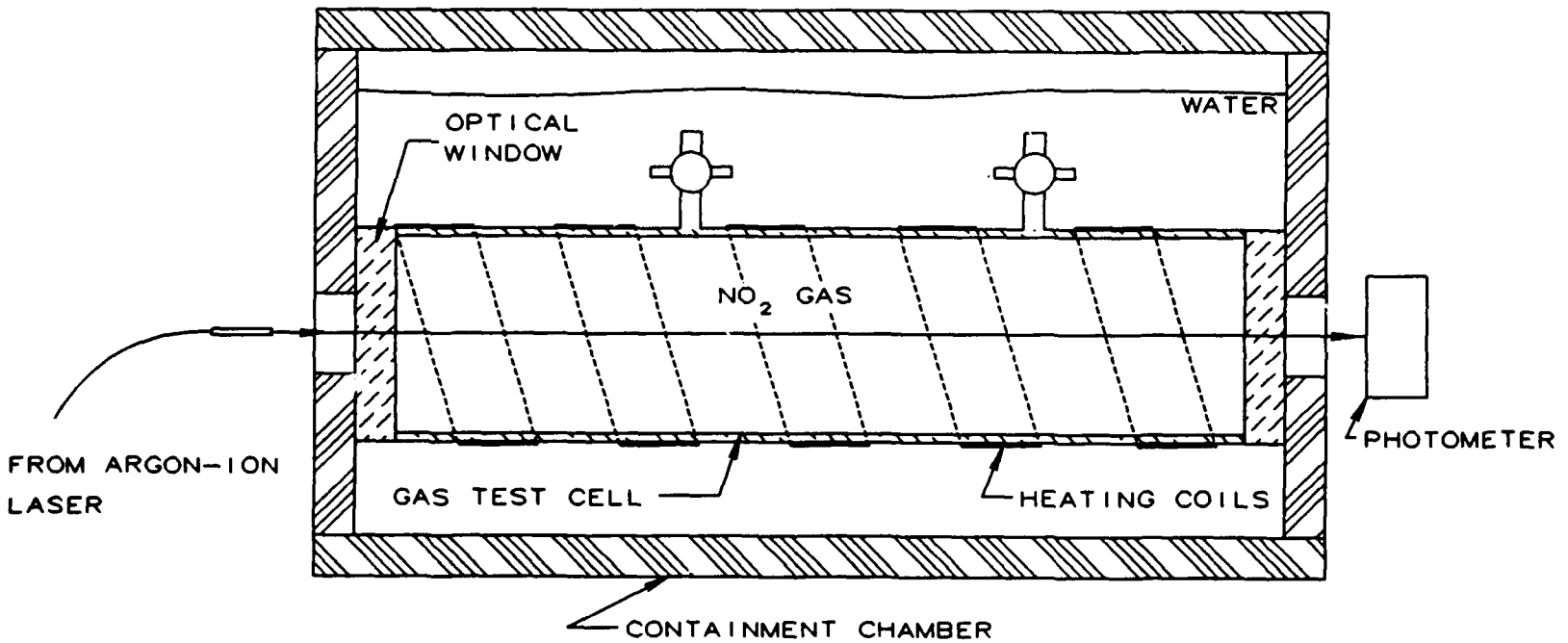

Figure 10. Schematic of NO_2 absorption test setup.

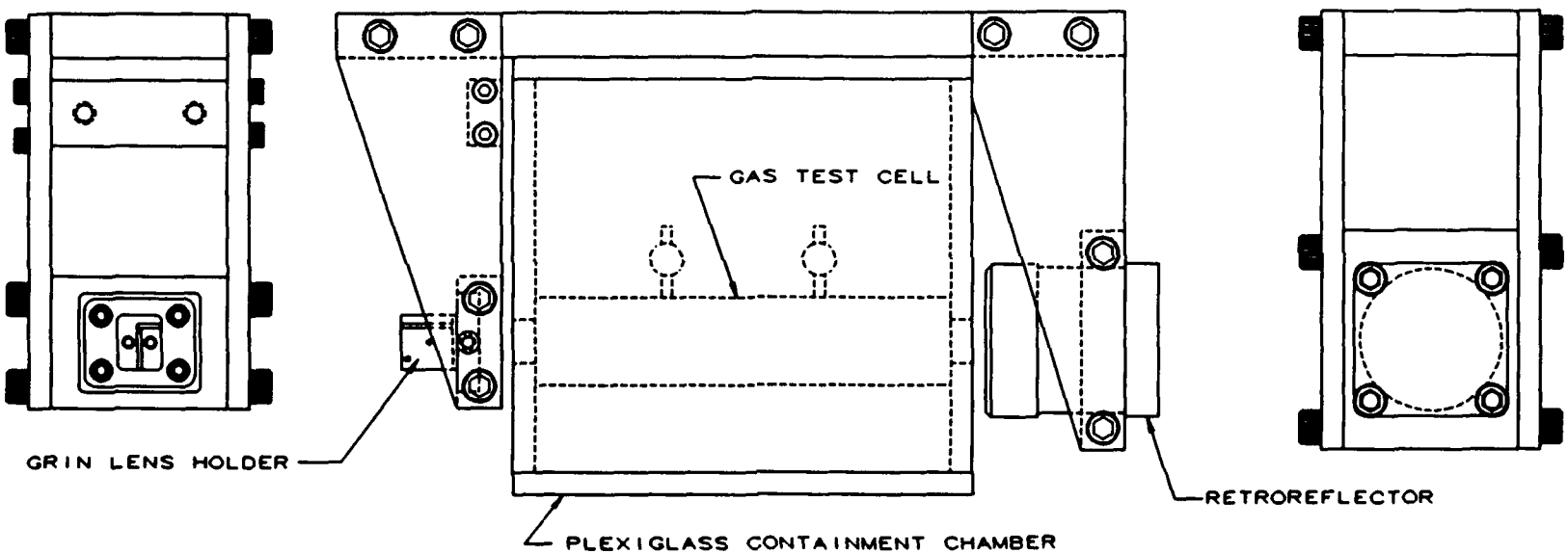

Figure 11. Schematic of double pass NO_2 absorption measurement apparatus.

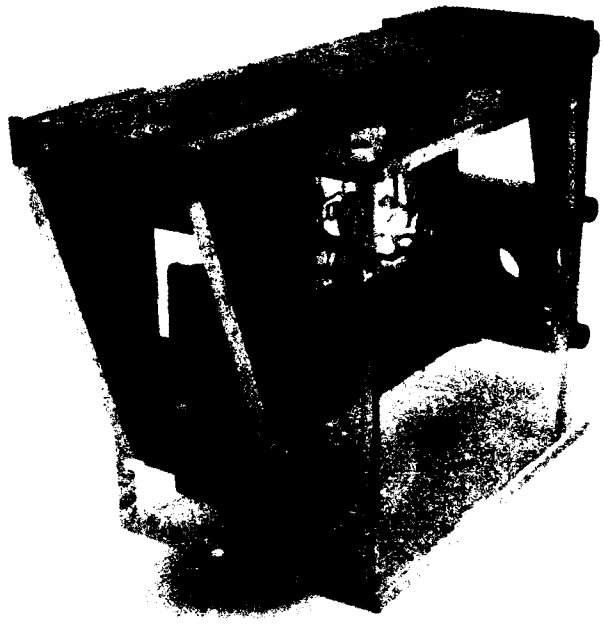

Figure 12. Photograph of double pass NO_2 absorption apparatus.

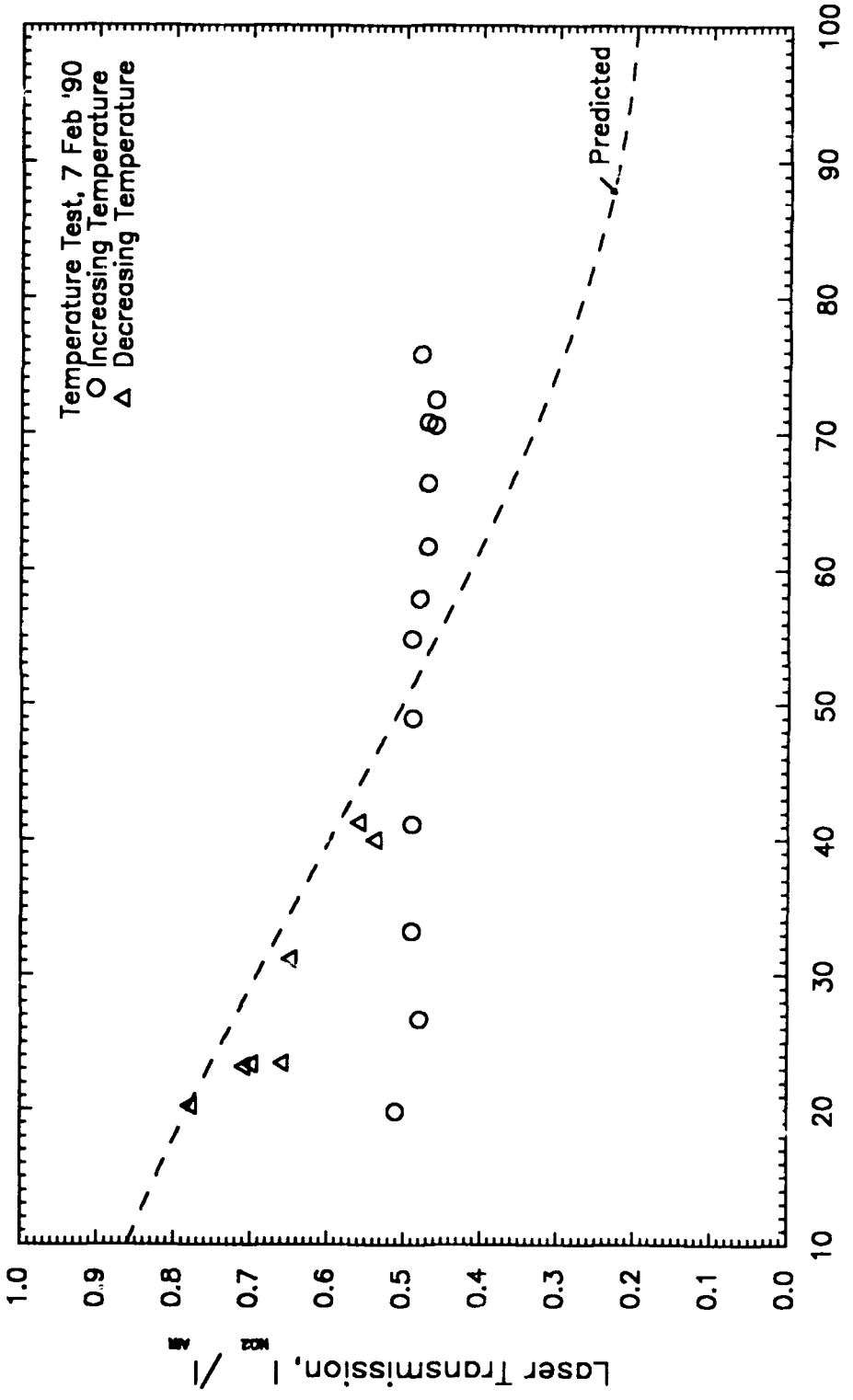

Figure 13. Laser transmission vs water bath temperature.

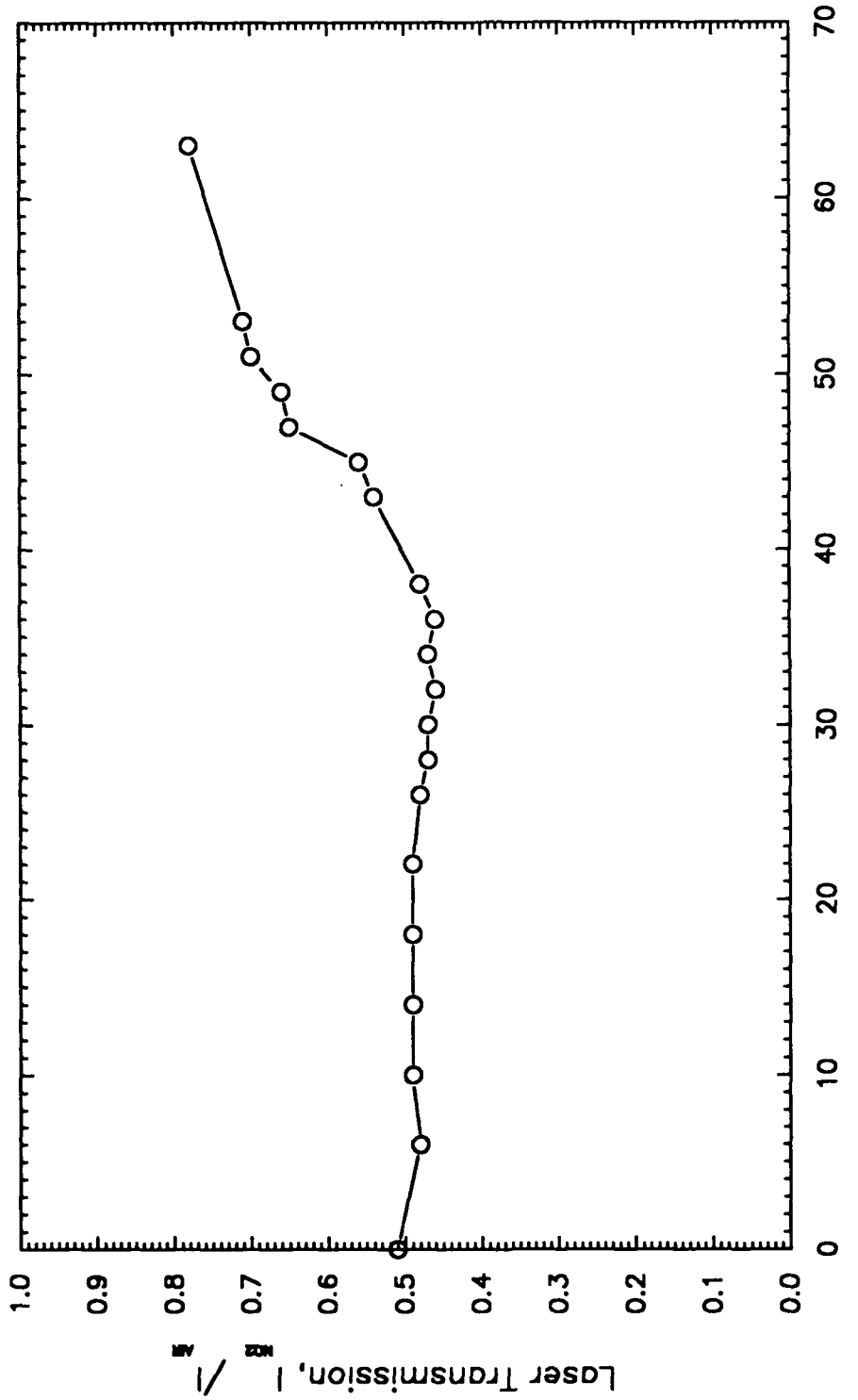

Figure 14. Laser transmission versus time.

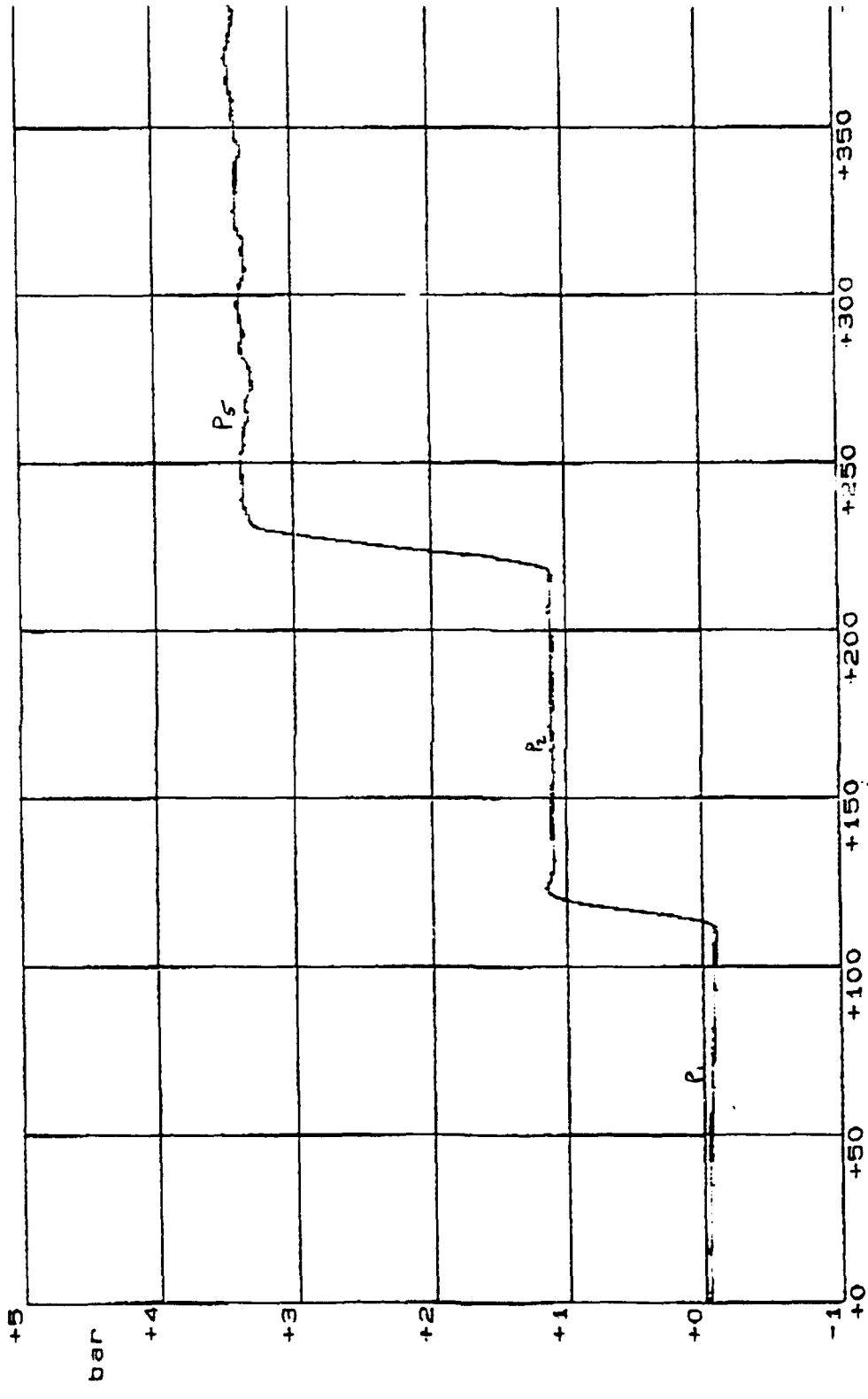

Figure 15. Pressure trace for run 13479.

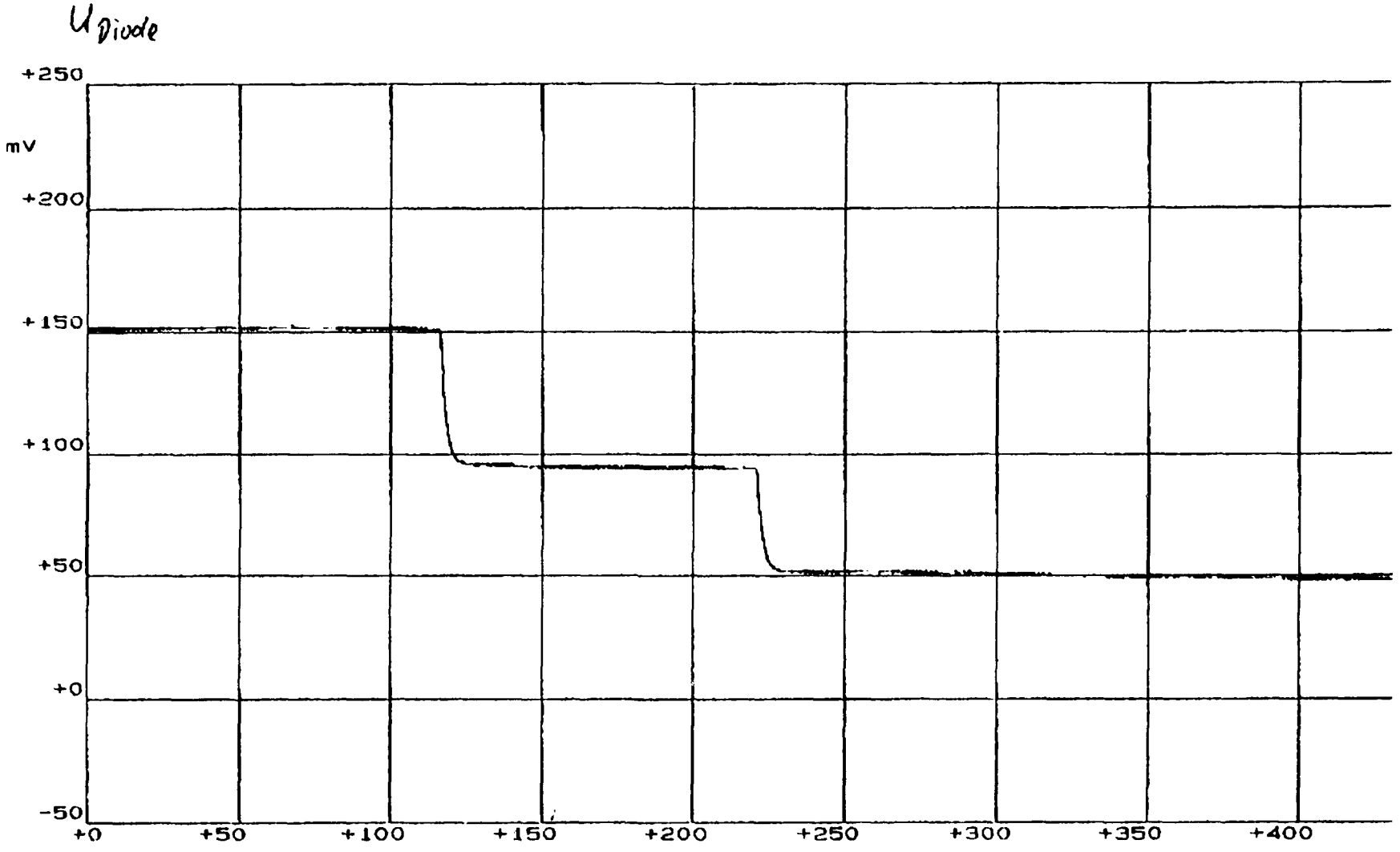

Figure 16. Laser attenuation time history for run 13479.

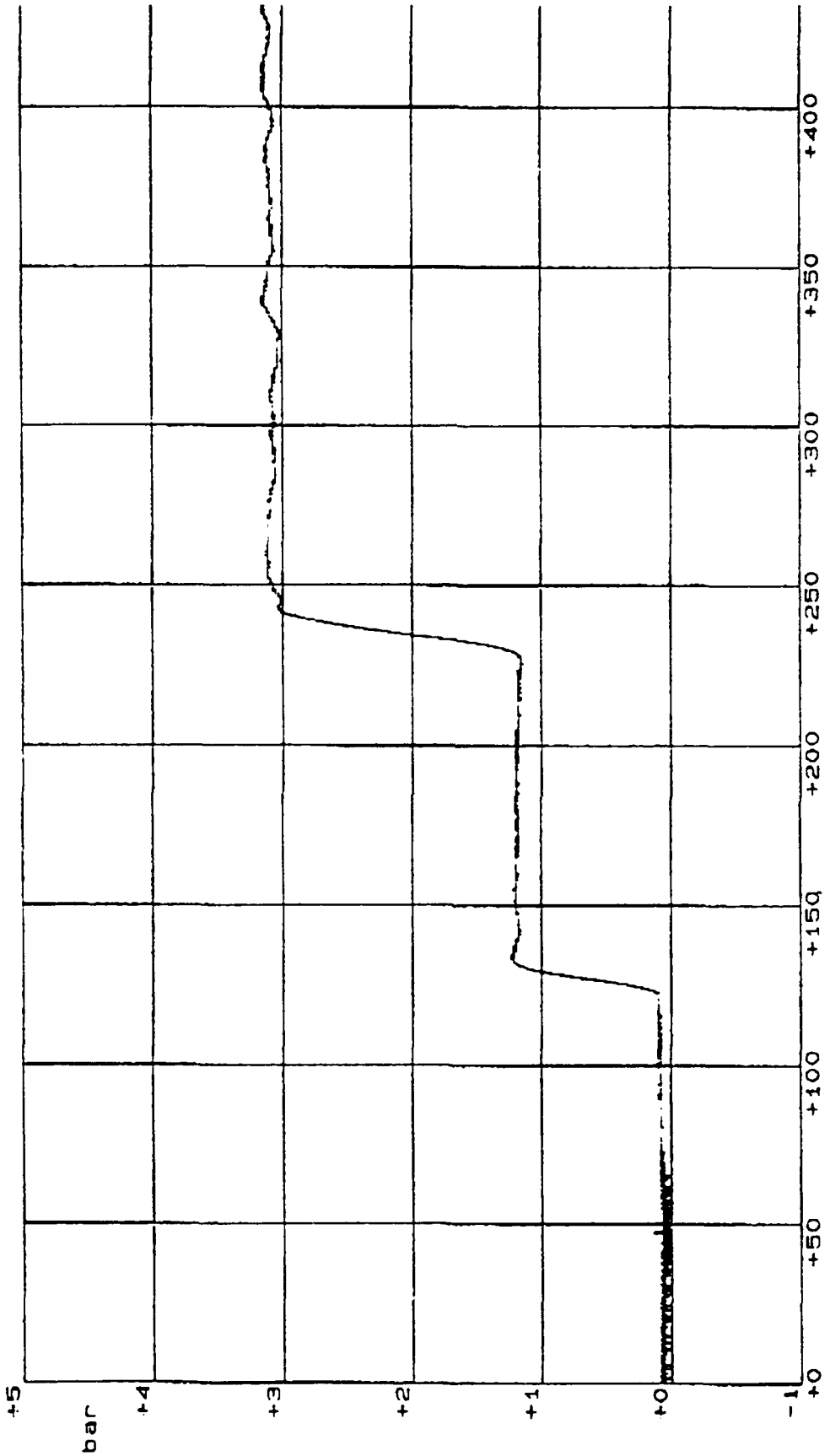

Figure 17. Pressure trace for run 13480.

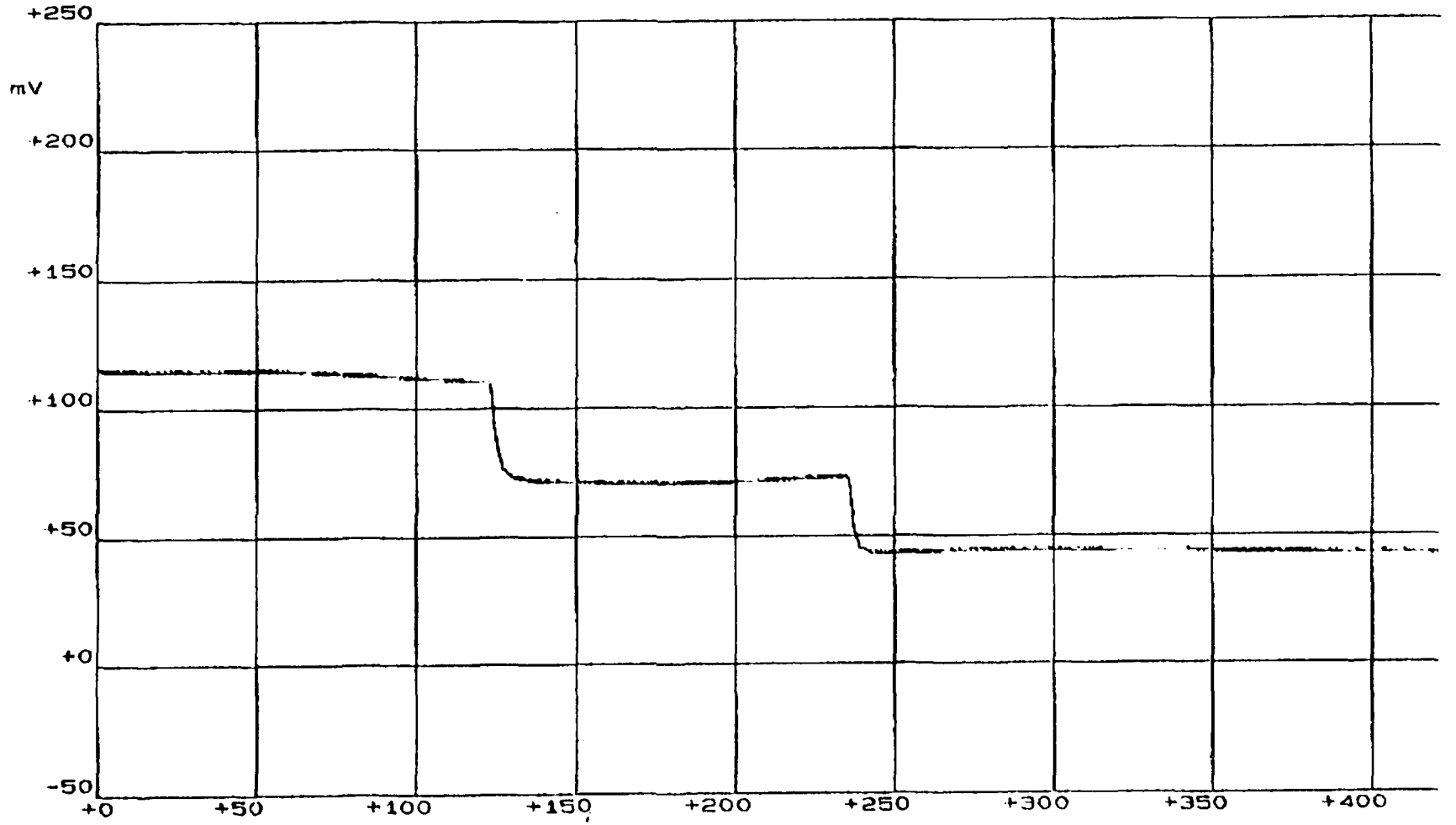

Figure 18. Laser attenuation time history for run 13480.

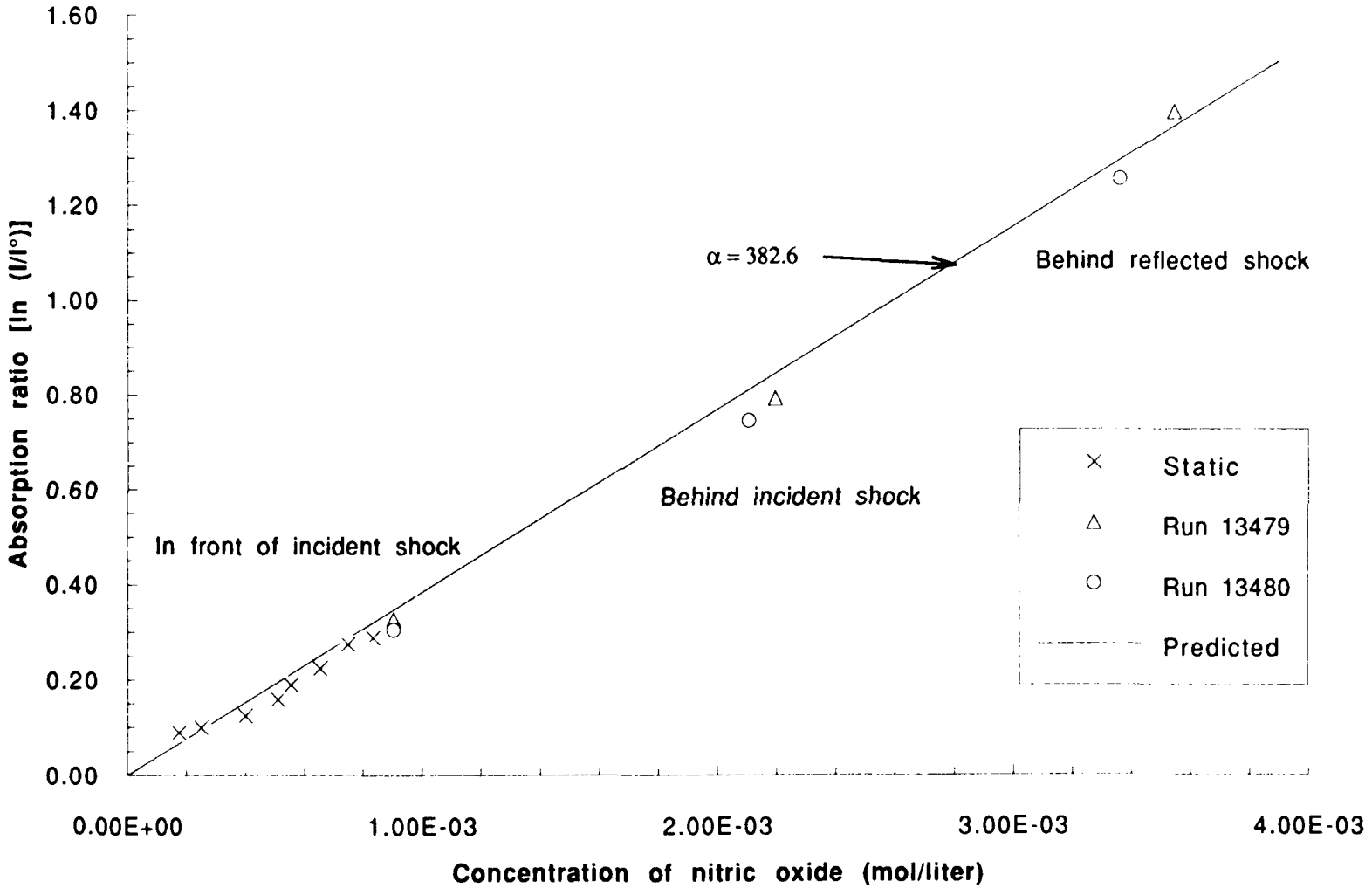

Figure 19. Laser attenuation versus NO_2 concentration.

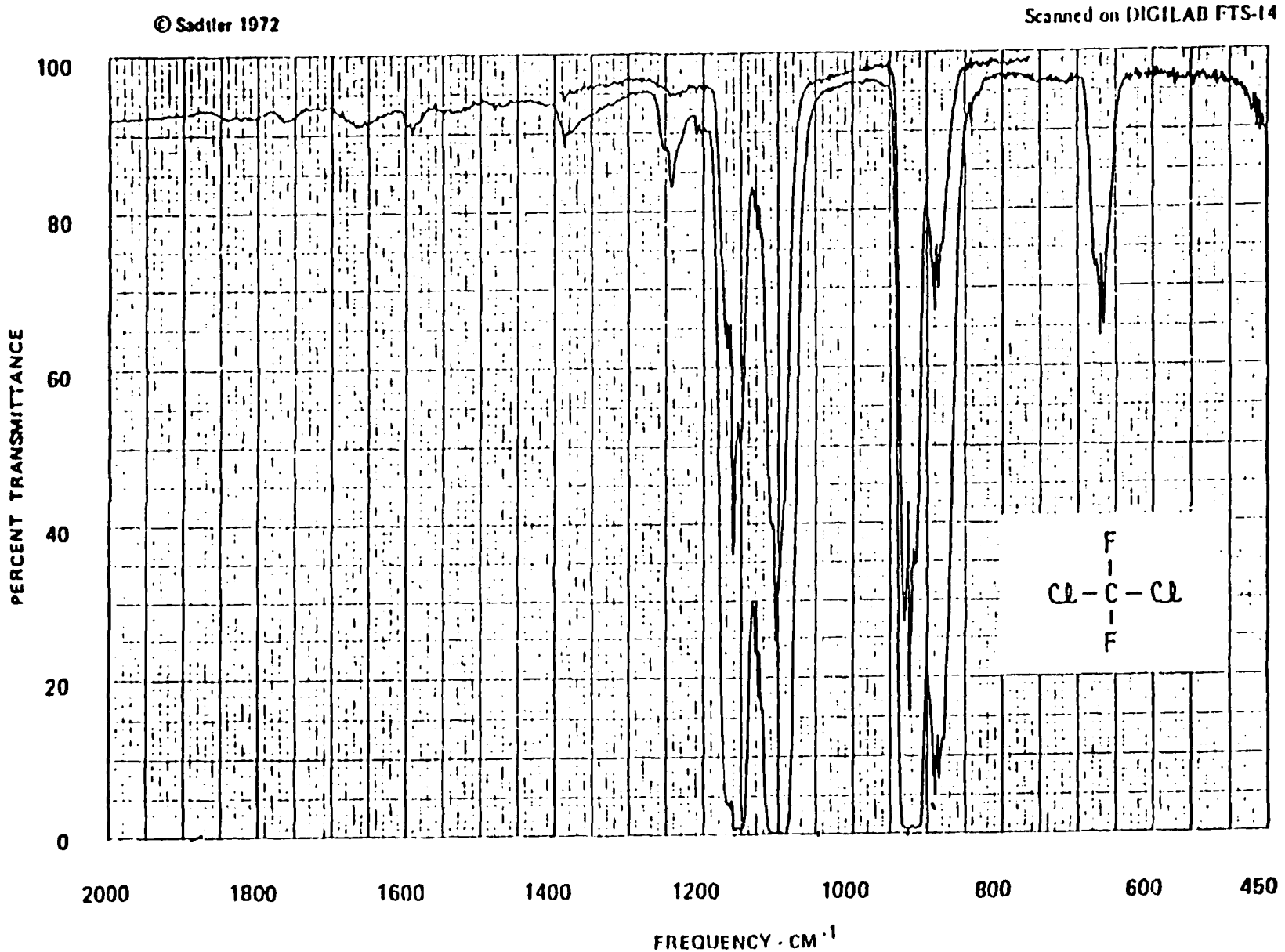

Figure 20. Transmission versus frequency for Freon 12.

SECTION 4

VELOCITY MEASUREMENT

4.1 LASER DOPPLER VELOCIMETER.

A four location simultaneous Laser Doppler velocimeter for EMI was designed. The velocities of interest ranged from 100 m/s to 1000 m/s.

Initially two types of LDV were considered for measuring the velocity in the shock tube. One was based on a reference beam to produce fringes at the detector (reference beam LDV) and the other on interference of two beams at the point of measurement to produce fringes (dual beam LDV). Schematics of the two methods are shown in Figures 21 and 22. A number of single location prototypes were developed and tested. Based on a number of considerations, with ease of alignment and operation being a deciding factor, a design based on the dual beam concept was chosen.

To confirm the theoretical estimation of the signal-to-noise reference beam technique, a single point system was fabricated and tested at EMI. This single point dual beam LDV was installed and tested at EMI. A typical signal is shown in Figure 23. The design of the final system is discussed in the following section.

4.2 LDV PROBE DESIGN.

Utilizing the C-section support fabricated to hold the transmitting and receiving lenses of the single point reference beam LDV, two separate housings for the transmitting and receiving optics were designed. An assembly drawing of these housings attached to the C-section support is shown in Figure 24. To obtain four probe volumes from a single source, a series of beam splitters were designed and fabricated. A schematic of the optical

layout for the transmitter of the four point LDV probe is shown in Figure 25. With a fringe spacing of 10 microns in conjunction with the 100 MHz transient recorders, the dynamic range for this probe is 30 to 500 m/s. Photographs of the installed probe are shown in Figures 26 to 28. For a faster measurement range either 200 MHz digitizers will have to be used making the dynamic range 30 to 1000 m/s, or electronic down mixing to reduce the frequency will be necessary making the dynamic range 500 to 1000 m/s. These options were not explored further during the present program.

4.3 PRELIMINARY TESTS AT ERNST MACH INSTITUTE.

The probe was installed at EMI and measurements listed in Table 2. were performed. Two flow conditions were used: 1) clean flow over a smooth floor and 2) clean flow over rough surface (outdoor carpet). Figure 29 shows a comparison of typical pressure traces for the two conditions. Figure 30 shows a typical velocity time history and a corresponding pressure for the rough floor condition. A velocity run for the smooth floor condition is shown in Figure 31. The degree of repeatability between two different runs at the same height for the smooth floor is demonstrated in Figure 32. Averaged velocities at various heights for the smooth wall condition are shown in Figure 33. The smooth wall boundary layer thickness was less than 2 mm during the test time. Having this small of a boundary layer thickness made it impractical to measure the velocity profile with sufficient spatial resolution.

Figure 34 shows the rough surface (carpet like synthetic material) that was installed as the ceiling of the shock tube. Measurements were made with the three probes placed in the centerline of the shock tube to find the free stream velocity. The average velocity plots for these three points are shown in Figure 35. It shows that the average velocity increased

with time. This behavior was not observed with the smooth floor data. Averaged velocities for the various heights measured are plotted in Figure 36. From the data obtained for the carpet flow it was possible to obtain the RMS velocity. Typical results for three different heights are presented in Figure 37.

For the carpet case, since the location where the velocity was zero was unknown, a scheme was implemented to approximate its location. The normalized velocities at a given time were plotted versus the initial measured heights above the carpet and with the addition of 2 mm and 4 mm to the heights on a log-log scale. These data were extrapolated to find the boundary layer height, δ. Assuming a power law curve fit to the data,

$$\frac{U}{U_o} = (\frac{y}{\delta})^n$$

results indicated that the initial heights above the carpet were off by 4 mm. This correction was made to the heights and the normalized velocity profile was obtained for the carpet flow and is presented in Figure 38. The coefficient n was found to be 0.59 ± 0.02. Comparison of this data to other flows is presented in Figure 39. This comparison shows that the flow over the carpet is similar to dusty flow conditions.

Table 2. LDV measurements made at EMI.

EMI Run #	File Name		Height Above Floor (mm)	P_2/P_1	Floor Condition
3626	May 8A	1.SIG	17.0	2.7	Smooth
		2.SIG	22.5		
		3.SIG	28.0		
		4.SIG	33.5		
3627	May 9A	1.SIG	1.7	2.6	Smooth
		2.SIG	6.9		
		3.SIG	12.6		
		4.SIG	17.9		
3628	May 9B	1.SIG	1.7	2.7	Smooth
		2.SIG	6.9		
		3.SIG	12.6		
		4.SIG	17.9		
3629	May 9C	1.SIG	1.7	2.8	Smooth
		2.SIG	6.9		
		3.SIG	12.6		
		4.SIG	17.9		
3632	May 10C	2.SIG	0.4	2.8	Smooth
		3.SIG	5.9		
		4.SIG	11.4		
3633	May 10D	2.SIG	0.4	2.7	Smooth
		3.SIG	5.9		
		4.SIG	11.4		
3634	May 10E	2.SIG	0.9	2.6	Smooth
		3.SIG	5.9		
		4.SIG	11.4		
3635	May 10F	2.SIG	0.4	2.9	Smooth
		3.SIG	5.9		
		4.SIG	11.4		
3636	May 10G	2.SIG	0.9	2.7	Smooth
		3.SIG			
		4.SIG	11.9		
3637	May 10H	2.SIG	0.9	2.7	Smooth
		3.SIG	6.4		
		4.SIG	11.9		
3638	May 10I	2.SIG	1.9	2.7	Smooth
		3.SIG	7.4		
		4.SIG	12.9		

Table 2. LDV measurements made at EMI (continued).

3641	May 14A 1.SIG	1.0	2.8	Sand Paper
	2.SIG	6.5		
	3.SIG	12.0		
	4.SIG	17.5		
3643	May 16A 1.SIG	3.0	2.6	Rough (Carpet)
	2.SIG	8.5		
	3.SIG	17.0		
	4.SIG	19.5		
3644	May 16B 2.SIG	2.0	2.6	Rough
	3.SIG	7.5		
	4.SIG	13.0		
3645	May 16C 2.SIG	2.0	N/A	Rough
	3.SIG	7.5		
	4.SIG	13.0		
3646	May 16D 2.SIG	1.0	2.7	Rough
	3.SIG	6.5		
	4.SIG	12.0		
3647	May 16E 2.SIG	1.0	2.7	Rough
	3.SIG	6.5		
	4.SIG	12.0		
3648	May 16F 2.SIG	3.0	2.7	Rough
	3.SIG	8.5		
	4.SIG	14.0		
3649	May 16G 2.SIG	3.0	2.7	Rough
	3.SIG	8.5		
	4.SIG	14.0		
3650	May 16H 2.SIG	4.0	2.6	Rough
	3.SIG	9.5		
	4.SIG	15.0		
3651	May 16I 2.SIG	4.0	2.6	Rough
	3.SIG	9.5		
	4.SIG	15.0		
3652	May 16J 2.SIG	2.0	2.6	Rough
	3.SIG	7.5		
	4.SIG	13.0		
3653	May 16K 2.SIG	42.0	N/A	Rough
	3.SIG	47.5		
	4.SIG	53.0		
3654	May 16L 2.SIG	42.0	N/A	Rough
	3.SIG	47.5		
	4.SIG	53.0		

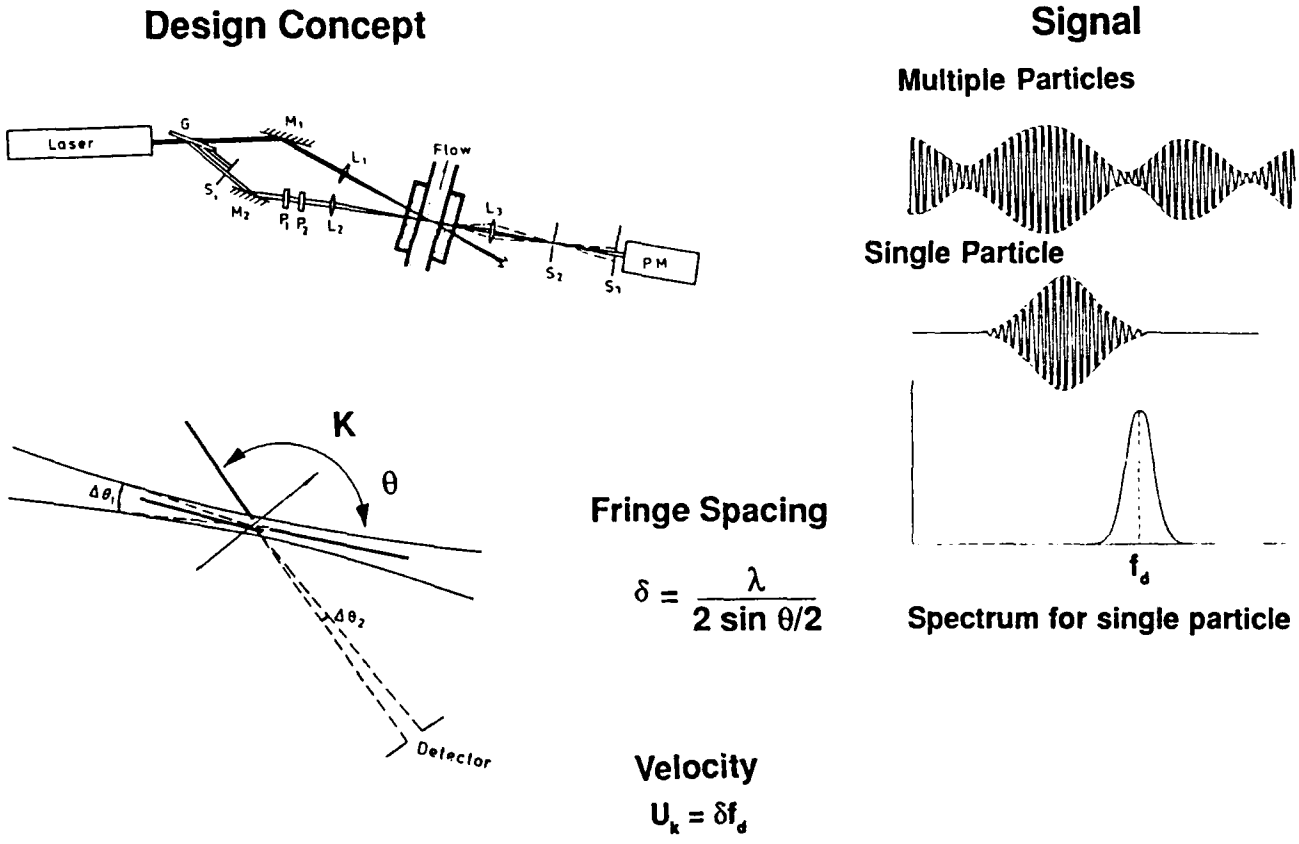

Figure 21. Reference beam LDV principle of operation.

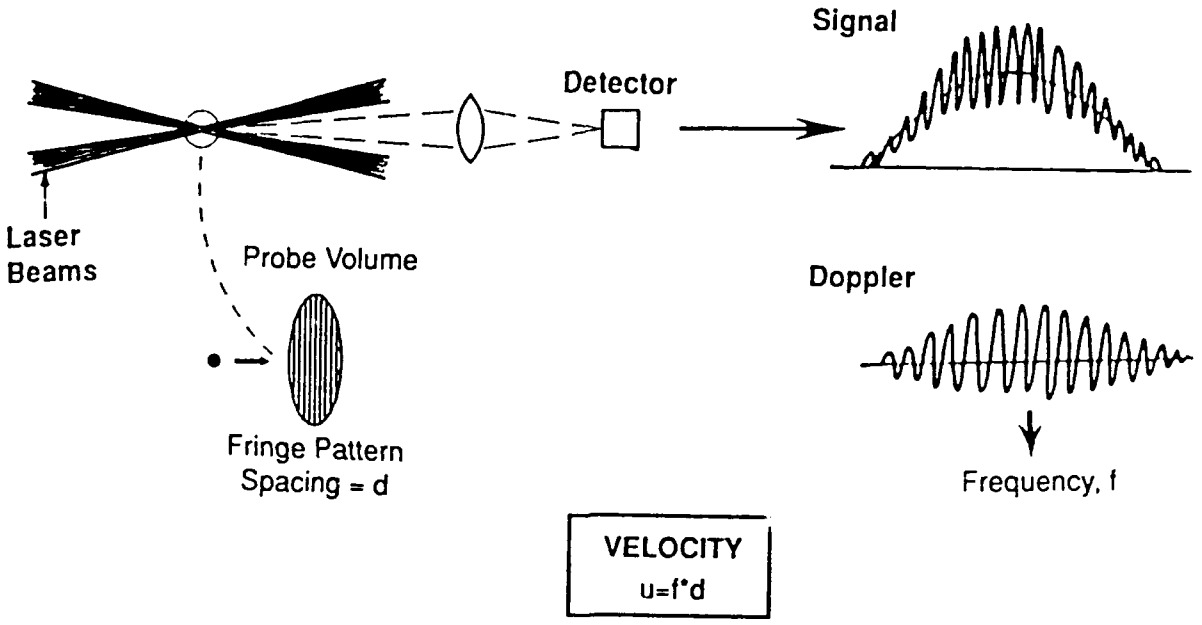

Figure 22. Dual Beam LDV principle of operation.

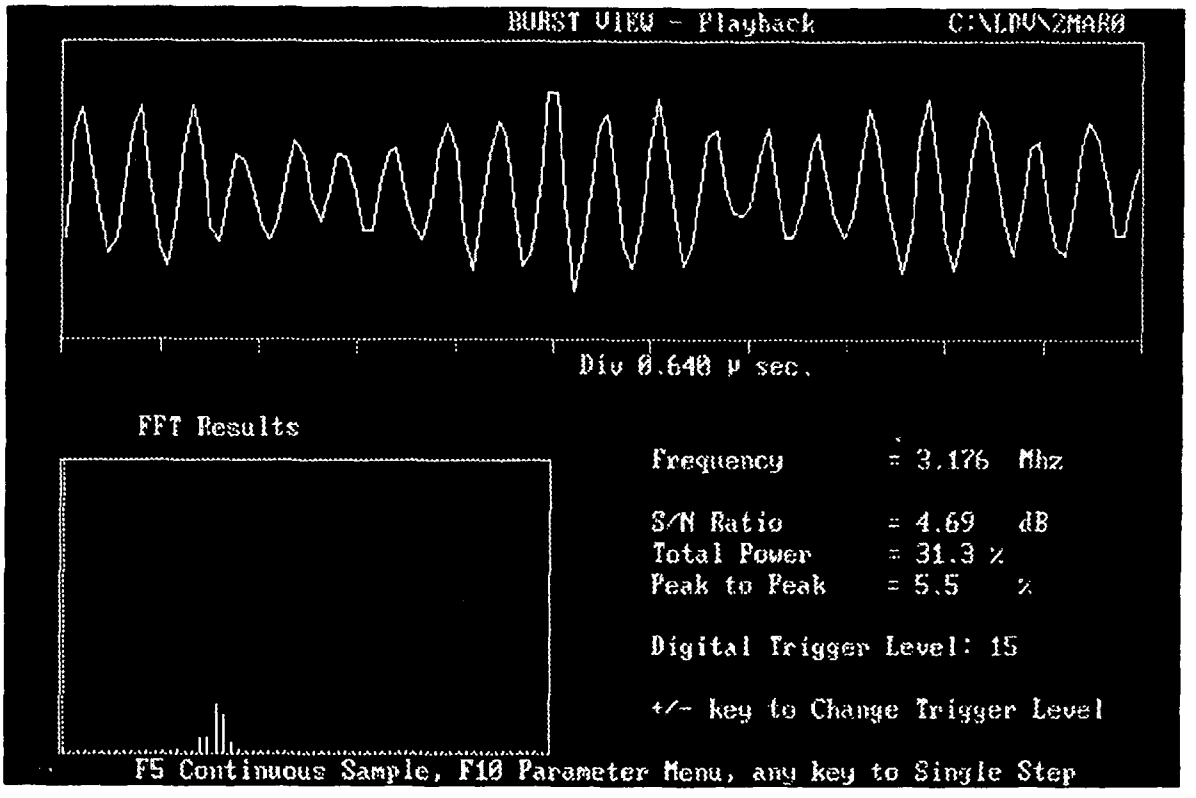

Figure 23. Sample burst and FFT from a tracer particle for single point LDV.

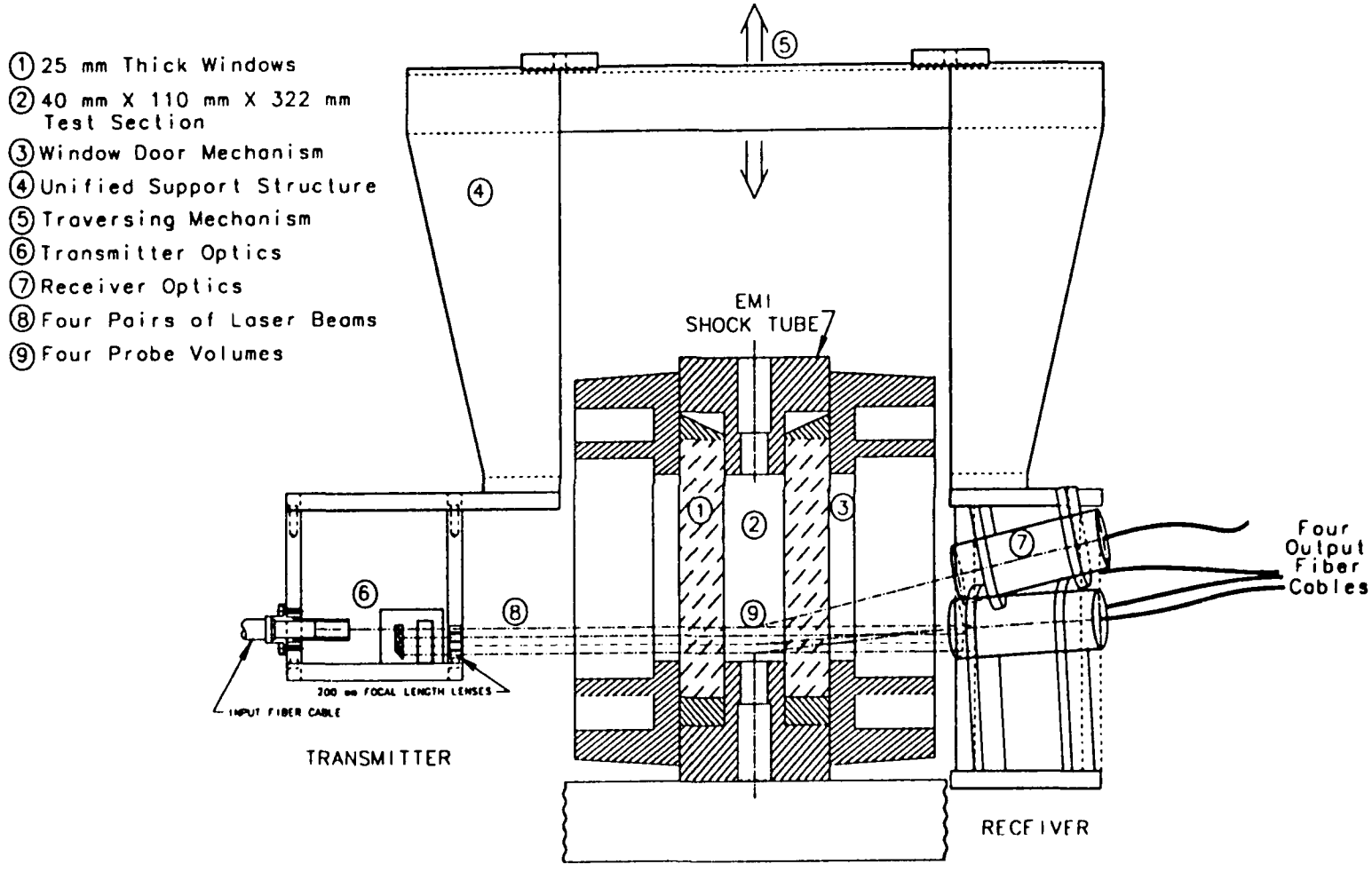

Figure 24. Schematic of four location LDV system at EMI.

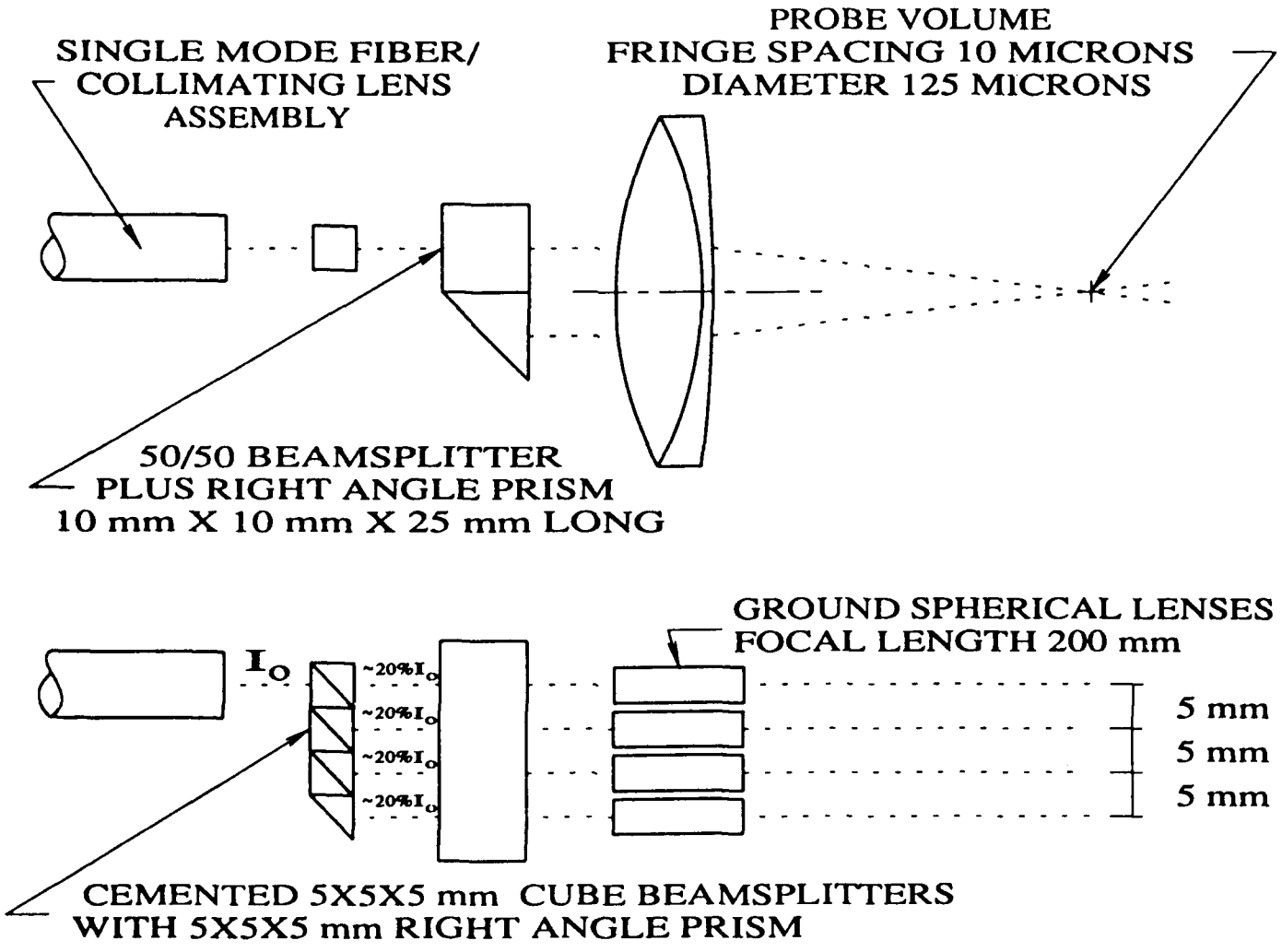

Figure 25. Optical schematic of 4 position LDV for EMI.

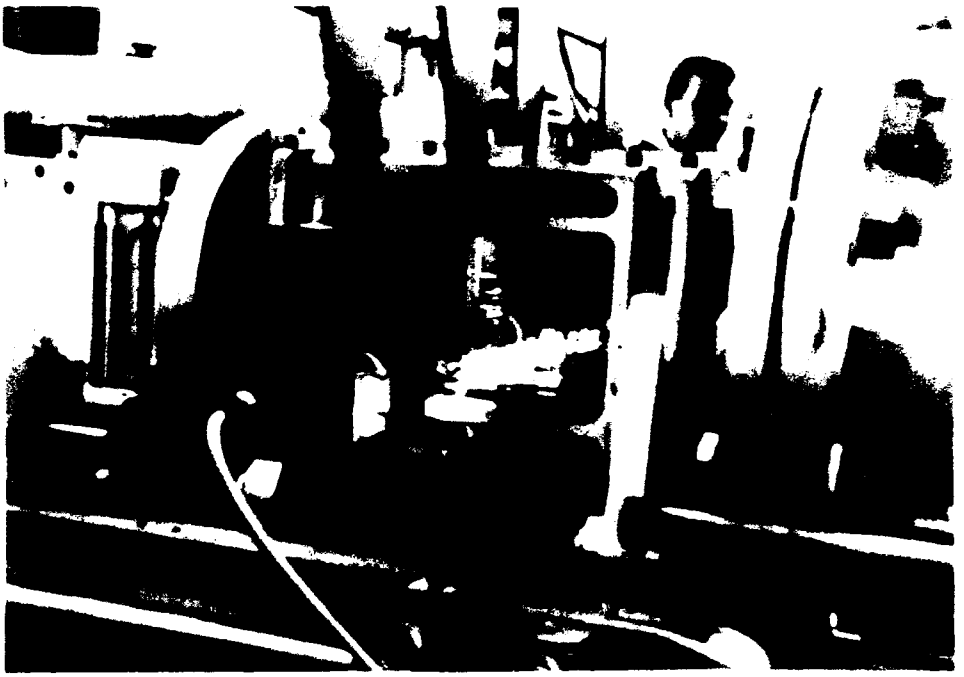

Figure 26. Photograph of LDV system installed at EMI.

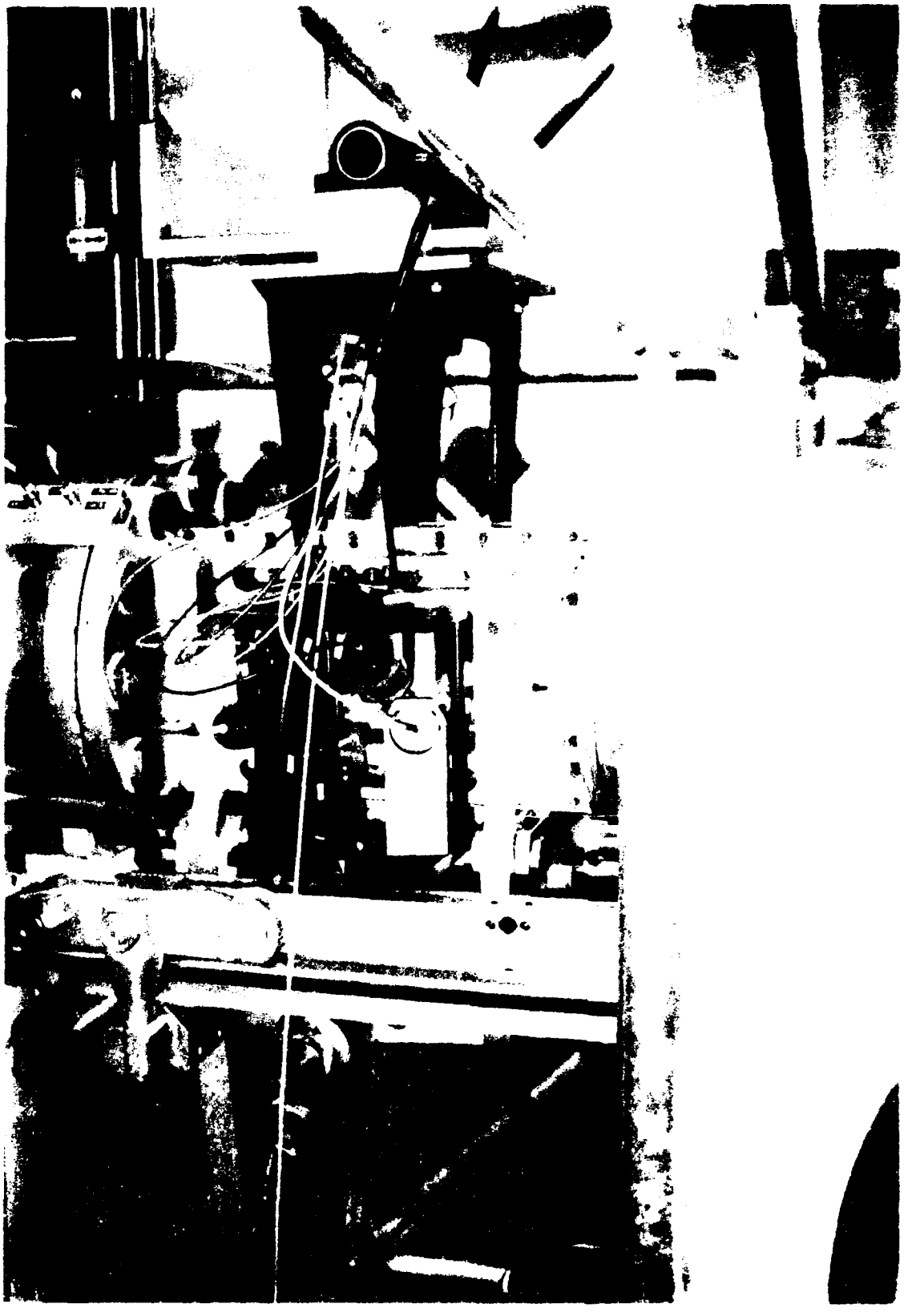

Figure 27. Photograph of probe's transmitting optics.

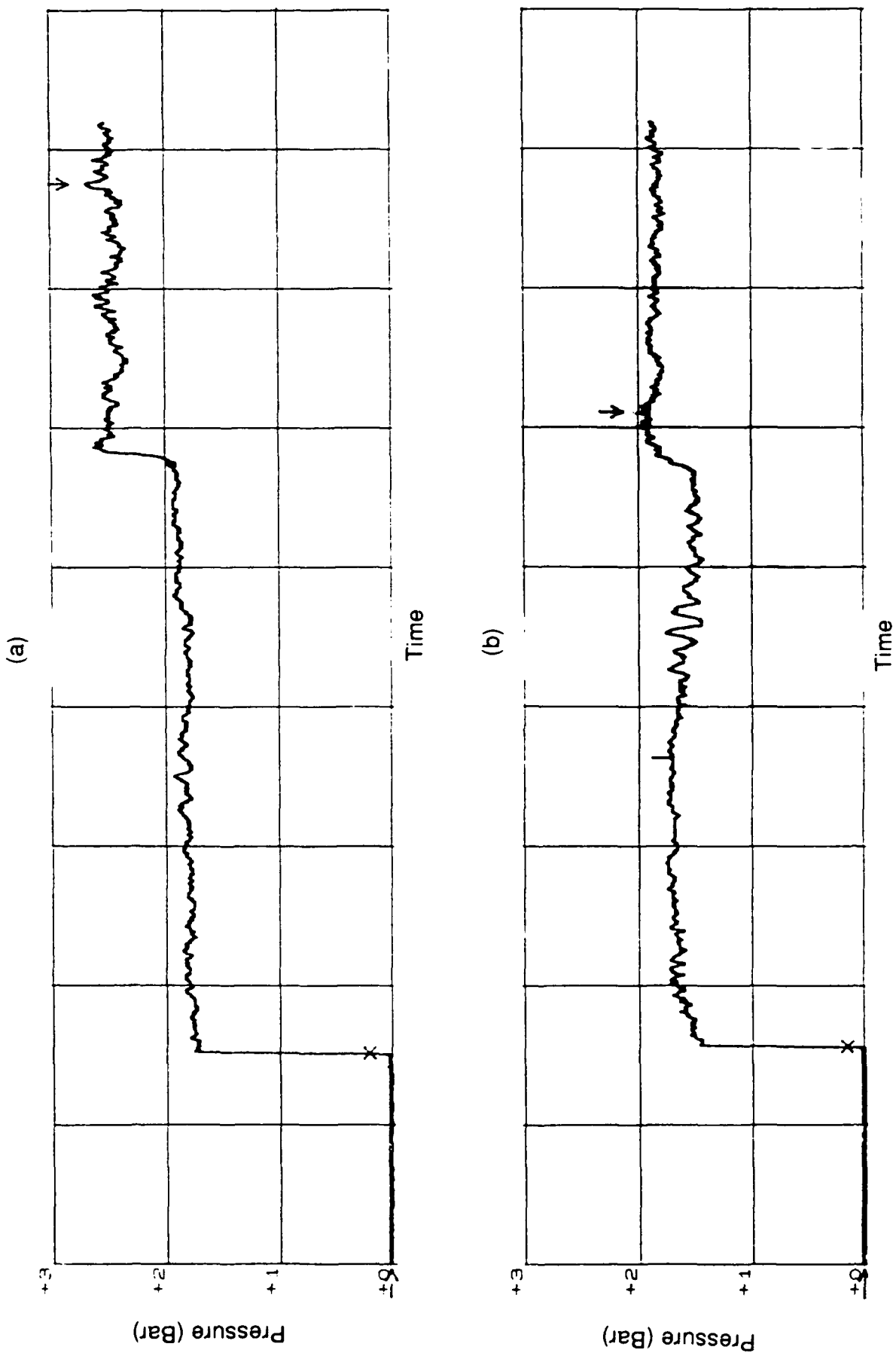

Figure 29. Typical pressure traces for a) smooth floor and b) rough floor.

- Individual velocity realizations represent mean and rms velocity time histories
- After 20 μs, the particles have reached 80% of gas velocity behind the shock
- Shock tube flow disturbances at 1 ms is apparent in velocity data

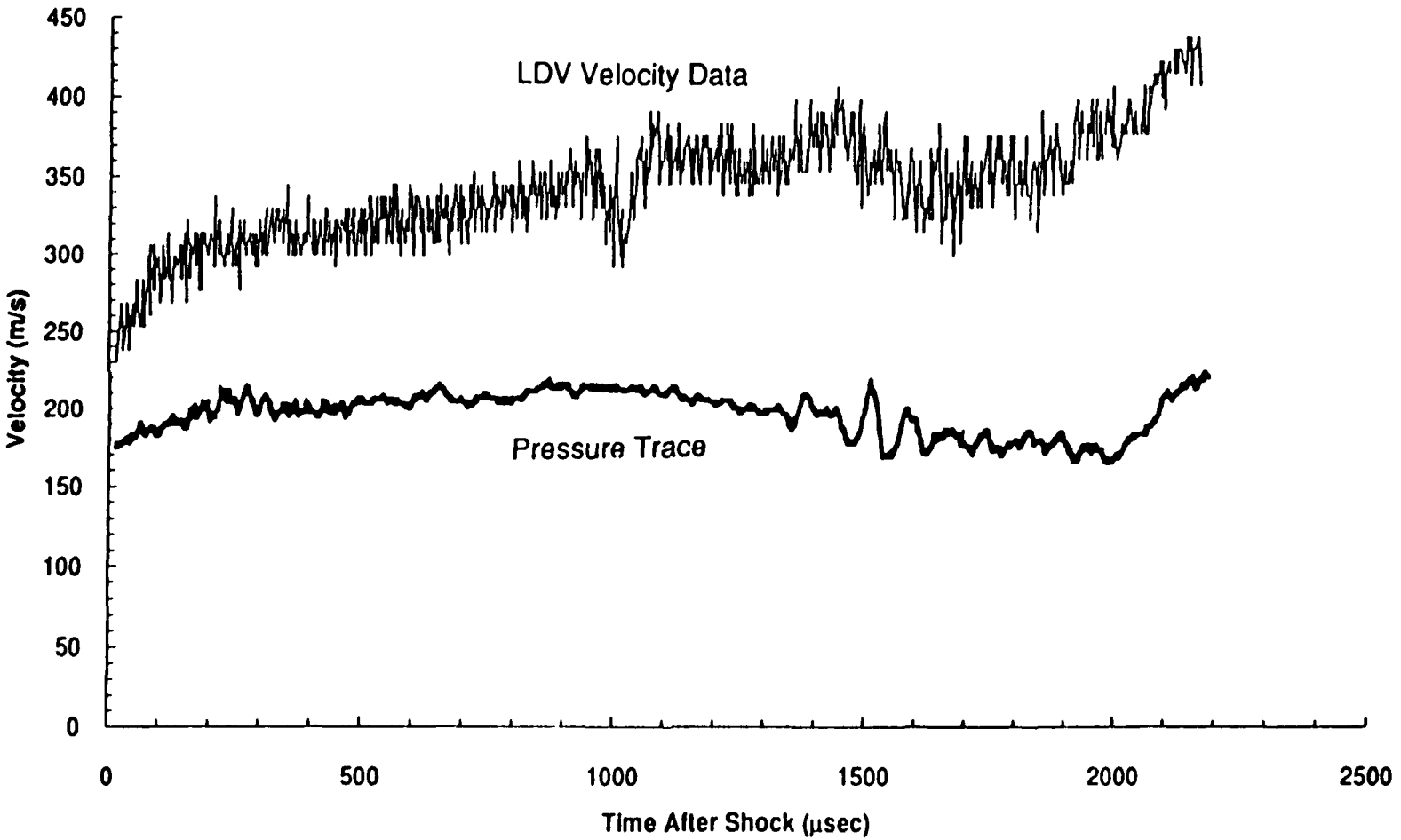

Figure 30. Freestream velocity data/pressure trace.

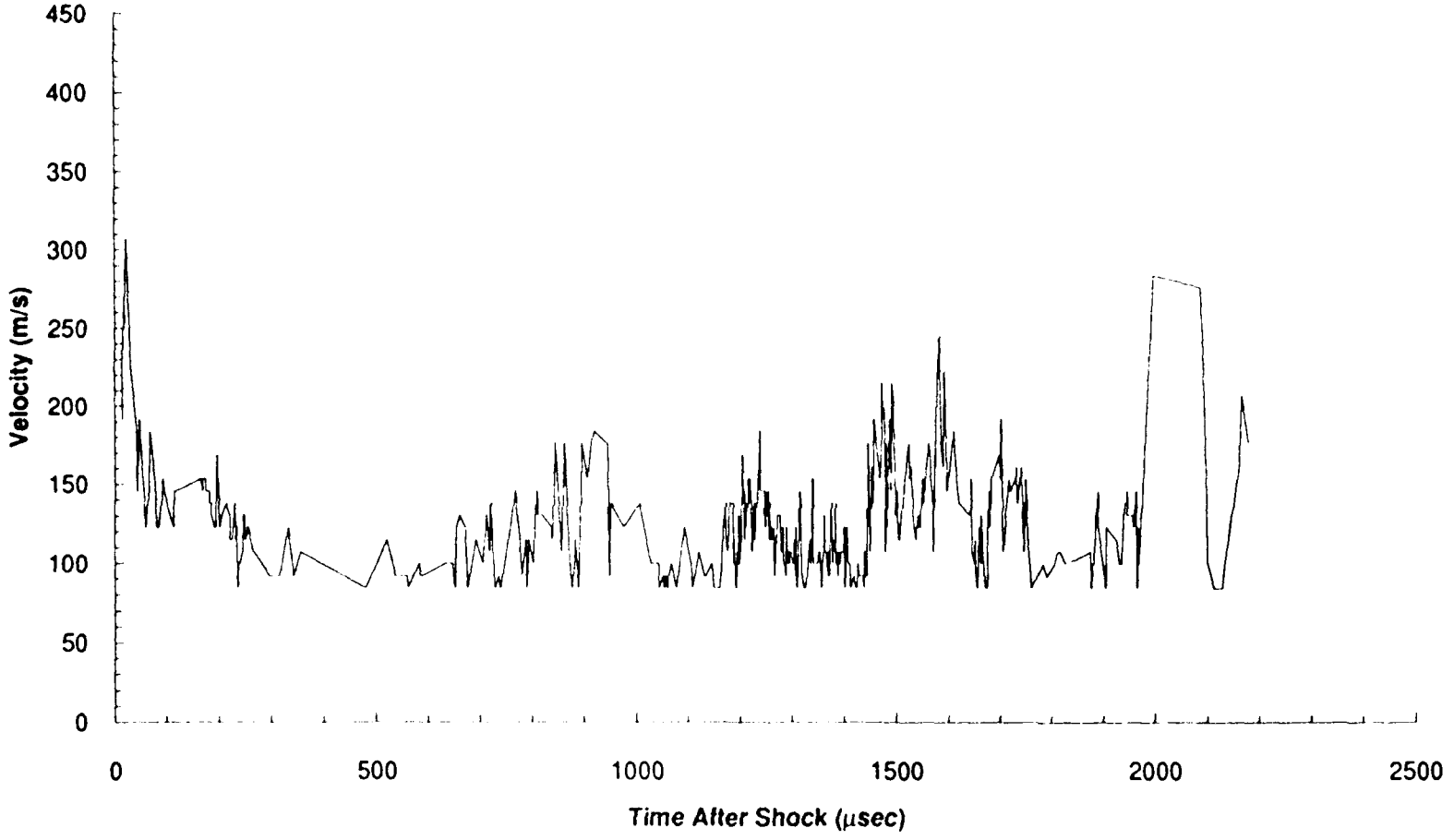

Figure 31. Individual velocity data 0.4 mm off smooth floor.

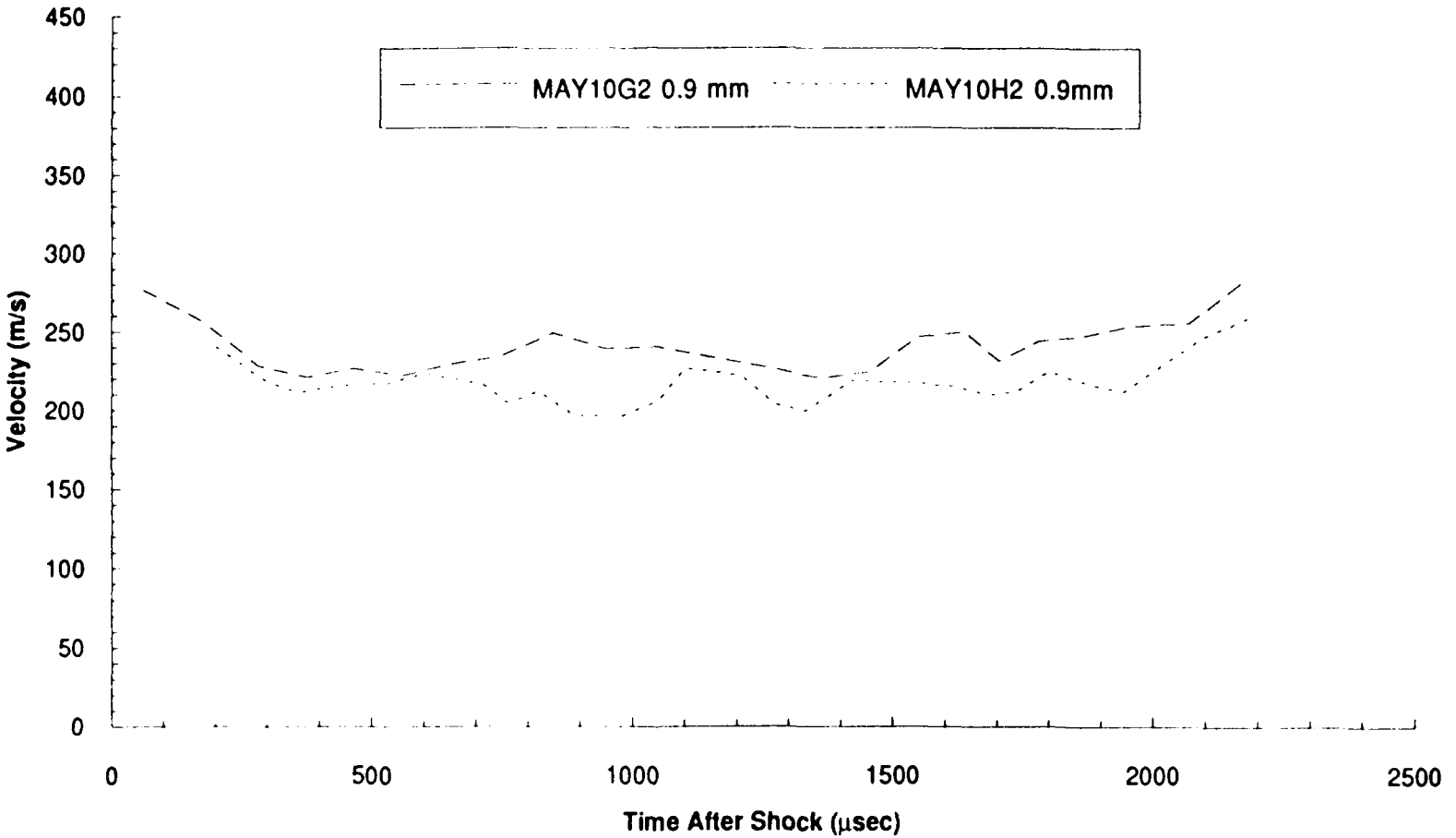

Figure 32. Velocity time histories for two different runs, smooth floor.

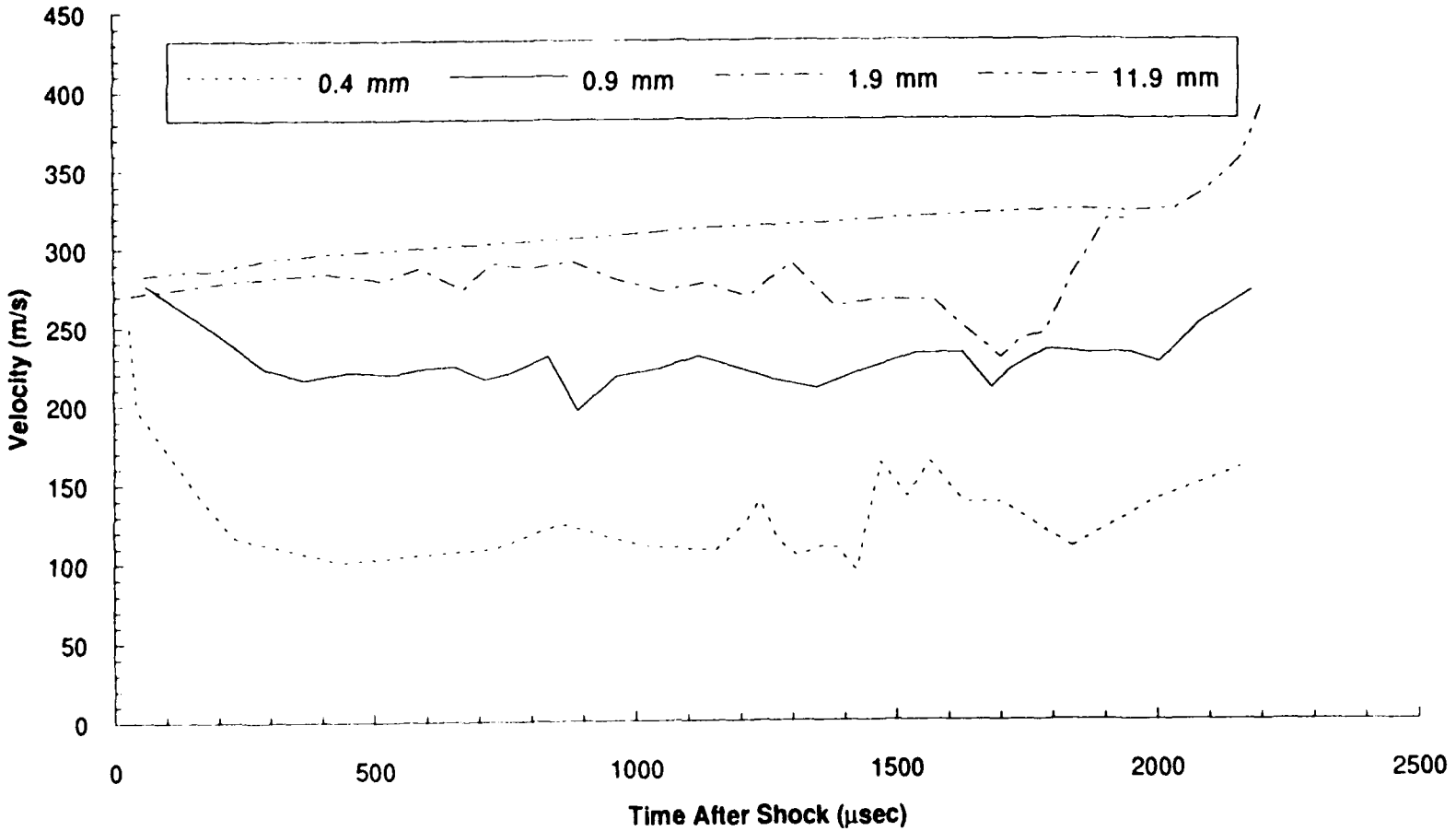

Figure 33. Velocity time histories for boundary layer developed behind a shock wave over a smooth floor.

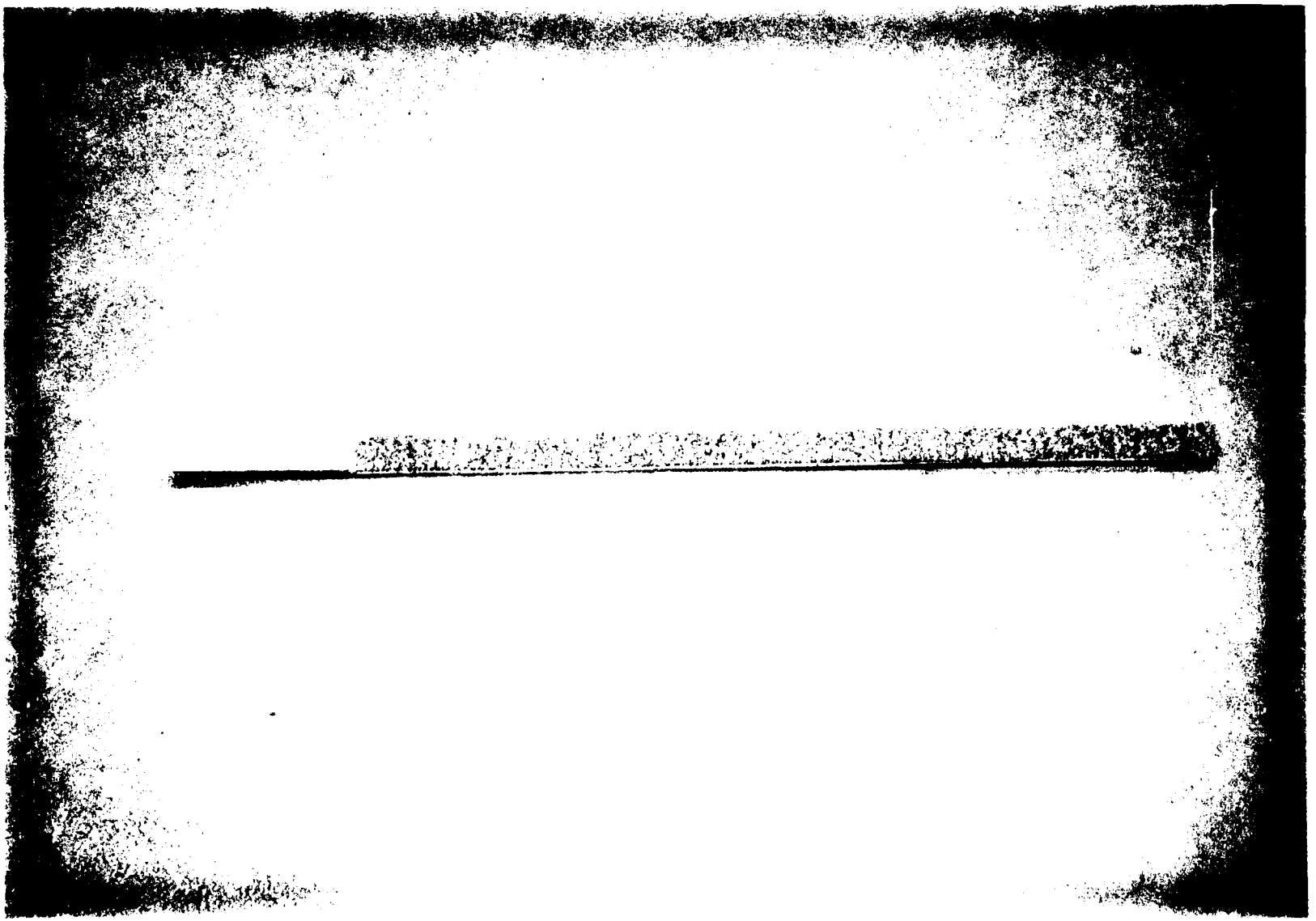

Figure 34. Photograph of test bed with carpet.

- Mean velocity time data for a single run
- This results demonstrate the precision/accuracy of three independent LDA measurements during one run
- Particles accelerate from rest to 80% - 90% of free stream velocity in ~15 micro-seconds corresponding to 0.3 micron size
- Velocity time histories display the disturbances reaching the test section at 1.0 and 1.5 ms

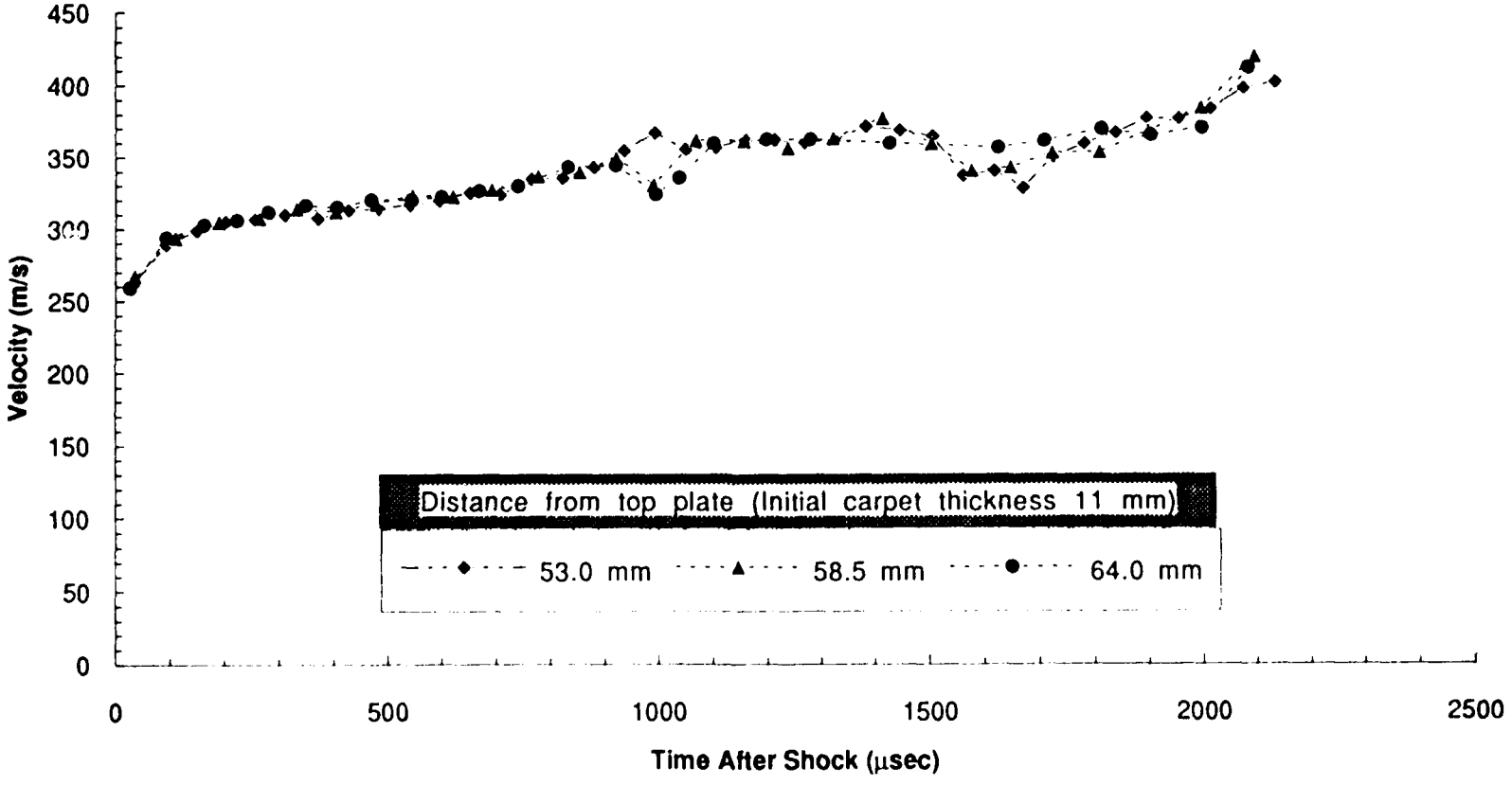

Figure 35. Three simultaneous freestream velocity time history.

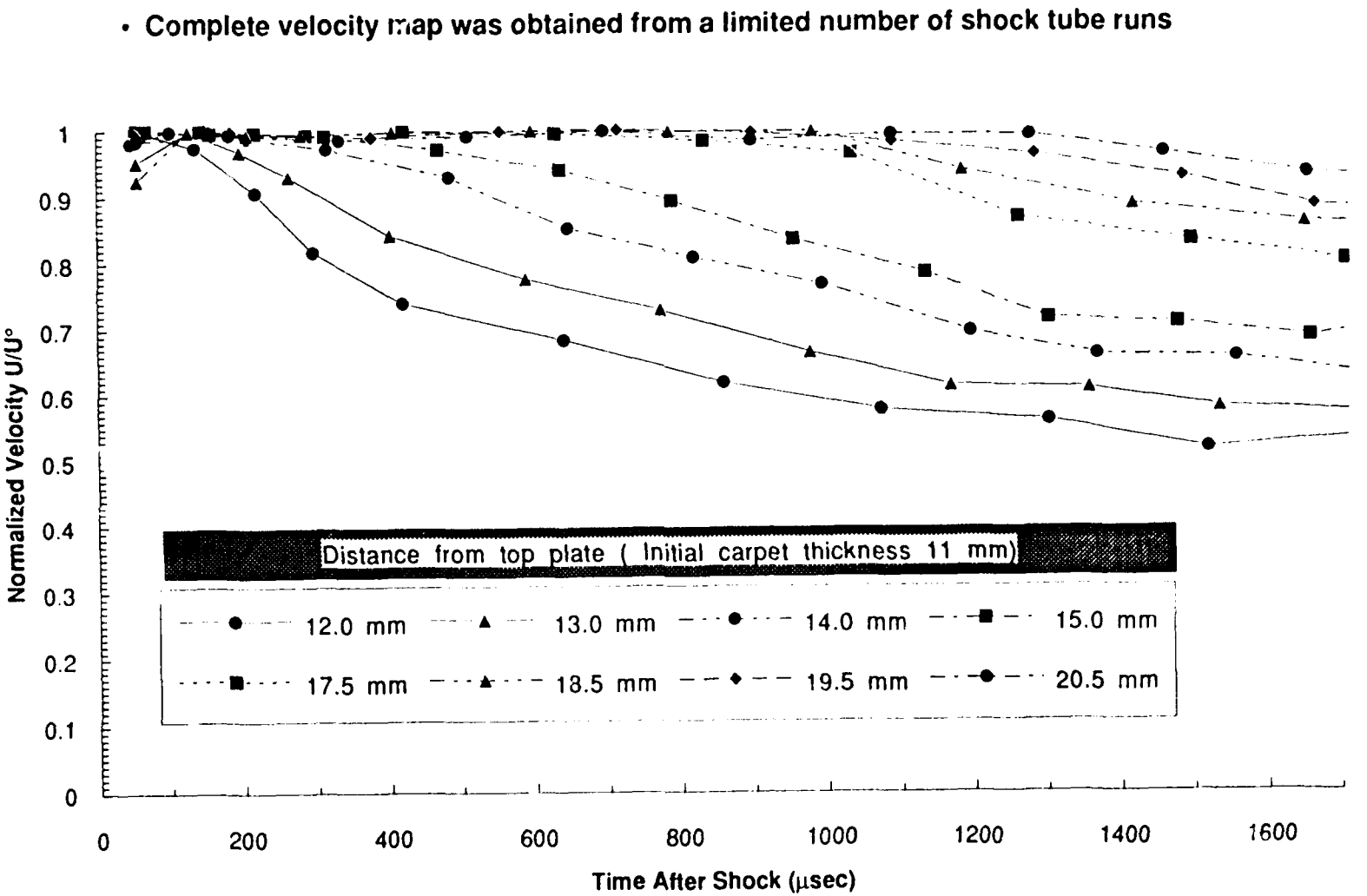

Figure 36. Normalized velocity time history for boundary layer developed behind a shock wave over rough surfaces.

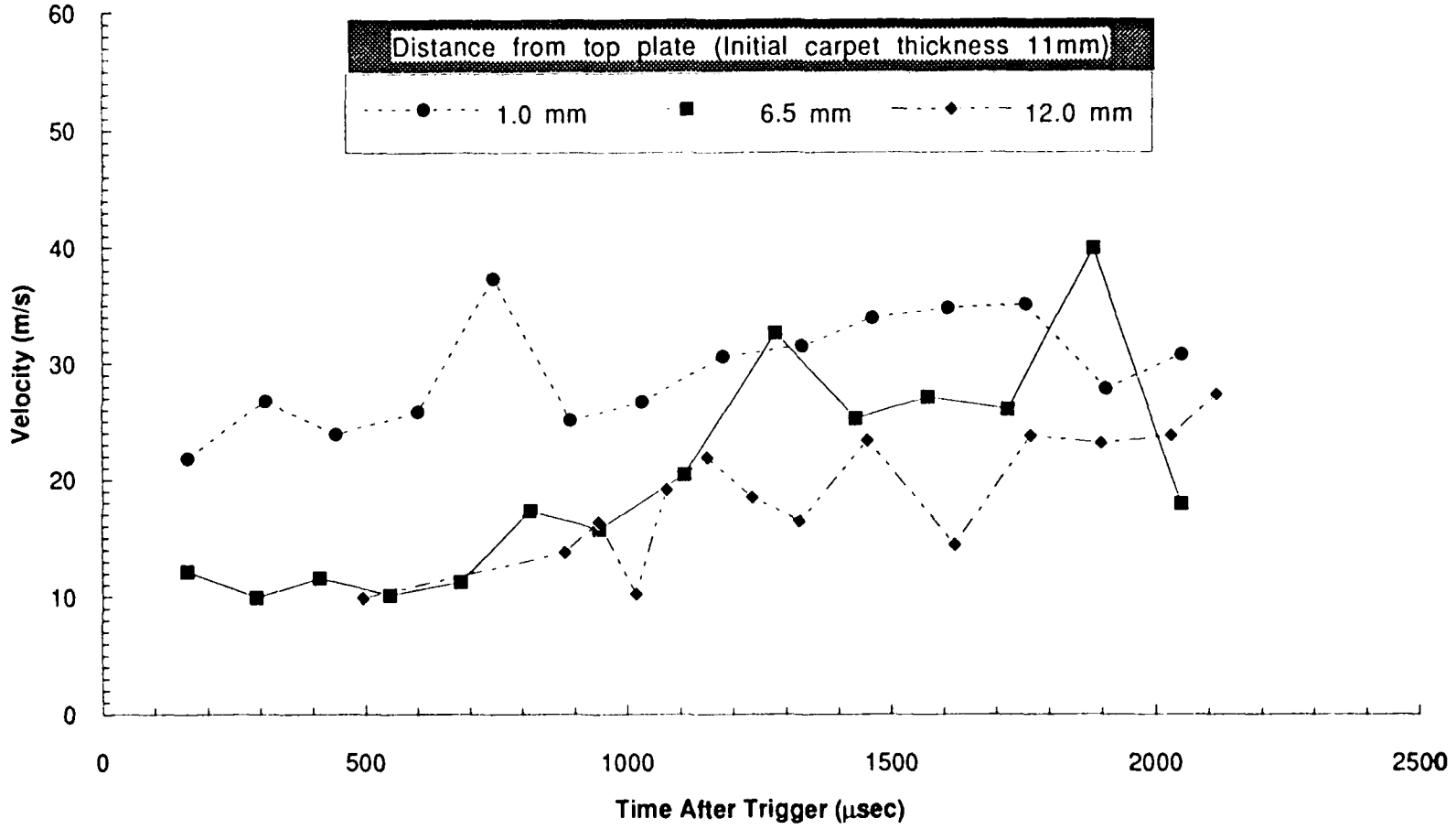

Figure 37. RMS velocity time history at different elevations.

- **Power law curve fit of boundary layer velocity profile over a rough surface**

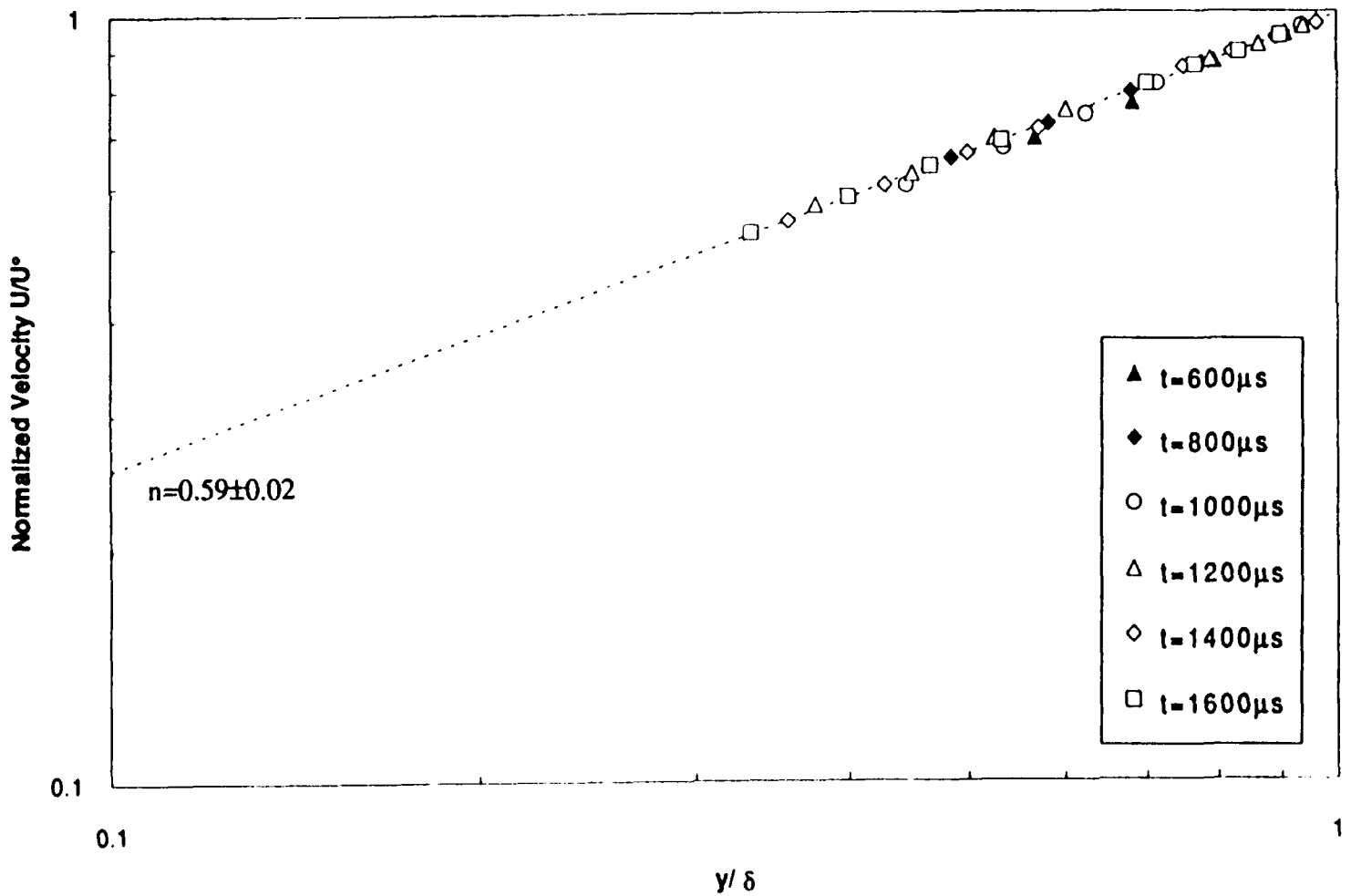

Figure 38. Normalized velocity profile.

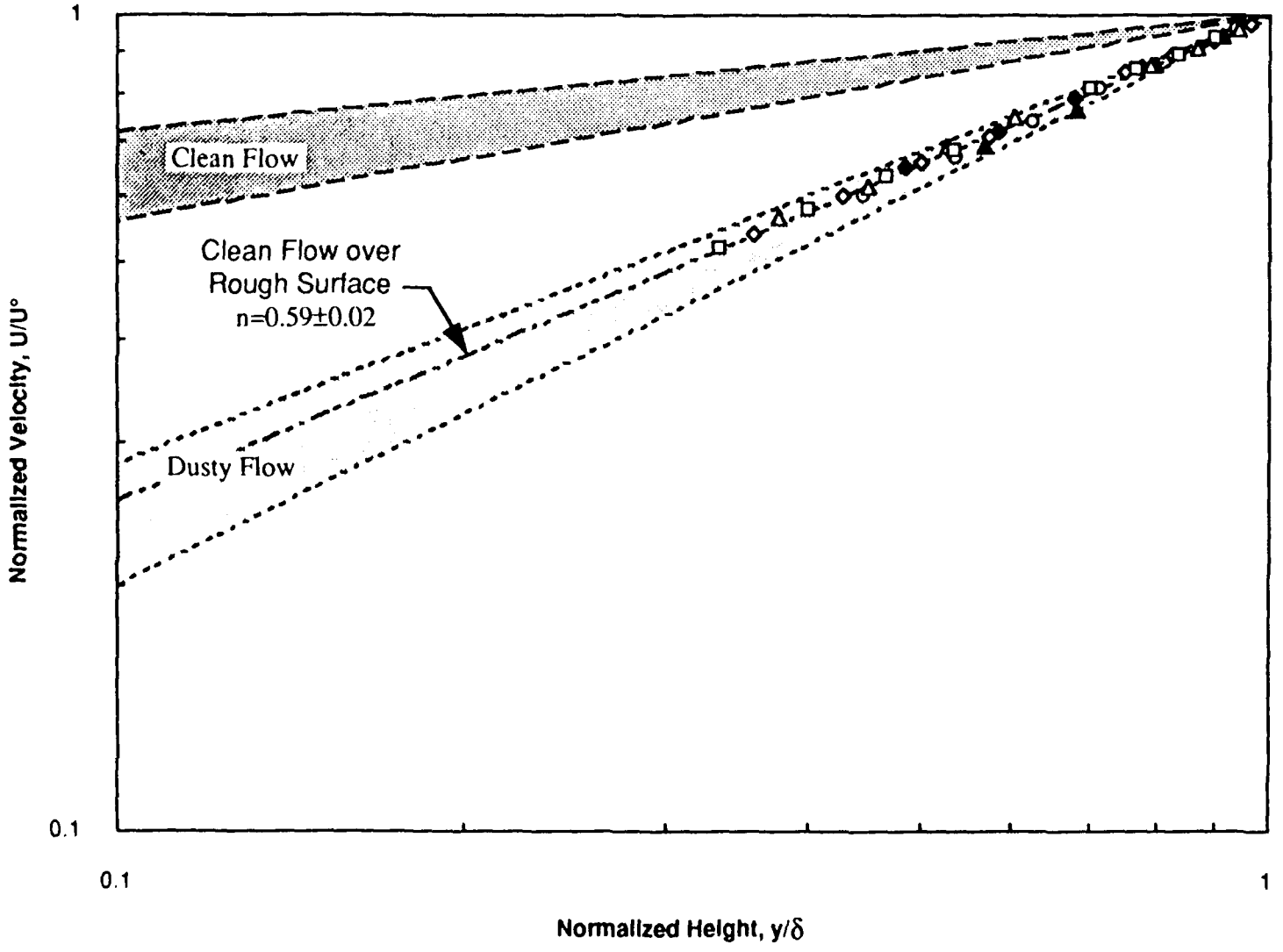

Figure 39. Comparison of normalized velocity profiles.

SECTION 5

CONCLUSION AND RECOMMENDATIONS

The tasks performed under this contract have enhanced the density measurement capabilities of the EMI shock tube for non-ideal airblast studies. Implementation of the fringe analysis software package provides for mapping of the pre-shock helium partial density in the shock tube with an accuracy previously unobtainable. This technique, however, does not allow for determination of the rapidly varying densities in the flow behind the shock wave. Possible techniques for accomplishing this were reviewed, and successful experiments using absorption spectroscopy were carried out. However, interaction of the NO_2 seed gas used with atmospheric moisture produced nitric acid corrosion of non-ferrous metal parts inside the shock tube. A further review of possible techniques was performed, and filtered Rayleigh scattering from Freon 12 was chosen as an acceptable alternative. Design factors for a system using this technique are presented in the report, with a proposal for an experimental test in the shock tube. Simultaneous multi-location measurements of flow velocity are also required for analysis of the non-ideal airblast flow. A four-point LDV instrument was designed and successful preliminary tests carried out during the contract. The initial tests measured a flowfield with characteristics resembling dusty non-ideal blast flow. On the basis of the results described, we make the following recommendations.

The proposed experiment for testing the filtered Rayleigh scattering technique for density measurements should be carried out. A number of approaches for upgrading the prototype design have been identified in this report. A prototype design and test experiment will indicate the optimum approach to obtaining the rapid density field measurements

needed for detailed understanding of non-ideal blast flow and validation of computer simulation models.

Further improvements for the above mentioned four-point LDV system are planned. These improvements would consist of modifying and adding to the software for data processing and modifying the optics of the transmitter and receiver. Presently, the software for data processing requires several steps to obtain the velocity time histories and it does not handle multiple particles crossing the probe volume (common occurrence for data taken). Improvements to the data processing software would entail making it more automated and altering the processing algorithms so that multiple particles can be processed. To improve the signal-to-noise ratio (SNR) of the signal, modification of the input optics needs to be done along with reducing the core diameter of the receiving fiber. A further benefit of reducing the core diameter of the receiving fiber would be a reduction in the number of the multiple particles detected. The Development of a multi-point laser Doppler velocimeter for the EMI shock tube should continue, since detailed knowledge of the flow velocity field is essential for characterizing the flow adequately.

SECTION 6

LIST OF REFERENCES

1. R. Miles and W. Lempert, "Two-Dimensional Measurement of Density, Velocity, and Temperature in Turbulent High-Speed Air Flows by UV Rayleigh Scattering," Applied Physics B 51, (1990), pp. 1-7.

2. R. B. Miles, W. R. Lempert, and J. Forkey, "Imaging Turbulent Structure in High-Speed Air by Filtered Rayleigh Scattering," 12th Symposium on Turbulence, University of Missouri-Rolla, September 24-26, 1990.

3. B. Yip, D. C. Fourguette, and M. B. Long, "Three-Dimensional Gas Concentration and Gradient Measurements in a Photoacoustically Perturbed Jet, " Appl. Opt. 25, (1986), p. 3919.

4. Shardanand and A. D. Prasad Rao, "Absolute Rayleigh Scattering Cross Sections of Gases and Freons of Stratospherics Interest in the Visible and Ultraviolet Regions," NASA Technical Note, #TN D-8442, March 1977.

5. H. Shimizu, K. Noguchi, and C. Y. She, "Atmospheric Temperature Measurement by a High Spectral Resolution Lidar," Applied Optics 25, (1986), p. 1460.

6. S. Yip and M. Nelkin, "Application of a Kinetic Model to Time-Dependent Density Correlations in Fluids," Physical Review 135 (1964), p. A1241.

7. V. V. Altunin, V. Z. Geller, E. A. Kremenevskaya, I. I. Perelshtein, and E. K. Petrov. English Editor, T. B. Selover, Jr. Thermophysical Properties of Freons: Methane Series, Part 2. Chapter 3: "Thermophysical Properties of Freon 12," (Hemisphere Publishing Corp., New York, 1987), p. 77.

8. D. R. Smith, J. Poggie, and A. J. Smits, "Application of Rayleigh Scattering to Supersonic Turbulent Flows," Fifth International Symposium on Application of Laser Techniques to Fluid Mechanics , Lisbon, Portugal, July 9-12, 1990, p. 1.4.

APPENDIX A

Operation Manual

INTERFERENCE FRINGE ANALYSIS IMAGE PROCESSING SYSTEM

Prepared for

Fraunhofer-Institut für Kurzzeitdynamik
Ernst-Mach-Institut
Eckerstraße 4, D-7800 Freiburg
Federal Republic of Germany

Prepared by

Dariush Modarress, Robert Padgug and Chris Wegener

February 10, 1990

Physical Research, Inc.
25500 Hawthorne Blvd., Suite 2300
Torrance, CA 90505-6828, U. S. A.

TABLE OF CONTENTS

Section			Page
1.0	INTRODUCTION TO THE SYSTEM		1
	1.1	Overview	1
	1.2	System hardware	2
	1.3	System software	2
2.0	PROGRAM IP - FRINGE PATTERN DIGITIZATION		5
	2.1	Purpose	5
	2.2	Using the program	5
3.0	PROGRAM PROCESS - FRINGE PATTERN ANALYSIS		9
	3.1	Purpose	9
	3.2	Using the program	9
4.0	PROGRAM FRINGE - FRINGE PATTERN VERIFICATION		15
	4.1	Purpose	15
	4.2	Using the program	15
Appendices			
A.	HOST COMPUTER REQUIREMENTS		19
B.	SYSTEM INSTALLATION		19

LIST OF FIGURES

Figure		Page
1.	IP main menu	6
2.	PROCESS control screen	10
3.	PROCESS image display	13
4.	PROCESS partial pressure of helium display	14
5.	FRINGE display of digitized fringe pattern	16
6.	FRINGE display with selected fringe highlighted	17

1.0 INTRODUCTION TO THE SYSTEM

1.1 OVERVIEW.

The Interference Fringe Analysis Image Processing System is an integrated system of hardware and software that automates much of the process of determining the partial pressure of helium at multiple locations in a shocktube. In investigations of blast wave propagation in non-ideal conditions, helium is introduced into the shocktube to form a gas layer with sound velocity greater than that of air, simulating a heated layer produced by thermal radiation and reradiation from the ground. Analysis of the experiment requires determination of the helium density distribution prior to shock arrival. With the image processing system, researchers may quickly digitize photographs of fringe patterns produced by Mach-Zehnder interferometry before and after introduction of the helium. The system performs an automated comparative analysis of the fringe patterns and calculates the helium distribution. Results of the analysis are displayed in graphical form, and are recorded in computer data files for further use.

An AT-class personal computer is required for operation of the image processing system. Requirements for the host computer and procedures for installation of the image processing system are set forth in Appendices A and B of the manual. Operation of the system is controlled from the computer keyboard, mouse and monitor. To use the system, a researcher places an interference fringe photograph in the field of view of a video camera mounted above an illuminated horizontal easel. The video representation of the photograph is presented on the system's monochrome display monitor, and command menus for controlling system operation are displayed on the host computer's monitor.

The functions performed by the image processing system under the control of the researcher are divided into three tasks:

1.) digitization of the interference fringe patterns in the photographs;

2.) comparative analysis of the digitized patterns for determination of partial pressure of helium in the flowfield;

3.) graphical presentation of the digitized fringe pattern for detailed examination and checking of the analysis results.

Within each of these tasks there is a normal sequence in which functions are usually performed. The researcher/system interface is designed to facilitate progression through this sequence. However, performance of individual functions is under the control of the researcher throughout the operation.

1.2 SYSTEM HARDWARE.

The hardware components of the image processing system are primarily devoted to performance of the first system task, digitization of the fringe pattern. These components are:

a.) an Image Action Plus® frame grabber board;

b.) a CCD video camera with adjustable f-stop settings;

c.) a monochrome display monitor;

d.) a copy stand (horizontal easel) with illuminating lamps;

e.) connecting cables.

The frame grabber board is installed in an expansion slot of the host computer and is controlled by an interactive program executing on the computer. Analog data signals from the video camera are digitized by the frame grabber. A digitized frame is 512 pixels wide and 480 pixels high. Each pixel is represented by one 8-bit byte of data, providing a grey scale range of 256 steps.

Operation of the system hardware is controlled through the host computer by the system software.

1.3 SYSTEM SOFTWARE.

Each of the three tasks performed by the system is controlled by a separate software program. These programs are provided as executable (.EXE extension) files, and their selection and execution is peformed under the DOS operating system installed on the host computer. The programs are:

IP
This program controls the system hardware during digitization of the interference fringe pattern.

PROCESS

This program performs the analysis of the digitized pattern and calculation of the partial pressure of helium in the flowfield.

FRINGE

This program presents the digitized data graphically and gives the researcher the capability to determine the spatial coordinates of specific points in the digitized image, in order to verify the correct performance of the digitizing and analysis tasks.

Utilization of each of these programs will be described in the following Sections of the manual.

2.0 PROGRAM IP - FRINGE PATTERN DIGITIZATION

2.1 PURPOSE.

The IP program controls the system hardware in the task of digitizing the photographs of interference fringe patterns observed before and after introduction of helium to the shocktube. Manual intervention by the researcher is required for placing the photographs, adjusting the video camera, designating reference marks in the shock tube and visible in the photographs as reference points for calibration, establishing the spatial coordinates with respect to the reference points, and controlling data storage and file name assignment. The program is therefore controlled interactively by the researcher through the host computer keyboard, mouse and monitor. The digitized image contains 480 horizontal rows of 512 pixels. Image brightness in each pixel is represented by one eight-bit data byte, providing a grey scale of 256 steps. An area of interest within the photograph is selected by the researcher for subsequent analysis in program PROCESS. Each image selected by the researcher for retention is stored as an individual file containing approximately 250 Kbytes of data. These data files are used by the PROCESS program.

2.2 USING THE PROGRAM.

2.2.1 Invocation.

To begin execution of the IP program, type "ip" at the DOS prompt. The default directory at the time must be the subdirectory containing the executable program files, or that subdirectory must have been specified by the PATH command in DOS.

2.2.2 Operation and Commands.

The IP program initially displays its Main Menu (Figure 1). Commands in the main menu appear in the order in which they are normally executed during a routine digitization procedure.

INITIALIZE

Select INITIALIZE only when the program is first executed.

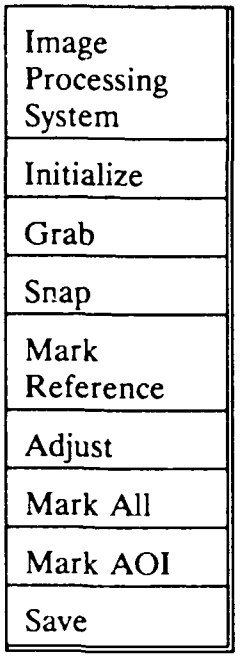

Figure 1. IP main menu

GRAB

Select GRAB to put the frame grabber board into continuous acquisition mode. In this mode the CCD video camera is in operation and the image is presented on the system display monitor. Position an interference fringe photograph on the horizontal easel. Adjust the camera for proper focus while viewing the image in the monitor, and then set the lens f-stop adjustment to produce maximum contrast in the image. NOTE: When performing a series of digitizations, try to place all photographs in the same location on the easel.

SNAP

When the camera has been adjusted for the best image, select SNAP. This command stops continuous acquisition and stores a single frame for digitization.

MARK FIRST

Select MARK FIRST to begin the process of calibration to shocktube reference marks visible in the photograph. The program presents this message:

Press left Mouse Button Drag crosshair cursor over Leftmost reference Mark Press right Mouse Button

Press the left mouse button to activate the crosshair cursor on the monitor. Center the cursor on the leftmost reference mark and press the right mouse button to return to the main menu.

ADJUST

Select ADJUST to continue the calibration procedure. The program presents this message:

Adjust the Photo till the three Reference Marks are centered upon the line. Press the right mouse button when done

A horizontal line passing through the leftmost reference mark appears on the monitor screen. Adjust the photograph so that all visible reference marks are located on the line. Press the right mouse button to return to the main menu.

MARK ALL

Select MARK ALL when all reference marks on the photograph are aligned with the horizontal line. The program presents this message:

Center cursor on reference mark and push left button Enter 1, 2, 3 or 4 for orientation from left margin Push right button when done.

Please enter distance between reference marks 1 and 2 in centimeters Distance: 0

Press the left mouse button to activate the cross hair cursor on the monitor. This cursor will only move to the left or right along the horizontal line through the leftmost reference mark. Center the cursor on the first reference mark, press the right mouse button and enter '1' to

identify the reference mark. Move the cursor to the second reference mark, click the right button, and enter '2'. The program prompts for the distance between the first and second reference marks. Enter the distance in centimeters. WARNING: If the carriage return is pressed before a number is typed, a value of zero is entered. Repeat for the third mark (and for the fourth mark, if any) the process of moving the cursor to the mark, identifying the mark, and entering the distance between marks. After entering the final distance, click the right mouse button again to return to the main menu.

MARK AOI

Select MARK AOI to define the area of interest (AOI) that is to be analyzed in program PROCESS after the reference marks have been identified and their spatial separations entered. The area must be wholly within the fringe area. The program presents this message:

```
Push left mouse button
Position crosshair at upper left corner of AOI
Press right mouse button
Drag box over AOI
Press right mouse button
```

Press the left mouse button to create the crosshair cursor, and position the cursor at the upper left corner of the area of interest that is to be processed. Press the right hand button to create a box and anchor the upper left corner of the box at the cursor location. Move the cursor to drag the lower right corner of the box until the box encloses the area of interest. Press the right hand button again to define the area of interest. The program returns to the main menu.

SAVE

Select SAVE to command the program to digitize the frame and store the data in a file. The program presents this message:

```
Please enter a file name
with a maximum of eight characters
the program will append an extension
File Name:
```

Enter a name. The program appends the extension ".IMG" and creates a file which contains the digitized image. Each image file contains approxmately 250 Kbytes of data.

3.0 PROGRAM PROCESS - FRINGE PATTERN ANALYSIS

3.1 PURPOSE.

The PROCESS program performs the automated analysis to calculate the helium partial pressure at each raster point in the designated area of interest, using the pair of digitized image files produced by the IP program from interference fringes photographed before and after introduction of helium into the shock tube. The partial pressure data are stored in a data file in ASCII format. PROCESS also creates an image file showing the center line of each fringe within the area of interest. This file is used with the FRINGE program in the task of checking the results of the IP and PROCESS programs. On request, PROCESS displays on the computer monitor the fringe images or the partial pressure distribution.

3.2 USING THE PROGRAM.

3.2.1 Invocation.

To begin execution of the PROCESS program, type "process" at the DOS prompt. The default directory at the time must be the subdirectory containing the executable program files, or that subdirectory must have been specified by the PATH command in DOS.

3.2.2 Operation and Commands.

The PROCESS program initially displays its Control Screen (Figure 2). The three boxed upper sections of this screen contain information about:

1.) the graphics display installation and data presentation mode,

2.) the image files being processed, and

3.) the coordinates of the area of interest.

Except for the video display adapter type and resolution, which are determined by the host computer hardware, the information displayed in the boxes is parameters set by the researcher.

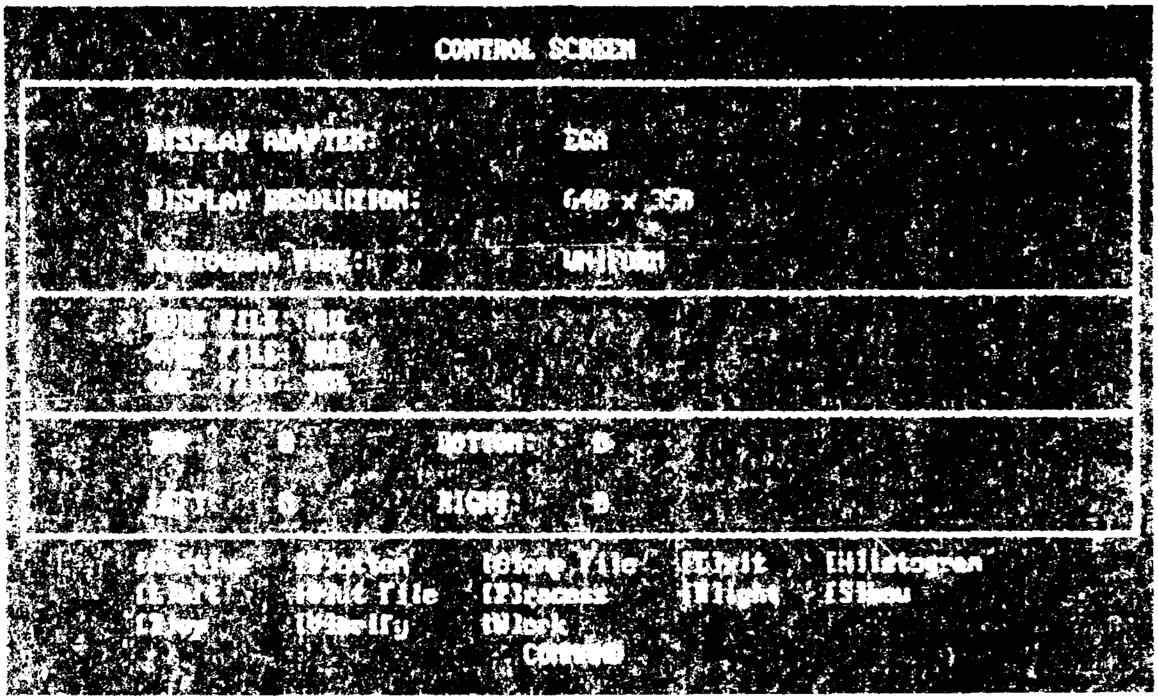

Figure 2. PROCESS control screen.

Histogram Type

There [illegible] three options for assigning colors to value ranges for display [illegible]

UNIFORM. Eight colors are used. Each is associated with [illegible] contiguous steps in the 256-step grey scale.

MAX ENTROPY. Eight colors are used. The range of grey [illegible] between the minimum and maximum actual data [illegible] and [illegible] band.

PF DISPLAY. [illegible] used. [illegible] the [illegible] range [illegible] pressure.

Files

WORK: The image file of fringes photographed after helium was introduced into the shocktube.

COMP: The image file of fringes photographed before helium was introduced into the shocktube, with which the work file is compared.

OUT: The image file of digitized helium partial pressure in percent.

At any time, one of the three image files is designated as the ACTIVE file and is marked by a '>' symbol to the left of the file type label. The image of this file can be displayed on the computer monitor. The ACTIVE file selection can be changed by the researcher.

Note that the file names include extensions. If any of the files is not in the current default director, the complete path to the file must be specified.

Area of Interest Boundary Coordinates

The TOP, BOTTOM, LEFT and RIGHT boundary coordinates (in raster units) of the area to be processed are displayed in the third box. These coordinates default to the values set in program IP, but may be changed in PROCESS by the researcher. The areas in the Work and Comp files should be the same. If the areas differ between files, the area common to both is analyzed.

Below the boxes is a list of the commands. To select a command, type only the initial letter of the command. As a reminder, in the control screen the initial letters of the commands are enclosed in square brackets. This convention will also be followed here. The commands are discussed in the order in which they would be selected in a typical execution of the program.

[W]ORK

Select [W]ork to designate the WORK file, which contains the image of the fringes after helium is introduced in the shocktube. The program will prompt for a file name. The file name must include the extension (usually .IMG). If the file is not in the current default directory, the complete path to the file must be specified.

[C]OMP

Select [C]omp to designate the COMP file, which contains the image of the fringes before helium is introduced in the shocktube. The program will prompt for a file name.

The file name must include the extension (usually .IMG). If the file is not in the current default directory, the complete path to the file must be specified.

[O]UT

Select [O]ut to designate the OUT file, which will contain the image of the helium partial pressure distribution calculated by PROCESS. The program will prompt for a file name. The file name must include the extension (usually .IMG). If the file is not in the current default directory, the complete path to the file must be specified.

[S]HOW

Select [S]how to display the image of the Active file on the computer monitor. An example of a WORK file is shown in Figure 3. The labeled reference marks and the boundaries of the area of interest appear in the image. Initially, these boundaries are those set in program IP. The researcher may adjust the boundaries in PROCESS. Take care that the designated area lies entirely within the fringe image, so that no part of the frame or copy stand is included.

[T]OP, [B]OTTOM, [L]EFT, [R]IGHT

Image file displayed on monitor screen

Select [T]op, [B]ottom, [L]eft or [R]ight to designate the corresponding boundary of the area of interest. To move the TOP or BOTTOM boundary, use the [Up Arrow] or [Down Arrow] keys for single pixel moves, or the [Page Up] or [Page Down] keys for moves of ten pixels. Similarly, for the RIGHT or LEFT boundary, use the [Right Arrow] or [Left Arrow] keys for single pixel moves, or the [Tab] or [Shift Tab] keys for moves of ten pixels. The boundary lines in the image move after a move command is entered, and the coordinate values in the third box are also changed. When the boundaries have been adjusted as desired, type [Esc] to return to the main menu.

Main menu displayed on monitor screen

Select [T]op, [B]ottom, [L]eft or [R]ight to designate the corresponding boundary of the area of interest. The program will prompt for a raster coordinate value. Enter the value. The coordinate value in the third box will change.

[A]CTIVE

Select [A]ctive to change the designation of the active file. Successive selections of [A]ctive select the WORK, COMP and OUT files cyclically.

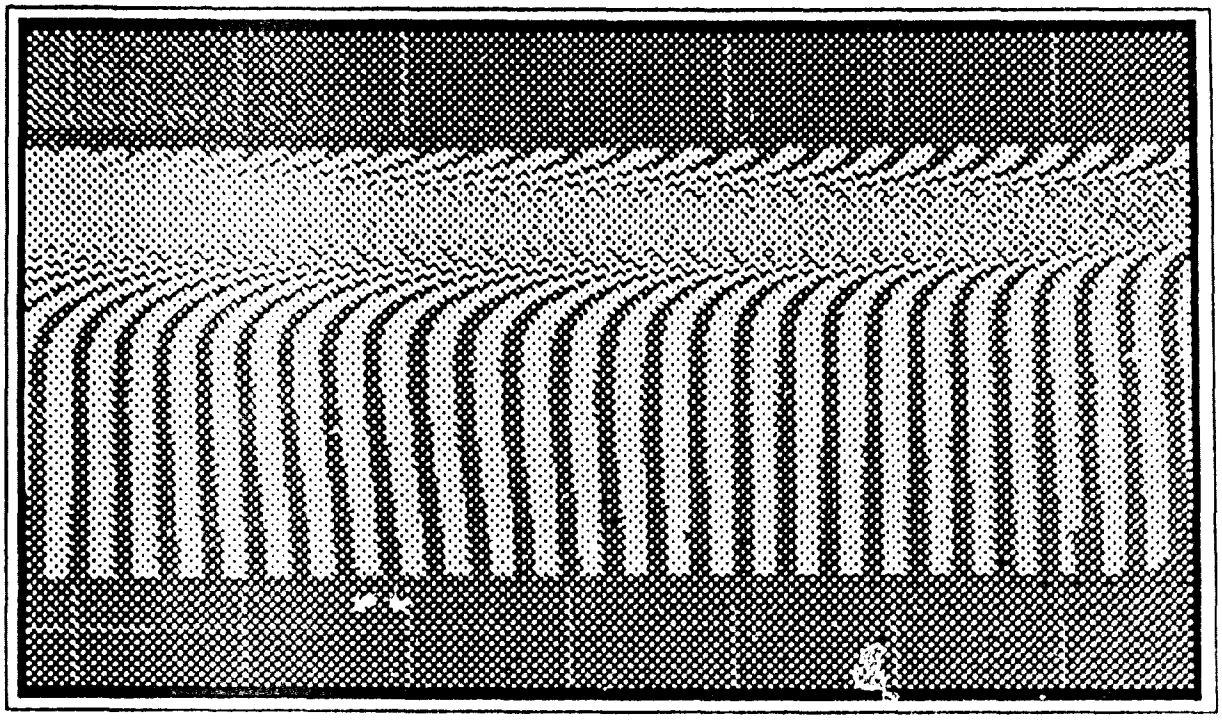

Figure 3. PROCESS image display.

[P]ROCESS

When the areas of interest have been properly adjusted in both WORK and COMP files, select [P]rocess to cause the program to calculate the distribution of partial pressure of helium within the area of interest. During the calculation the program display indicates the file on which the program is working and the line number being processed.

To see the results of the calculation, select [H]istogram to set the color assignment to PP Display, select [A]ctive to designate OUT as the active file, and select [S]how to display the helium partial pressure distribution as a filled contour plot (Figure 4). Recall that eight colors are used cyclically over the 32 bands of partial pressure in per cent units.

[V]ERIFY

Select [V]erify to cause the program to generate an image file, named VFILE.IMG, that shows the center line of each fringe within the area of interest. This image is displayed on the computer monitor when the file is generated. The VFILE.IMG file will be used by the FRINGE program in the task of checking the digitization and analysis performed by programs IP and PROCESS.

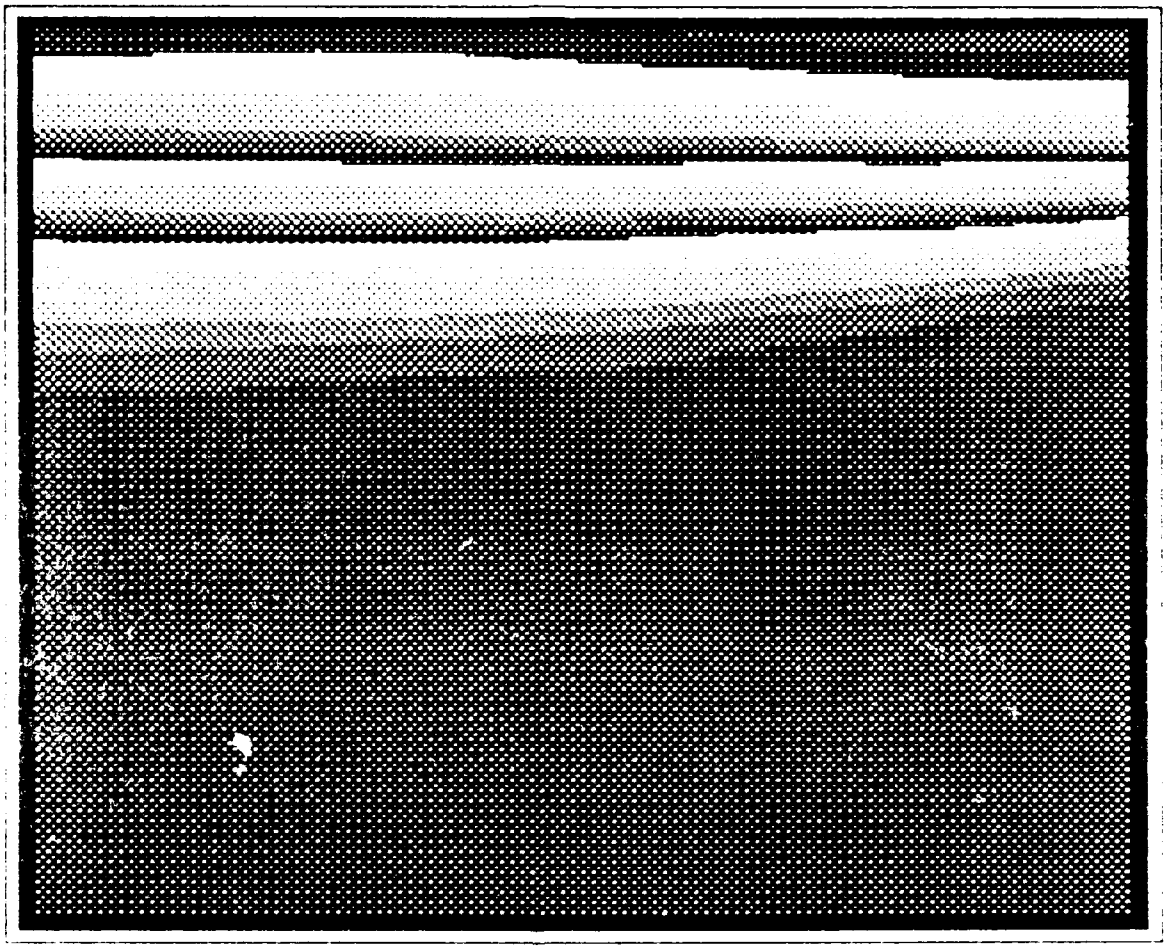

Figure 4. PROCESS partial pressure of helium display.

3.3 SAVING PROCESS OUTPUT FILES.

In addition to the VFILE.IMG file produced with the [V]erify command, PROCESS produces a file in ASCII format named LOGFILE. This file contains the partial pressure of helium at every pixel location within the area of interest. For large areas of interest, the LOGFILE may be up to 2 Mbytes in size and will require several seconds to write. NOTE: Both VFILE.IMG and LOGFILE are assigned their names by the program. If the files are to be preserved, they should be renamed with the DOS command REName before PROCESS is again executed.

4.0 PROGRAM FRINGE - FRINGE PATTERN VERIFICATION

4.1 PURPOSE.

The FRINGE program allows researchers to verify the results of the digitation by program IP and the fringe pattern analysis by program PROCESS. FRINGE displays the fringe pattern image generated in program PROCESS with the [V]erify command on the computer monitor. A researcher may select individual fringes and read positions on that fringe in raster coordinates or distances from the leftmost reference mark in the digitized data images generated by program IP. The coordinates may be used by the researcher for calculations to verify the helium partial density distributions calculated in program PROCESS.

4.2 USING THE PROGRAM.

4.2.1 Invocation.

To begin execution of the FRINGE program, type "fringe" at the DOS prompt. The default directory at the time must be the subdirectory containing the executable program files, or that subdirectory must have been specified by the PATH command in DOS.

4.2.2 Operation.

The FRINGE program initially displays this message:

```
Please enter a path and a file
with a maximum of eight characters
File Name:
```

Enter the name of a fringe image file created with the [V]erify command in program PROCESS. If the file is not in the current default directory, include the complete path in the name. The default name for a fringe image file is VFILE.IMG, but if multiple fringe image files have been created and saved, each file will have an individual name.

FRINGE has no specific commands. The fringe image is displayed on the host computer monitor (Figure 5). The cursor may then be moved along the fringe with the

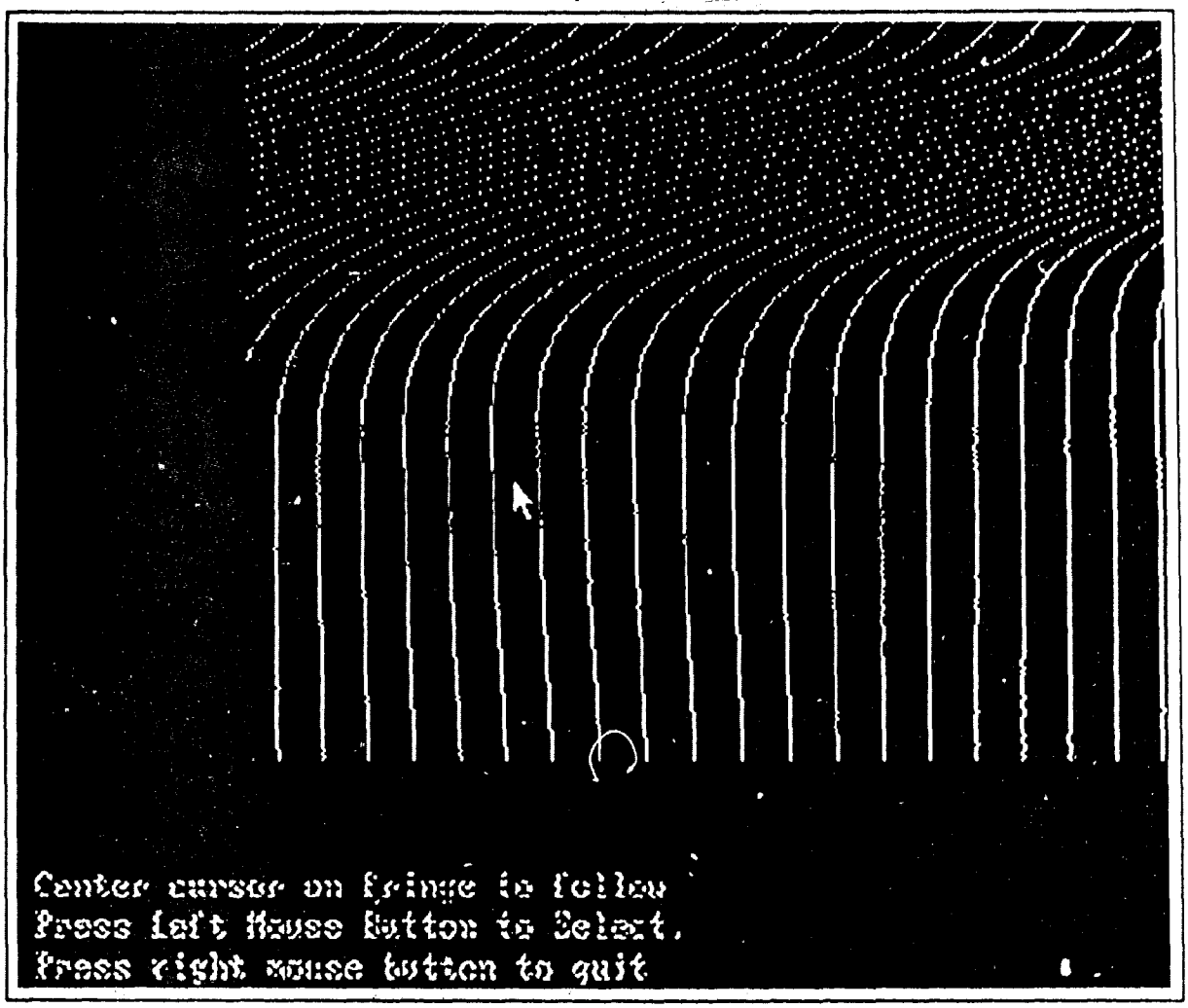

Figure 5. FRINGE display of digitized fringe pattern.

mouse. A cursor in the image is controlled by the mouse. Place the cursor on a fringe centerline in the lower part of the frame and press the right mouse button to select the fringe. The selected fringe will be highlighted in red in the image (Figure 6). The cursor may then be moved along the fringe with the mouse. The location of a pixel on which the cursor is positioned may be read in raster coordinates or in distance in centimeters from the leftmost reference mark. To select another fringe for study, press the right mouse button again. To exit the program, press the right mouse button when no fringe is highlighted.

Warning: attempting to select a fringe with the cursor on a sloping part of the fringe may lead to an error which causes the red highlighting to jump from fringe to fringe. If this occurs, press the right button, move to a lower portion of the fringe, and select again.

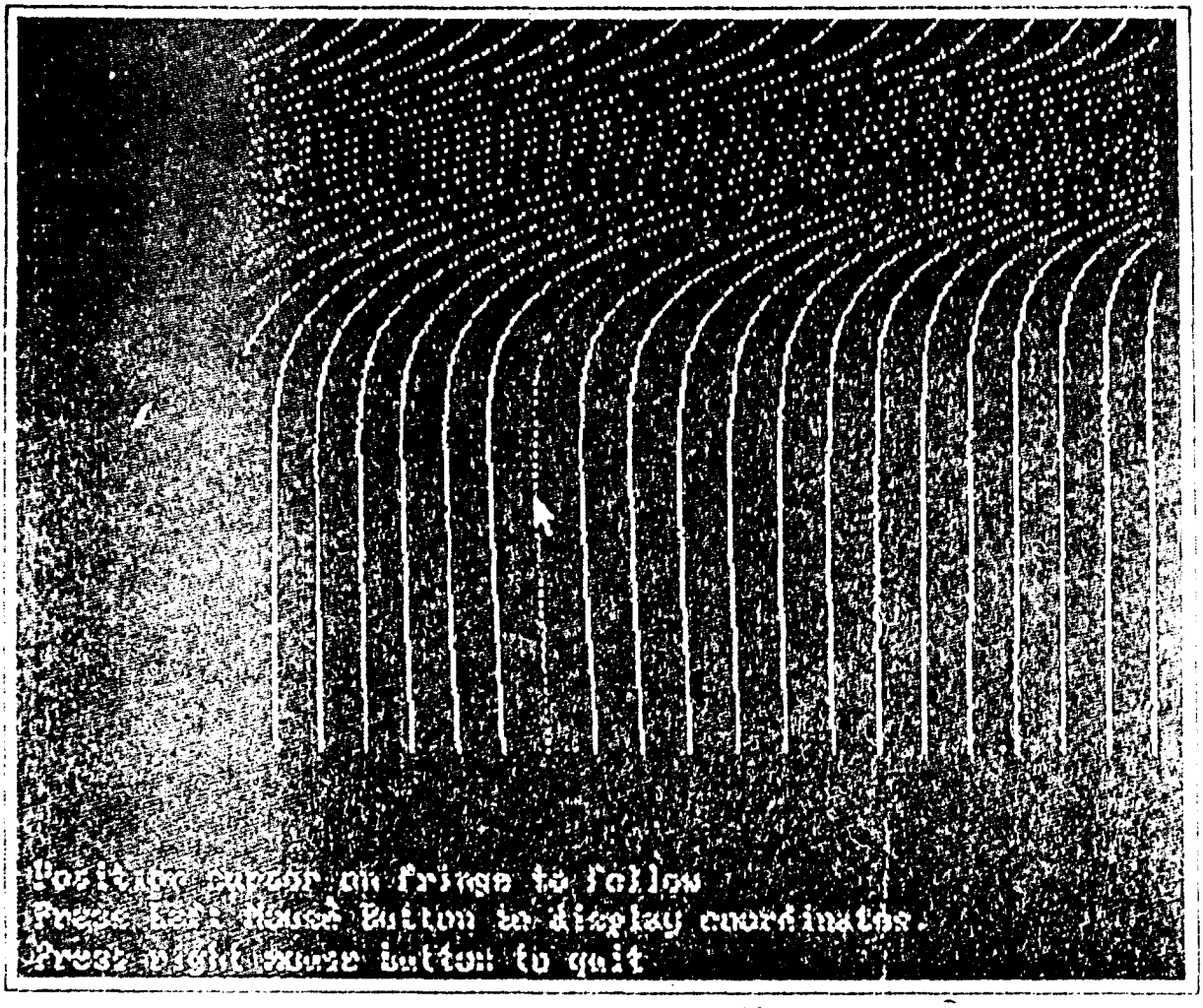

Figure 6. FRINGE display with selected fringe highlighted.

APPENDIX A. HOST COMPUTER REQUIREMENTS

The Interference Fringe Analysis Image Processing System (IPS) requires an AT-class personal computer with a hard disk, operating under Version 2.0 or later of DOS, as a host. The computer must have either an EGA or a VGA video display.

It is not required that the computer be dedicated solely to IPS operation. However, at least 4 MBytes of storage must be set aside on the hard disk for storage of the system software, and additional storage will be required for the data files produced.

An expansion slot must be available for installation of the Image Action Plus® frame grabber board. The manufacturer's manual for the board contains installation instructions.

APPENDIX B. SYSTEM INSTALLATION

Installing the software

The system software is supplied on three 5-1/4" DOS-formatted floppy disks. Installation requires only copying the files from the floppy disks to the host computer hard disk. It is recommended that a separate subdirectory be established to contain all of the system files. The choice of name for this subdirectory is left to the user; the authors have used "ip". It may prove convenient to have separate subdirectories for programs and data files. In this case the PATH command in the DOS operating system must be used. Use of batch files (.BAT extension) is also recommended for convenience of operation.

Disk 1 contains executable files (.EXE extension) for the three system programs, IP, PROCESS and FRINGE. Source code for the programs is also provided in subdirectory "\source" on Disk 1. The IP and FRINGE programs were written in Microsoft C version 5.1 and require CSCAPE version 2.0 from the Oakland Group. The PROCESS program was written in MicroSoft FORTRAN version 4.1.

Several image files are included with the system software for use in gaining familiarity with the program. These files are located on Disk 2, and all have the .IMG file extension.

Refer to Sections 2 through 4 for descriptions of the various image files.

TEST1

This is a compensation image (see Section 2) with no helium introduced.

TEST2

This is a work image (see Section 2) after helium has been introduced into the flow.

TEST3

This is the helium partial pressure distribution from the analysis of TEST1.IMG and TEST2.IMG in program PROCESS (see Section 3).

VFILE

This is the fringe verification image file see (Section 3) of the analysis of TEST1.IMG and TEST2.IMG.

Also included for familiarization is the ASCII output file LOGFILE (see Section 3) produced in the analysis that generated TEST3.IMG. This LOGFILE is stored in Disk 3 in the DOS BACKUP utility format, and the RESTORE utility must be used to retrieve the file from the disk.

Configuring the frame grabber board

For operation with the IP program, the Image Action Plus® frame grabber board must be set to the DUAL Frame configuration. Directions for setting the jumpers to this configuration are contained in the manual supplied with the board.

The factory setting for the register address is 300H. To use the frame grabber card with an EGA or VGA video display card, the base memory address must be changed from the factory setting. Use the manual to determine the new address. (D0000H is a good location.) The register address and base memory address default to the factory settings, but either or both addresses may be changed by passing them as optional parameters when the IP program is invoked. The command line has the format

ip *[optional parameter] [optional parameter]*

The form of the parameter for the register address is *rnnn*, where *nnn* is the three-digit hexadecimal address. Similarly, the form of the parameter for the base memory address is

m*nnnnn*, where *nnnnn* is the five-digit hexadecimal address.

Since the addresses will in general remain constant once determined, a simple way to invoke the IP program is to rename the program executable file and to create a batch file (.BAT extension) to invoke the program and pass the parameters. For example, the executable file might be renamed XIP.EXE and a batch file IP.BAT created. The batch file would contain one line,

xip r*nnn* m*nnnnn*

(recall that only the changed addresses need be supplied). The program would then be invoked by typing "ip" to execute the batch file.

APPENDIX B

Required equipment for Rayleigh scattering.
(Note: European prices are approximately 1.4 x U.S. prices.)

LASER SYSTEM	US PRICES	
Continuum		
NY61 Laser	$33,000	*
Injection-locking option	$25,000	**
Double pulse option	$5,000	*
Frequency doubling package	$4,300	*
Wavelength separation package	$1,600	*
Frequency quadrupling package	$6,300	
Wavelength separation package	$2,600	

European Sales -- West Germany
Contact: Optilas
Boschstreasse 12
D-8039, Puchheim
West Germany
Tel: (49) 89-80-10-35

TIMING		
Stanford Research Systems		
DG535 Four channel digital delay/pulse generator	$3,500	**

CAMERA SYSTEM		
Double intensified UV-sensitive camera 25mm microchannel plate intensifiers with tapered fiber connection to TN2707 camera.	$42,000	**

* Recommended initial purchase by EMI.

** Recommended to DNA for initial planning.

DISTRIBUTION LIST

DNA-TR-91-224

DEPARTMENT OF DEFENSE

ASSISTANT TO THE SECRETARY OF DEFENSE
ATTN: EXECUTIVE ASSISTANT

DEFENSE INTELLIGENCE AGENCY
ATTN: DB-TPO
ATTN: DIW-4

DEFENSE NUCLEAR AGENCY
ATTN: DDIR G ULLRICH
ATTN: OTA P ROHR
ATTN: SPSD
ATTN: SPSD LT COL ARTMAN
ATTN: SPSP DR P CASTLEBERRY
ATTN: SPWE
ATTN: SPWE C GALLOWAY
ATTN: SPWE T FREDERICKSON
ATTN: TDTR
2 CYS ATTN: TITL

DEFENSE TECHNICAL INFORMATION CENTER
2 CYS ATTN: DTIC/FDAB

DEPARTMENT OF DEFENSE EXPLO SAFETY BOARD
ATTN: CHAIRMAN

FIELD COMMAND DEFENSE NUCLEAR AGENCY
ATTN: FCNV

FIELD COMMAND DEFENSE NUCLEAR AGENCY
ATTN: ENIE N GANTICK
ATTN: FCNM
ATTN: FCTP E MARTINEZ
ATTN: FCTP E RINEHART
2 CYS ATTN: FCTT W SUMMA

STRATEGIC AND THEATER NUCLEAR FORCES
ATTN: DR E SEVIN

THE JOINT STAFF
ATTN: JKCS

DEPARTMENT OF THE ARMY

DEP CH OF STAFF FOR OPS & PLANS
ATTN: DAMO-SWN

HARRY DIAMOND LABORATORIES
ATTN: SLCIS-IM-TL

U S ARMY ARMAMENT MUNITIONS & CHEM CMD
ATTN: MA LIBRARY

U S ARMY BALLISTIC RESEARCH LAB
2 CYS ATTN: SLCBR-SS-T

U S ARMY CORPS OF ENGINEERS
ATTN: CERD-L

U S ARMY ENGINEER DIV HUNTSVILLE
ATTN: HNDED-SY

U S ARMY ENGINEER DIV OHIO RIVER
ATTN: ORDAS-L

U S ARMY ENGR WATERWAYS EXPER STATION
ATTN: C WELCH CEWES-SE-R
ATTN: CEWES J K INGRAM
ATTN: CEWES-SD DR J G JACKSON JR
ATTN: J ZELASKO CEWES-SD-R
ATTN: RESEARCH LIBRARY

U S ARMY FOREIGN SCIENCE & TECH CTR
ATTN: AIFRTA

U S ARMY MATERIAL TECHNOLOGY LABORATORY
ATTN: DRXMR J MESCALL
ATTN: TECHNICAL LIBRARY

U S ARMY NUCLEAR & CHEMICAL AGENCY
ATTN: MONA-NU DR D BASH

U S ARMY RESEARCH DEV & ENGRG CTR
ATTN: STRNC-YSD G CALDARELLA

U S ARMY STRATEGIC DEFENSE CMD
ATTN: CSSD-H-SA
ATTN: CSSD-SA-E
ATTN: CSSD-SD-A

U S ARMY STRATEGIC DEFENSE COMMAND
ATTN: CSSD-SA-EV
ATTN: CSSD-SL

U S ARMY WAR COLLEGE
ATTN: LIBRARY

USA SURVIVABILITY MANAGMENT OFFICE
ATTN: SLCSM-SE J BRAND

DEPARTMENT OF THE NAVY

NAVAL POSTGRADUATE SCHOOL
ATTN: CODE 1424 LIBRARY

NAVAL RESEARCH LABORATORY
ATTN: CODE 2627 TECH LIB
ATTN: CODE 4040 D BOOK
ATTN: CODE 4400 J BORIS

NAVAL SURFACE WARFARE CENTER
ATTN: CODE R44 P COLLINS
ATTN: CODE R44 R FERGUSON

NAVAL WEAPONS EVALUATION FACILITY
ATTN: CLASSIFIED LIBRARY

OFFICE OF CHIEF OF NAVAL OPERATIONS
ATTN: OP 03EG

OFFICE OF NAVAL RESEARCH
ATTN: CODE 1132SM

DEPARTMENT OF THE AIR FORCE

AIR FORCE ENGINEERING & SERVICES CTR/DEMM
ATTN: R FERNANDEZ

AIR UNIVERSITY LIBRARY
ATTN: AUL-LSE

HEADQUARTERS USAF/IN
ATTN: IN

PHILLIPS LABORATORY
ATTN: BLDG 497

STRATEGIC AIR COMMAND/XPSW
ATTN: XPS

DEPARTMENT OF ENERGY

LAWRENCE LIVERMORE NATIONAL LAB
ATTN: C E ROSENKILDE L-084
ATTN: J BELL L-316
ATTN: L-203 R SCHOCK
ATTN: L-81 R PERRETT

LAWRENCE LIVERMORE NATIONAL LABORATORY
ATTN: ALLEN KUHL

LOS ALAMOS NATIONAL LABORATORY
ATTN: REPORT LIBRARY

MARTIN MARIETTA ENERGY SYSTEMS INC
ATTN: DR C V CHESTER

SANDIA NATIONAL LABORATORIES
ATTN: A CHABAI DIV 9311
ATTN: DIV 5214 J S PHILLIPS
ATTN: DIV 9311 L R HILL
ATTN: TECH LIB 3141

U S DEPARTMENT OF ENERGY
OFFICE OF MILITARY APPLICATIONS
ATTN: OMA/DP-252MAJ D WADE

OTHER GOVERNMENT

CENTRAL INTELLIGENCE AGENCY
ATTN: OSWR/NED

DEPARTMENT OF DEFENSE CONTRACTORS

AEROSPACE CORP
ATTN: H MIRELS
ATTN: LIBRARY ACQUISITION

APPLIED & THEORETICAL MECHANICS, INC
ATTN: J M CHAMPNEY

APPLIED RESEARCH ASSOCIATES
ATTN: R FLORY

APPLIED RESEARCH ASSOCIATES, INC
ATTN: J KEEFER
ATTN: N ETHRIDGE

APPLIED RESEARCH ASSOCIATES, INC
ATTN: J L BRATTON

APPLIED RESEARCH ASSOCIATES, INC
ATTN: R FRANK

APPLIED RESEARCH ASSOCIATES, INC
ATTN: J L DRAKE

BDM INTERNATIONAL INC
ATTN: E DORCHAK
ATTN: J STOCKTON

CALIFORNIA RESEARCH & TECHNOLOGY, INC
ATTN: J THOMSEN
ATTN: K KREYENHAGEN

CARPENTER RESEARCH CORP
ATTN: H J CARPENTER

E-SYSTEMS, INC
ATTN: TECH INFO CTR

FLUID PHYSICS IND
ATTN: R TRACI

GEO CENTERS, INC
ATTN: B NELSON

IIT RESEARCH INSTITUTE
ATTN: DOCUMENTS LIBRARY
ATTN: M JOHNSON

INFORMATION SCIENCE, INC
ATTN: W DUDZIAK

INSTITUTE FOR DEFENSE ANALYSES
ATTN: CLASSIFIED LIBRARY

KAMAN SCIENCES CORP
ATTN: L MENTE
ATTN: LIBRARY
ATTN: R RUETENIK

KAMAN SCIENCES CORP
ATTN: JOHN KEITH

KAMAN SCIENCES CORP
ATTN: D MOFFETT
ATTN: DASIAC
ATTN: E CONRAD

KAMAN SCIENCES CORPORATION
ATTN: DASIAC

LOCKHEED MISSILES & SPACE CO, INC
ATTN: TECH INFO CTR D/COLL

LOGICON R & D ASSOCIATES
ATTN: C K B LEE
ATTN: D SIMONS
ATTN: LIBRARY
ATTN: T A MAZZOLA

LOGICON R & D ASSOCIATES
ATTN: B KILLIAN
ATTN: E FURBEE

LOGICON R & D ASSOCIATES
ATTN: G GANONG
ATTN: J WALTON

LOGICON R & D ASSOCIATES
ATTN: E FURBEE
ATTN: J WEBSTER

LTV AEROSPACE & DEFENSE COMPANY
2 CYS ATTN: LIBRARY EM-08

MCDONNELL DOUGLAS CORPORATION
ATTN: R HALPRIN

MOLZEN CORBIN & ASSOCIATES, P.A.
ATTN: TECHNICAL LIBRARY

NEW MEXICO ENGINEERING RESEARCH INSTITUTE
ATTN: J JARPE
ATTN: N BAUM
ATTN: R NEWELL

NICHOLS RESEARCH CORPORATION
ATTN: R BYRN

PACIFIC-SIERRA RESEARCH CORP
ATTN: H BRODE
ATTN: L E JOHNSON
ATTN: L SCHLESSINGER

PDA ENGINEERING
ATTN: J E WUERER

PHYSICAL RESEARCH INC
2 CYS ATTN: D MODARRESS
2 CYS ATTN: T HOEFT

RAND CORP
ATTN: B BENNETT

S-CUBED
ATTN: C PETERSEN
ATTN: G SCHNEYER
ATTN: J BARTHEL
ATTN: K D PYATT JR
ATTN: P COLEMAN
ATTN: T PIERCE

S-CUBED
ATTN: C NEEDHAM

SCIENCE APPLICATIONS INTL CORP
ATTN: C HSIAO
ATTN: F Y SU
ATTN: G EGGUM
ATTN: G T PHILLIPS
ATTN: H WILSON
ATTN: TECHNICAL REPORT SYSTEM

SCIENCE APPLICATIONS INTL CORP
ATTN: DIV 411 R WESTERFELDT

SCIENCE APPLICATIONS INTL CORP
ATTN: J WILLIAMS

SCIENCE APPLICATIONS INTL CORP
2 CYS ATTN: D HOVE
2 CYS ATTN: H SINGER
ATTN: J COCKAYNE
ATTN: W LAYSON

SCIENCE APPLICATIONS INTL CORP
ATTN: K SITES

SCIENCE APPLICATIONS INTL CORP
ATTN: G BINNINGER

SCIENCE APPLICATIONS INTL CORP
ATTN: R ALLEN

SRI INTERNATIONAL
ATTN: D KEOUGH
ATTN: DR B S HOLMES
ATTN: J SIMONS
ATTN: M SANAI

TECHNICO SOUTHWEST INC
ATTN: S LEVIN

THE TITAN CORPORATION
ATTN: LIBRARY

TRW SPACE & DEFENSE SECTOR
ATTN: HL DEPT/LIBRARY
ATTN: OUT6/W WAMPLER

WASHINGTON STATE UNIVERSITY
ATTN: PROF Y GUPTA

WEIDLINGER ASSOC, INC
ATTN: H LEVINE

WEIDLINGER ASSOCIATES, INC
ATTN: T DEEVY

WEIDLINGER ASSOCIATES, INC
ATTN: I SANDLER
ATTN: M BARON